DEVELOPMENT OF A NEW TECHNOLOGY--RICH/LEAN COMBUSTION OF PULVERIZED COAL

Zuohe Chi, Qiang Yao, Jinhu Zhou, Xiao Jiang, Baomin Sun,
Xinyu Cao, and Kefa Cen

The Institute for Thermal Power Engineering
Zhejiang University, Hangzhou, China

ABSTRACT

In this paper, a new technology named rich/ lean coal combustion is introduced. The technology is used for the low load flame stabilization of pulverized coal without support oil and the prevention of furnace wall slagging. A specially designed two phase flow test facility was set up in Zhejiang University to develop a technology of air--coal mixture separation. The cross section of test pipe is 250 × 250mm. The maximal air flow in the tester can reach 6000 m^3/h and particles flux is up to 3-4 t/h. The pulverized coal in primary air is separated and two streams of air- coal-- rich pulverized coal stream and lean pulverized coal stream are formed. Rich pulverized coal steam is guided to the high temperature area facing the flame. This contributes to ignition and flame stability of pulverized coal. The lean pulverized coal stream is guided to low temperature area located behind the flame and forms a air film near furnace wall that benefits to reduce the slagging on the wall. The rich/lean combustion also lows NOx emission.

The test results of new developed equipment shows that the ratio of the concentration of rich pulverized coal side to concentration of lean side is 7-12:1. Namely, if average C/A is equal to 0.6, then C/A in rich side reaches about 1.1 and C/A in lean side is about o.1. The pressure drop of the separate equipment is about 3000-4000Pa.

The retrofit of several utility boilers have been made. These include 200MW, 125MW, 100MW, and 50MW utility boilers and the coal types used include brown coal, bituminous coal and anthracite coal. The industrial tests showed that this technology is successful to meet the above three goals. The lowest boiler load of about 40-50% to keep coal flame steady has been obtained without supporting oil. The flow pattern in furnace is good and no slagging is formed on the wall of the retrofitted boilers. The combustion efficiency of the boiler to burn bituminous coal is improved apparently after the retrofit of the boilers.

INTRODUCTION

For pulverized coal furnace, in order to prevent pulverized coal to block up the piper line the primary air velocity is generally chosen as 20-30m/s. Under the condition the coal concentration C/A is about o.5-0.7kg/kg. However, from the view of ignition and flame stability of pulverized coal the coal concentration is too low. So, a new pulverized coal rich/lean combustion technology is developed.

The technology divides the air-coal flow into two steams, one is the rich pulverized coal flow and the other is the lean pulverized coal flow. The rich pulverized coal flow is guided to the high temperature area facing flame and the lean pulverized coal flow is guided to the low temperature area located behind flame. The combination of high pulverized coal concentration with high temperature contributes to the ignition of coal and coal flame stability. Lean coal stream forms a air film near furnace wall that benefits to reduce the slagging on the wall.

Test results have shown that ignition temperature of air-coal mixture decreases , the heat required for igniting air-coal stream lows and the ignition time shorts with the increase of coal concentration. Fig.1 shows ignition index varies with coal concentration for parts of typical Chinese coal. Fig.2 is experimental results of ignition distance of coal via coal concentration. A large number of hot model experimental data were summered. Optimum pulverized coal concentration is as follows: For brown coal C/A is about 0.6-0.8, for bituminous C/A is about o.8-1.2, for low-rank bituminous、lean coal and anthracite C/A is larger than 1.2.

This paper first describes the experimental results of concentration distribution at the exit of bending tubes, and then introduces the separate efficiency of the new developed guiding separate equipment. Based on the test data the mechanisms of coal flame stability and resistant-slagging are discussed. Finally, industrial application results of the new technology are represented.

TEST RIG AND AIR -SOLID FLOW SIMULATION

A large test rig was built to test pulverized coal separation from air through centrifugal force of bend tubes and to test separate efficiency of a specially designed guiding-separate equipment. The system of test rig are shown in Fig.3. The cross-section 0f test duct is 250 × 250. Air flow rate through the test duct is up to 6000 m^3/h and powder flux can reach 3-4 t/h. Air flow rate is adjusted by damper and is measured by Venturimeter. The powder flux is adjusted by changing the rotation speed of feeder and measured by isokinetic sampling probe. A large test room is located at the exit of test duct, which is made from plexiglass, to observe and test the air- solid separation. The air-solid mixture under the test room continue to be transported to cyclone separator. After the separation of air-solid the air is introduced to the inlet of F.D fan, which forms a close circulation. In order to maintain the negative pressure of the test duct a pressure balance pipe is used.

According to simulation theory the numbers w_p/w, ρ_p/ρ, Re number, Fr number and Stk number should be kept equal between model and original(where w –velocity , ρ –density). However, due to $\rho_p/\rho >>1$ it is acceptable to consider $(\rho_p/\rho)_m$ is equal to $(\rho_p/\rho)_o$. The relative velocity between air and powder is low. So, $(w_p/w)_m$ can approximately considered to be equal to $(w_p/w)_o$. $(\mathrm{Re})_m$ and $(\mathrm{Re})_o$ do not need to be equal. However, they must be large enough to enter the second simulating region. Fr number is the ratio of inertia force to centrifugal force or weigh force. Stk number is given by

$$Stk = \rho_p \cdot w^n \cdot d_p^{n+1} / (C_D \cdot \rho \cdot \upsilon^n)$$

If the particle diameter d_p is small, then C_D=24, n=1.

The talcum powder of 150 mesh was taken as experimental medium during the experiments. The real density of the talcum powder is 2700kg/m^3 and its average diameter is 50 um. The simulation numbers of the model experiment and original are shown in Table 1.

Table 1. the simulation numbers of the model experiment and original

Re(original) / Re(model)	Fr(original) / Fr(model)	Stk(original) / Stk(model)
5.8×10^5 / 3.8×10^5	11.8 / 12.8	0.94 / 1.48

THE SEPARATION EFFICIENCY OF DIFFERENT BENT TUBES

The air-solid two phase flow tests were conducted for several typical bent tubes to know separate results. Fig.4 shows the test value of the concentration distribution at the exit of the bent tube under the conditions that the ratio R/D (R-curved radius of the bent, D-diameter of the bent tube) is equal to 2, air velocity is 21.6m/s and the curvature angle is 110°During the experiments the average concentration C/A was 0.246. A separate plate is arranged at the center of the exit section. The separation efficiency is defined as the ratio of the average concentration in the rich side to that in lean side, The average concentration in the rich side or in the lean side is given by

$$C_{av} = \frac{\sum V_i C_i S_i}{\sum V_i S_i}$$

Where V_i and C_i are respectively the velocity and concentration at the test location. S_i is the small area around the test points. The concentration ratio of the rich side to the lean side can reach 10-12:1 for 110° bent tube. The curve 1 in Fig.5 gives the results of concentration distribution at the exit section for 45° bent tube. The concentration ratio is 4-5:1. A reflect block is added at the inlet of the bent tube shown in Fig.6 to enhance the separation efficiency of 45° bent tube and the concentration ratio of 8-10:1 is reached, shown in curve 2 of Fig.5. Table 2 is the test results for different curvature angle bent tubes.

A large number of test results show that: (1) The separation efficiency is affected by the concentration of pulverized coal. In the experimental range of which C/A is smaller than o.6 the separation efficiency is slightly decreased with the increase of pulverized coal concentration. (2) In the

Table 2 the separation efficiency for different curvature angle bent tube

operating conditio	average velocity in rich side (m/s)	average velocity in lean side (m/s)	concentration in rich side, C/A	concentration in lean side, C/A	concentration ratio
45° bent tube	21.6	19.8	0.463	0.116	4.4 : 1
45° bent tube with reflection block	23.5	20.4	0.635	0.072	10.2 : 1
45° bent tube	22.1	19.9	0.501	0.052	9.6 : 1
110° bent tube	21.5	20.1	0.471	0.0463	11.1 :1

experimental range of which curvature angle is smaller than 110° the separation efficiency increases with the increase of curvature angle. (3) The larger the radius of curvature , the better the separation efficiency .

A NEW TYPE OF COLLISION SEPARATION EQUIPMENT

It is certain that the rich coal sides in two corners of tangentially fired boilers of which the primary line are located horizontally are located behind the coal flame when the separation of bent tube is used. Furthermore, there is often a long straight tubes before the burner for some large boilers. Using directly bend tubes to separate air coal mixture the possibility of choking tube caused by pulverized coal of high concentration in rich side is increased. In order to guide rich pulverized coal flow to the side facing coal flame and not to increase the possibility of choking tube a collision separation equipment is designed and tested. The schematic diagram of the separation is shown in Fig.7. The important technical parameters of the separator are the height of the collision block, the collision angle of the block facing air flow ,the distance between the block and the separate plate and the curve shape of the plate located at the opposite of the collision block. A good combination of these parameters would make the separator reach a high separation efficiency and low flow pressure drop and obtain almost the same velocity distribution in each side of the plate. Fig.8 shows the distribution of the concentration and velocity tested in rich side and lean side. Parts of the test results of the collision separator is listed in Table 3.

From Table 3 the following facts can be observed : (1) The guiding block has a good separation efficiency and the separation efficiency an change by changing the height of guiding block , which most benefits to the load change of boiler and the change of coal type. When the load of boiler is lowed and the quality of coal becomes inferior, the height of guiding block increase to increase separation efficiency. (2) The velocity difference between the rich side and lean side of the separate plate increases with the increase of the height of the guiding block. (3) If the height of the guiding block is fit, the separation efficiency can reach high range of 7-12:1 and the velocity difference between the rich side and lean side can be controlled in an accepted range of 4-5m/s.

Table 3 parts of the test results of the collision separator

height of the guiding block (mm)	velocity in rich side(m/s)	velocity in lean side (m/s)	concentration ratio of rich side to lean side
40	25.9	22.5	2.9 : 1
60	26.2	22.1	7.1 : 1
60	15.9	15.3	5.9 : 1
60	21.2	19.1	7.2 : 1
80	28.4	20.1	13.5 : 1

THE MECHANISM OF COAL FLAME STABILITY WITH LOCAL HIGH PULVERIZED COAL

Owing to the increase of difference between peak load and valley load of electrical network many boilers must often operate at low load. Furthermore, the price difference between coal and fuel oil greatly increases in recent year. Many power plant require that boiler can operate steadily at low load without support of oil to improve the economy of power plant. To meet these requirements a coal flame stability technology is developed. The key points of the technology are to produce a local region with high concentration of coal pulverized, which is space-interception shown in Fig.9. The guiding separator is used to produce a layer with high concentration of pulverized coal and to introduce the layer to the side facing flame. the test results show the C/A in the layer can reach 1.6-2.0 kg/kg. On the other hand, a V-shape body is horizontally located in burner shown in Fig.9, which produces a reflux zone. At the edge of the reflux zone a thin layer with high concentration is also formed. The high concentration layers caused by V-shape body and by guiding separator intercept in space. The layer facing flame is directly impacted by the flue gas of high temperature from upstream so that the exchange of heat and mass between coal pulverized and flue gas is very strong. In the same way the high concentration layer at the edge of the reflux zone has a very strong mass and heat exchange. The coal pulverized in the layers is promptly heated and ignited. A good igniting resource is provided and coal pulverized flame is kept steady at the low load.

THE RESISTANT-SLAGGING PRINCIPLE OF RICH/LEAN COMBUSTION OF PULVERIZED COAL

To keep coal-pulverized flame steady at low load often makes the slagging in furnace become serious at high load because the temperature in furnace is higher and igniting points are nearer to burners. To solve the slagging problem some technical measures are taken as follows:

(1) The air-coal flow is separated as rich coal stream and lean coal stream . Rich coal stream is guided to the side of burner facing flame and lean coal stream is guided to the side of the burner behind the flame. The lean coal stream which has a concentration C/A of 0.1-0.2 forms a prevention layer around the waterwall to prevent the rich coal flow directly to impinge the waterwall.

A number of particles trace experiments were made in a cold test rig with 1090mm length × 960mm width × 3300mm height to demonstrate the resistant-slagging of the arrangement. Some compounds particles used as tracer were injected into the model primary line and carried into furnace with the primary air. The tracers that impinge the wall were caught by the Vaseline coating on the wall. Many samples were taken and analyzed by chemical analysis to determine the deposit quantity in the samples. Then the total relative deposit quantity was approximately calculated in four walls. The test results show that the relative deposit quantity on four walls is 10-15% without separation of air-coal mixture. When guiding separator is used and lean coal stream is arranged to the side of burner behind flame the relative deposit quantity is only 5-6%. The relative deposit quantity is greatly reduced by using the separator. That is , the possibility of coal-pulverized impinging the waterwall is reduced. The slagging on the waterwall is lighted to a certain degree.

(2) It is important to select the match of the blocking ratio of the V-shape body and the slagging properties of coal used . For the coals with high slagging the blocking ratio of the V-shape stabilizer is selected to be low so that the size of the reflux zone is not very large and the igniting point is not very near burners. On the other hand for high slagging coal the height of guiding separator is lowed to reduce the separation efficiency. The data about the optimum match of the V-shape stabilizer and the coal slagging property are being accumulated through the field tests of actual boilers. Actually the slagging never takes place for several boilers retrofited using the rich/lean coal combustion.

Also, that the V-shape flame stabilizer is arranged horizontally or vertically has a strong influence on the slagging of furnace. Cold model and field tests show when the V-shape body is located vertically the "stiffness" of the primary air greatly reduced and the primary air has strong deflection. Furthermore, when primary air flows through the V-shape body , the primary air is separated to two streams. One stream of the primary air enters the furnace in a angle which is nearer the waterwall. This causes pulverized coal in the stream very easily to impinge waterwall to result in slagging. For V-shape flame stabilizer located horizontally the "stiffness" of the primary air is slightly reduced and there is no problem of a stream of the primary air extending to the waterwall. From the view of resistant-slagging the V-shape located horizontally is better than that located vertically.

INDUSTRIAL APPLICATION OF RICH/LEAN COAL COMBUSTION

The new developed technology has been used for retrofits of many power plants. Some of the power plants are No.9 boiler (670t/h) of Shaoguan Power Plant in Guandong Province, No.1 and No.2 boilers (420t/h) of Xiaoshan Power Plant in Zhejiang Province and No.7 boiler(300t/h) of Liyujiang Power Plant in Hunang Province. The boiler of Shaoguan Power Plant burns anthracite which has 40-45% ash content, 7-9% volatile matter and 20300-21700 kj/kg LHV on as received basis. Because the igniting and firing properties of the coal are very bad, much refractory liner are used on the waterwall to increase the temperature in the furnace. This causes seriously slagging on the refractory liner. The burners were retrofitted by using the technique of rich/lean coal combustion and a part of refractory liner was removed.

After the retrofit the coal flame can keep steady at 75% boiler load without support of oil. The slagging on the waterwall is greatly reduced. The No.7 boiler of Liyujiang Power Plant was produced

by Dongfang Boiler Work. The rated power of the set is 70MW. The pressure and temperature of the main stream are respectively 9.8Mpa and 540℃. The fired coal is local low-rank bituminous. The coal composition is W=9.79%, A=47.2% and LHV=13272 kj/kg on as received basis. The boiler needs to operate at low load of 30 MW during night time. To reduce the supporting oil consumption the guiding collision separator was used to retrofit the burners. During the performance tests the set operated at constant pressure from 70% boiler load to 40% boiler load, and then when the load continued to low the variable pressure operating method was taken. The set was kept to operate for 8 hours at the load of 30-31MW and at the load of 27MW the boiler kept to operate steadily for about half an hour without supporting oil. The pressure drop of the guiding separator is 380 Pa. The performance tests show the retrofit is successful, the rich /lean coal combustion has strong coal flame stability at low load and the contract conditions of the retrofit are completely fulfilled.

The operation of many other boilers has demonstrated that the technique of rich/lean coal combustion using the guiding separator is of the advantages of low flow resistance, good flame stability, easy and simple to operate and resistant-slagging in a certain degree.

ACKNOWLEDGEMENTS

The paper is financially supported by the Fund of Nature Science of Zhejiang Province.

REFERENCE

(1) Chi Zuohe ,Jiang Xiao, Cen Kefa, The Research of Improving 200MW boiler slagging by Adding Guiding -Plate at the Burner, JSME-ASME International Conference on Power Engineering, 1993, Tokyo, Japan

(2) Masayasu sakai, Tangential Corner Fired Boiler with Low Volatile Matter Content Coal, TECHNICAL REVIEW, June, 1986

(3) Han Caiyuan, Developing Status in Combustion Theory and Technology of High Concentration Pulverized Coal, POWER SYSTEM ENGINEERING, Vol.9 No.3 1993

(4) Fu Weibiao, Prospect Analysis of Application of Anthracite in Four Corner Tangential-fired Pulverized Coal Bioler, POWER SYSTEM ENGINEERING (BIMONTHLY), Vol.10 No.5 (Ser. No.41)

(5) Cen Kefa, Boiler Combustion Test Methods and Measurement Technology, Hydraulic and Electrical Power Publisher, 1986

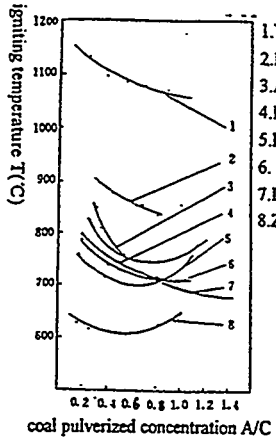

1.Yongan anthracite
2.Fongfong meager coal
3.Anyuang bituminous
4.Dadong bituminous
5.Huolinghe brown coal
6. Buchuen meager coal
7.Dianba bituminous
8.Zhaqiouncer brown coal

Fig.1 the experimental results of the igniting temperature via pulverized coal concentration

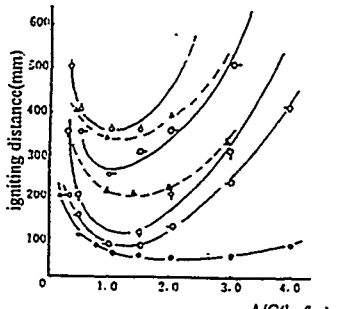

○--V_{af}=10.4 % ○--V_{af}=12.5 % ○--V_{af}=1.94 %
○--V_{af}=27.2 % ●--V_{af}=37.8 % ▲--Xishang meager coal
△--Dadong bituminous

Fig.2 the experimental results of igniting disfance via coal concentration

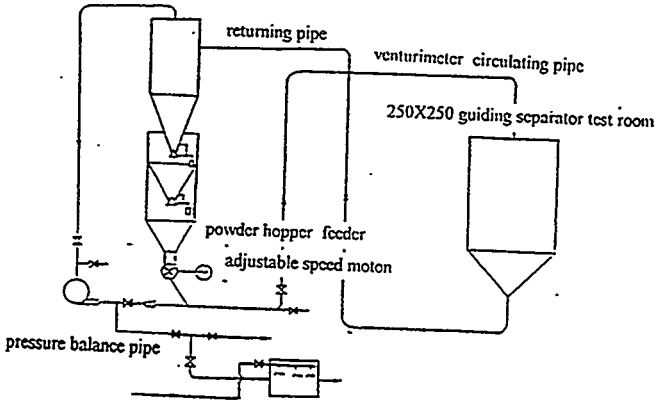

Fig.3 system diagram of air-solid two cyclone separator

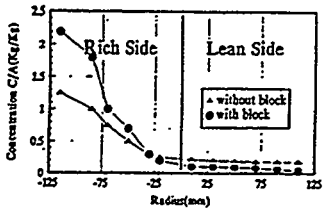

Fig.5 the concentration distribution of 45° bend tube with and without block body

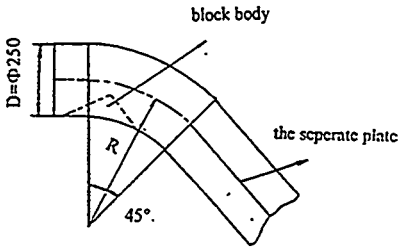

Fig.6 the diagram of 45° bend tube adding block body

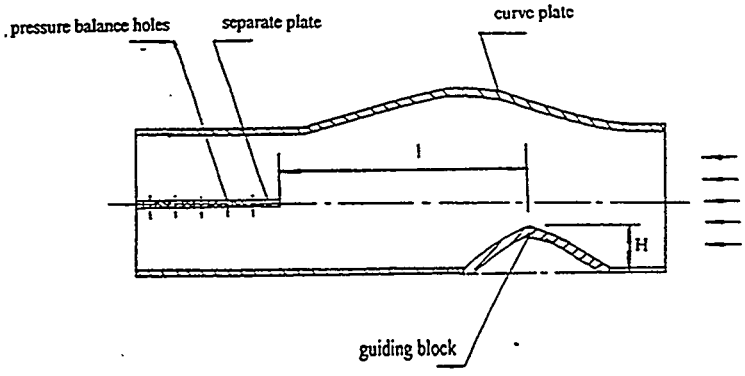

Fig.7 the sketch drawing of guiding seprartor

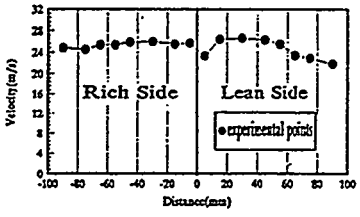

a—velocity distribution

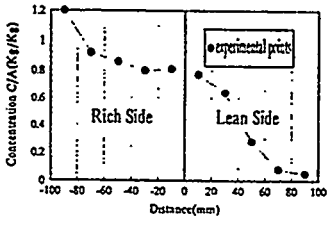

b—concentration distribution

Fig.8 the velocity and concentration distribution in rich side and in lean side

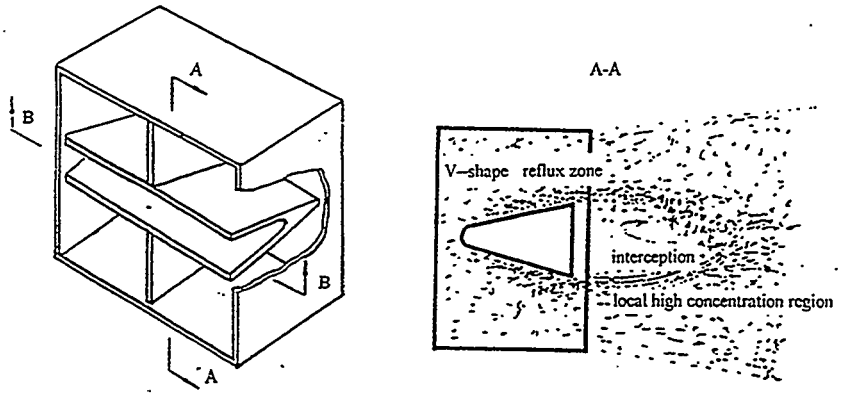

a–V-shape stabilizer

b–local high concentration rigion from A-A view

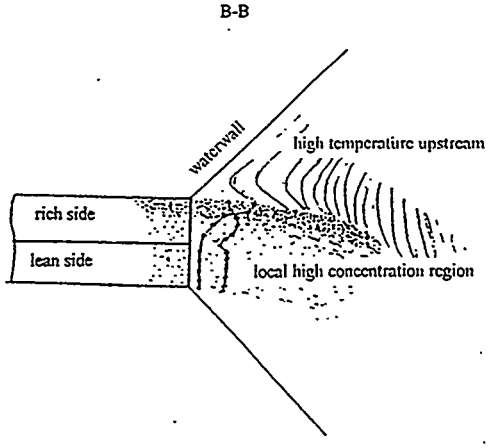

c–local high concentration region from B-B view

fig.9 the local high concentration region of space

Ash Deposition in Low NOx Burner Flames of Beneficiated Coal Fuels, *L.E. Barta, J.M. Beer, P. Lewis, D. Teare and V. Wood, Massachusetts Institute of Technology; and O.K. Chow, ABB Power Plant Laboratories, Combustion Engineering, Inc., USA*

Dr. Laszlo E. Barta
Scientific Advisor
EGI Contracting/Engineering Co. Ltd.
33-34 Bem rkp.
Budapest, HUNGARY 1027

This paper was unavailable at the time of publication and may be obtained directly from the author.

The Milling and Combustion Behaviour of Coal Blends

H. Maier, H. Spliethoff, K.R.G. Hein

University of Stuttgart, IVD
Pfaffenwaldring 23, 70569 Stuttgart, Germany
Tel./Fax: #49-711-685-3762 / #49-711-685-3491

Abstract

The European Union is one of the biggest areas importing bituminous coal from overseas areas and countries like Australia, Colombia, North America, and Indonesia/Asia. Overseas coals are less known in Europe as far as the milling and combustion behaviour is concerned but there will be specific problems with regard to both behaviours, e.g. fouling, slagging, ignition, etc. To get an improved knowledge of foreign coals, a lot of coal analysis data were investigated to find out about the specifics of fuel nitrogen, fuel sulphur, ash, and inertinite content of coals from different areas. As for coals from the southern hemisphere, the results reveal low sulphur and high inertinite contents and for coals from South-Africa and Asia, higher ash contents.
The investigations concerning the milling behaviour of coals were focused on the effect of the blending technique on the achievable coal particle size distribution. The results for milling the raw blended coal show in most cases that a finer particle distribution resulted in lower NO_x emissions and better burnout compared with the pulverised coal blending, but this behaviour depends on the used coal. NO_x emissions with respect to different primary air ratios show the highest values of about 940 vpm for a high volatile bituminous German coal in unstaged combustion conditions. For the in-furnace air-staged combustion with a primary air ratio of about 0.6 NO_x emissions between 270-290 vpm were measured for all coals. One significant aspect depending on the primary air ratio is that the NO_x emission of the blendings can be either between, higher or lower than the NO_x emission of the single coals. Advanced investigations concerning the double in-furnace air-staging show the lowest NO_x emissions of about 100 vpm.

Introduction

In 1993, the total coal exploration of hard coal in the world was about $3.5 \cdot 10^9$ t where more than 90 % altogether was produced by China, the USA, India, the Russian Confederation, South Africa, Australia, Poland, the Ukraine, Kazakhstan and Great Britain.
The German mining capacity with about 2 % of the world production is very small compared with the 55 % produced by the USA and China together /1/. The increase of the world population and the industry production in the next few decades especially in the fast growing areas of South-East Asia, Africa, Central and South America, will make the demand of energy rise equivalently, and one of the major fuels for power generation will be coal. In consideration of the coal mining price and the economical aspects in Western Europe, the mining capacity will be reduced in the next years. The contrary effect will happen in countries like Australia, Indonesia, Colombia, etc. which are growing export countries to serve the world coal trading market. The biggest import areas of coal nowadays and in the near future are the countries of the European Union (EU), Japan and the other countries in Asia.
However, considerable problems occur by using imported coals in power plants in Europe

concerning the combustion behaviour e.g. fouling, slagging, ignition, and the milling. One possibility of using imported coals is to blend these coals with the well-known domestic ones. In order to solve specific environmental problems, the use of coal blendings offers another important possibility, i.e. the utilization of low quality (domestic) coals with:
- high ash content in blend with low ash coals,
- low volatile content in blend with high volatile coals and
- higher sulphur content in blend with low sulpher coals.

Because of the fact that the EU (12 in 1993) with 32 % (360 . 10^6t) is the biggest area importing bituminous coal by sea transport /1/, there is a great effort to get more information about the combustion behaviour of foreign coals unknown in Europe and their behaviour as blending coal to solve the above mentioned particular problems.

Experimental

The growing market of imported coal or coal blendings in the near future in Europe stimulated the EU to increase the investigations concerning imported coals and coal blendings in order to get a better understanding about the combustion and grinding behaviour for energy utilization. The measurements were carried out at the semi-industrial 0,5 $MW_{(th)}$ coal combustion facility of the IVD (Institute of Process Engineering and Power Plant Technology). The design and operation of the test facility have been published elsewhere /2,3/. Nevertheless, one should know that the IVD milling system is equipped with a high speed impact mill with integrated wing classifier. By varying the classifier speed, the coal particle size distribution can be changed thus offering a great flexibility with regard to different fuels. For the investigations different coals and blendings were tested which are described by the proximate and ultimate analyses in table 1.

Table 1: Analyses data (wt%) of coals

Coal	Ash (db)	VM (daf)	C	H	N	S	Ho	ASTM class
				(daf)				
Göttelborn (GB)	10,2	36,5	79,5	4,9	1,5	1,0	52	HV
Emil Mayrisch (EM)	8,5	14,3	89,3	4,2	1,5	0,9	81	LV
Phoenix (PH)*	12,0	33,3	82,3	5,0	1,9	1,3	48	HV
Middleburg (MB)*	14,3	28,8	80,1	5,3	1,6	0,5	55	MV
Blends:								
(1) 40%GB-60%EM	9,1	23,6	85,3	4,5	1,5	1,0		MV
(2) 70%GB-30%EM	9,5	30,1	83,4	4,6	1,5	1,0		MV
(3) 30%GB-70%PH	11,5	34,3	81,5	5,0	1,8	1,2		HV
(4) 60%GB-40%PH	10,9	35,2	80,6	4,9	1,7	1,1		HV
(5) 30%GB-70%MB	13,2	30,9	79,9	5,2	1,6	0,6		MV
(6) 50%GB-50%MB	12,3	32,5	79,8	5,1	1,6	0,7		HV
(7) 70%GB-30%MB	11,5	34,0	79,7	5,0	1,5	0,8		HV

* coal from South Africa

The analysis data of the different blendings tested can be calculated based on the analysis data of the original coals and the blend ratio based on the heating value of the single coals.

Results

The first step in the project was to characterise the imported coals which are intended to be used as single or blending coals with for e.g. domestic coals with regard to their content of sulphur, volatile, ash and macerals. For this purpose coal analysis data taken out of literature were used and some characteristical results are shown in fig. 1 - 4. Fig. 1 concerning the coal sulphur content over the volatile matter of the coals shows that coals from Europe will have the highest value, except for some high volatile coals from North America. The low sulphur content of the imported coals in Europe offers the possibility to reduce the primary SO_x emission level in power plants as well as the gypsum production of $DeSO_x$-facilities. An interesting point is that for the most coals independent of their origin, except for the coals from Asia, the sulphur content increases with an increasing volatile matter content.
The fuel nitrogen content in fig. 2 shows a significantly higher amount compared with coals from the other regions in the world. Only some coals from Australia with volatile matter contents below 30 % may have a higher fuel nitrogen content. The tendency in fig. 2 shows that by using imported coals as single coal or blending coal the NO_x emission should be reduced with regard to the NO_x formation based on the fuel nitrogen. So it is possible to run a power plant with imported coals as blending coal far below the governmental limits without any problems and to save ammonia by using a catalytic $DeNO_x$ unit.

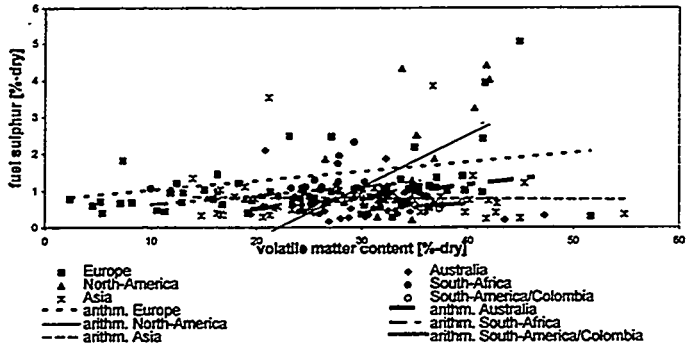

Fig. 1: Fuel sulphur content of coals from different areas in the world

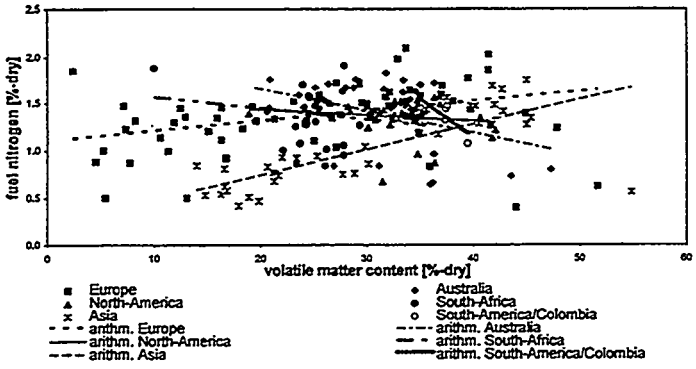

Fig. 2: Fuel nitrogen content of coals from different areas in the world

The analysis data of the maceral inertinite in fig. 3 show great differences for coals from Europe/North America and for coals from Australia, Asia and South Africa. Coals from Europe or North America have nearly the same low inertinite content of about 20 % over the total range of volatiles whereas the content of coals from the southern hemisphere ranges from 0 % up to about 63 %. This high inertinite amount of coals from the southern hemisphere makes one expect that the ignition behaviour of the coal particles should be lower compared with coal particles with lower inertinite content like the ones in Europe. The ash content of coals dependent on their origin is plotted in fig. 4. The results show that coals mainly from Europe, North America, and Colombia have lower ash contents than coals from South Africa, Australia, and Asia where the coals from Asia can have ash contents up to nearly 70 %. This higher amount of ash is very important for the design of the ash handling systems, and most of these high ash/low volatile coals can only be fired in pf-systems in a blending with high volatile coals. For high ash coals problems regarding the fouling and slagging behaviour in boilers are expected.

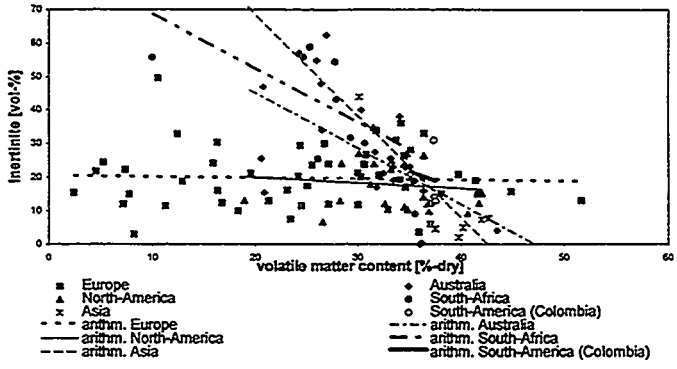

Fig. 3: Inertinite content of coals from different areas in the world

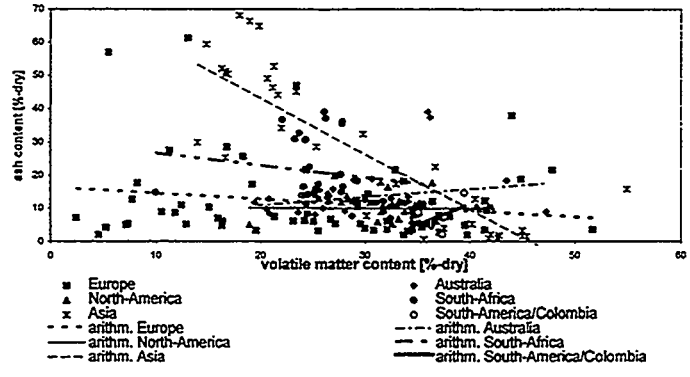

Fig. 4: Ash content of coals from different areas in the world

The next part was to study the grinding behaviour of coal blendings compared with the single coals as well as the influence of the blending technique by varying milling parameters like

Coal Blending Techniques

Nevertheless, the coal-psd of the coal blending of 50 % GB-MB being quite similar, input-output combustion tests were carried out to show whether or not the blending technique can influence the emission and the burnout behaviour. Fig. 7 shows the comparison of the coal-psd with respect to the blending of 50 % GB-MB whereas the result of the combustion behaviour is plotted in fig. 8 and fig. 9.

Using the raw coal blending technique, the results concerning the total particle residue show a slightly finer behaviour, the particle size distribution, of course, nearly show the same. The combustion behaviour concerning the NO_X emission (fig. 8) and the unburned carbon in the flue ash (fig. 9) shows lower NO_X emissions and a slightly lower unburned carbon content of about 1 % in the flue ash for the coal blended before the milling process.

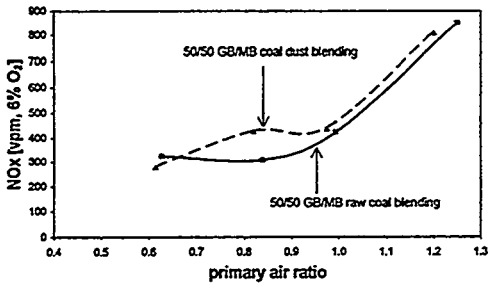

Fig. 8: Effect of coal blending technique on NO_X emission at the IVD test rig

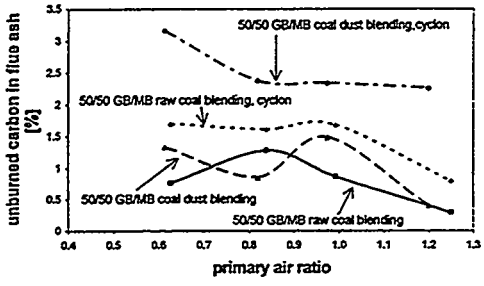

Fig. 9: Effect of blending technique on unburned carbon in the flue ash at the IVD test rig

Both the lower NO_X emissions and the lower unburned carbon are influenced by the finer coal particles as well as by a possible different particle surface or by particle cracking regarding different particle interactions in the mill. The influence of a finer coal particle size is resulting in an increase of the residence time in the primary NO_X reduction zone and higher NO emission levels in the flame by the higher fuel nitrogen release with the coal volatiles. Firing the coal particles in air-staged conditions, see experimental results shown in fig. 8 lower NO_X emissions are observable for the slightly finer coal by using the raw coal blending.

The corresponding results of the unburned carbon in fig. 9 show an increase with decreasing the primary air ratio. It is significant that using the raw coal blending technique a lower unburned carbon content in the flue ash was measured in the cyclon ash and also in the flue ash sampled in the combustion chamber. The unburned carbon content in the cyclon ash is a little bit higher than measured in the chamber because the very small ash particles without any corbon content pass the cyclon.

Effects of the Blend Ratio

Investigations were carried out for the coals GB, MB, and three blendings of the two at different primary air ratios. In fig. 10 the results with respect to the unstaged combustion of

- coal mass flow,
- air volume flow,
- classifier speed, and
- blending ratio.

For that, different coal particle size distributions (coal-psd) and characteristic values e. g. mean volumetric particle size D[v,0.5] were compared according to the two blending techniques of raw coal and pulverised coal blending. Fig. 5 will show the results for the coal blending 30 % Göttelborn (GB)-70 % Emil-Mayrisch (EM) and fig. 6 for the coal blending 30 % GB-70 % Phoenix (PH).

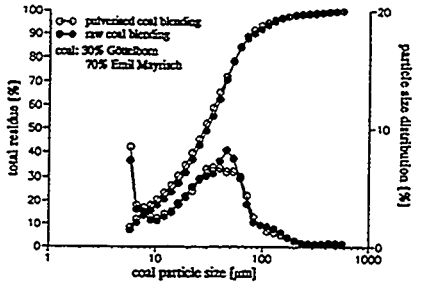

Fig. 5: Effect of coal blending technique on coal particle fineness

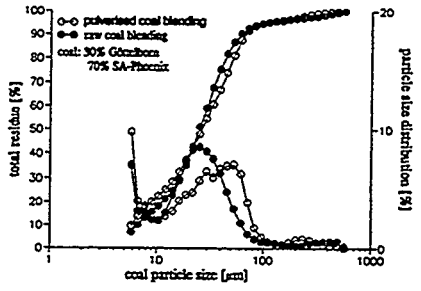

Fig. 6: Effect of coal blending technique on coal particle fineness

The coal-psd for the coal blending 30 % GB-70 % PH shows that there are large differences especially in the particle range from 5 μm to 100 μm. For these two coals, the technique will be the raw coal blending in order to get a finer coal-psd compared with the pulverised coal blending where the respective single coals are milled separately. This result could be observed for the demonstrated blend ratio of 30 % GB-70 % Ph as well as for the ratio 60 % GB-40 % Ph.

The used coals playing a key role among the above mentioned influences can be seen in figure 6 where one result of the two coals GB and EM is plotted. The coal-psd for a blending of these two coals (70 % GB-30 % EM) shows nearly the same curve regardless of whether the coals were blended in pulverised or raw conditions. Also, the blending with the ratio 40 % GB-60 % EM shows no significant difference in the achievable coal-psd and the same was measureable for the following blendings 40 % GB-60 % EM, 70 % GB-30 % MB, 50 % GB-MB and 40 % GB-60 % MB.

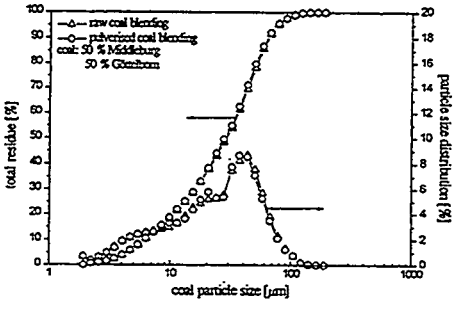

Fig. 7: Raw coal and pulverised coal blending, particle fineness for coal 50 % MB-50 % GB

$\lambda = 1.2$ show NO_X emissions of the GB coal of about 940 vpm and of the coal MB of about 700 vpm whereas the blendings of them are between these two values. Surprising is, however, that an increase of the percentage ratio of MB coal up to 100 % goes along with a decrease of the NO_X emissions, the fuel nitrogen content of the MB coal, of course, is higher than the one of the GB coal. This tendency may be caused by the lower volatile content of the MB coal, perhaps, by different ignition and devolatilization behaviours of volatiles and fuel nitrogen forming local substoichiometric zones and by a more homogenious temperature distribution in the flame.

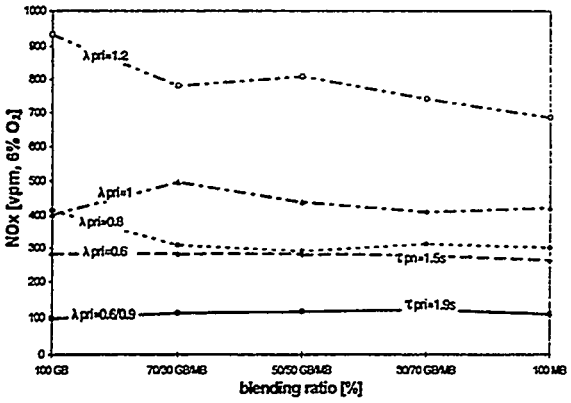

Fig. 10: Effect of blend ratio on NO_X emission

Using the in-furnace air staging technique with different primary air ratios of 0.6 to 1.0, NO_X emissions can be reduced to about 100 vpm with the lowest emissions for the double air-staging. The NO_X emissions of both the two coals and the three blendings are always on the same level so the NO_X does not depend on the blend ratio. This behaviour is caused by the relatively long residence time of coal particles and gas emissions in the primary reduction zone.

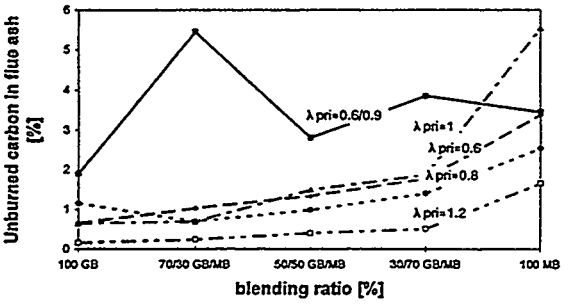

Fig. 11: Effect of blend ratio on unburned carbon in the flue ash

The content of unburned carbon in the flue ash is plotted in fig. 11 where the results show a slight increase with all primary air ratios by increasing the partial amount of MB coal in the blending. For the GB coal the value of unburned carbon in the flue ash lies between 0.3 and 2 % whereas for the MB coal the values range from 1.6 to 5.5 %. It is significant that the content of carbon in ash is nearly always less than 5 %, hence mostly below the respective limit set by the German government for using the ash by the concrete industry as additional material, i.e. in fact 5 %. The higher unburned carbon content for double air-staged flames is due to the totally longer residence of about 1.9 s in the first zone compared with the shorter residence time of about 1.4 s for the single air staged flames.

Effects of the Primary Air Ratio

The effect of the primary air ratio on NO_X emissions with respect to coal blendings was investigated for burner air-staging and in-furnace air-staging. The experiments with **burner air-staging** were carried out with the HVB-coal and LVB-coal EM for both the single coals and two kinds of blendings of it. The results in fig. 12 show mean values of input-output measurements with different secondary and tertiary air input velocities. Decreasing the primary air ratio from 1.2 to 0.6, the NO_X emissions can be reduced by about 50 % from 800 to 480 vpm for the HVB-coal. By increasing the proportion of low volatile coal up to 100 % LVB-coal, NO_X reduction by burner air-staging decreases to 10 %. The NO_X emissions from the two investigated coal blendings correspond to the product of the blend ratio and the NO_X emissions from the single coals. The test runs for **in-furnace air-staging** were carried out with the coals GB and MB, and the NO_X emission behaviour is reported in fig. 13. It can be seen that by decreasing the primary air ratio from about 1.2 to 0.6, the NO_X emission of the coals GB and MB and blendings of both can be reduced from 940 vpm (GB) and 700 vpm (MB) down to about 270-290 vpm for all coals. However, the results reveal different NO_X emission behaviours depending on the primary air ratio. In the case of unstaged combustion conditions λ_{Pri} = 1.15-1.25, the NO_X emissions of the coal GB is the highest one and for the coal MB the lowest one whereas the emissions of the three blendings is nearly between the minimum and the maximum value of the single coals. In the region of stoichiometric combustion (λ_{Pri} = 1.0) the NO_X emissions of the coal blendings are higher compared with the emissions of the single coals.

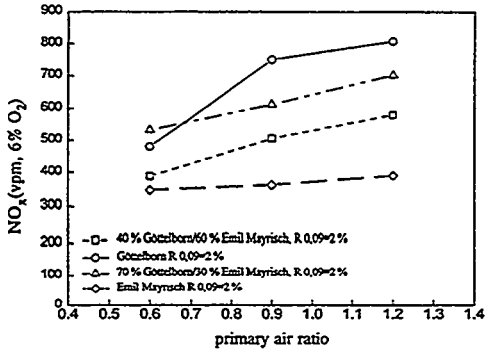

Fig. 12: Effect of primary air ratio on coal blendings for burner air-staging

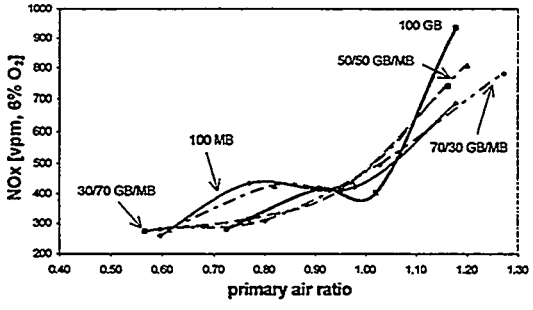

Fig. 13: Effect of primary air ratio on NO_X emission for a HVB-coal, MVB-coal and their blendings

furnace air-staging tests. The comparable combustion conditions with respect to primary air ratios of $\lambda_{Pri} > 1.0$ are demonstrated by the similar NO_X emission behaviour in both air staging concepts. Lower NO_X emissions of coal blendings than the ones of the original single coals are reported with respect to primary air ratios of $\lambda_{Pri} < 1$. This behaviour can be caused by in-flame reburning effects based on different ignition and devolatilization behaviours of both coals. The possibility to achieve lower NO_X emissions with coal blendings rather than with the original coals is also reported by Rozendaal et al. /4/.

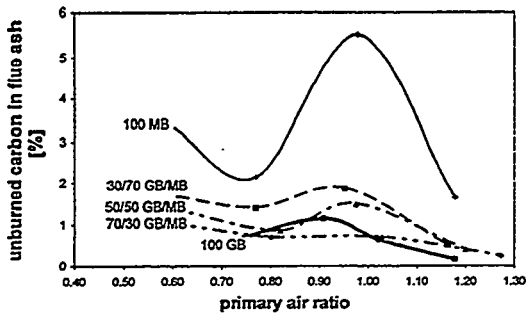

Fig. 14: Effect of primary air ratio on unburned carbon in flue ash for a HVB-/ MVB-coal and their blendings

The effect of the primary air ratio on the unburned carbon in the flue ash for the different tested coals is plotted in fig. 14. The results show a increasing of the unburned carbon in the flue ash with decreasing the primary air ratio from $\lambda_{pri} = 1.2$ up to 0.6 because the amount of unburned coal and coke particles in the primary combustion zone will increase and these particles must be oxidized after the burnout air injection.

Conclusions

1. **Coal Analysis.** The analysis data in some cases showed great differences in behaviour with regard to world trade coals from Europe, North America, Australia, Asia, and South Africa. As for the fuel sulphur, coals from the northern hemisphere may have higher contents than coals from e.g. Australia and South Africa. Using low sulphur coals, by the way, reduces the SO_X emissions of power plants. The data of the maceral inertinite show high amounts up to 70 % for coals from Asia, Australia, and South Africa. So, taking the inertinite as reference for the ignition behaviour of coals, it can be seen that the use of such coals is likely to rise ignition and burnout problems. The results for the ash content show higher values for coals from South Africa and Asia. Hence, it is very important to design the ash handling system according to this higher ash content and to be prepared for fouling and slagging problems in boilers.

2. **Coal-PSD and Blending Technique.** The results show that the blending technique of the coal can have an influence on the achievable coal fineness. This influence is strongly related to the used coals. In most cases the raw coal blending will be the preferable technique in that a finer coal psd for the same milling parameter can be obtained. With a raw coal blending lower NO_X emissions and an improved performance with respect to the unburned carbon content can be achieved.

3. **Primary Air Ratio for Burner and In-Furnace Air-Staging.** The NO_X emission of the blendings can be either lower or higher than, or between the emission levels of the single coals. With burner air-staging lower NO_X emissions could not be achieved. With in-furnace

air- staging, the NO_X emission of the blendings were between the levels of the single coals in the case of unstaged combustion, for stoichiometric combustion the emissions came higher, and for primary air ratios from 0.6 to 1.0 the emissions stayed lower or between the ones of single coals.

4. Blending Ratio, Unstaged, Single and Double In-Furnace Air-Staged Combustion

For the unstaged combustion the coal MB has lower NO_X emissions of about 250 vpm probably caused by the different ignition and devolatilization behaviour forming local NO_X reduction zones and a more homogeneous temperature distribution in the flame. By in-furnace air-staging up to primary air ratios of 0.6 and a residence time of about 1.4 s NO_X emissions of 290 vpm were achievable independently of the blend ratio. Increasing the residence time up to about 1.9 s and using the double air-staging technique, lowest NO_X emissions of about 100 vpm could be measured. Under improved combustion conditions emissions lower than the German limit of about 100 vpm are expected using primary NO_X reduction technologies.

References

/1/ Ewers, J.; Joppich, H.; Oberthür, C.; Schiffer, H.-W.: Welthandel mit Steinkohle. Rheinbraun AG, 1994

/2/ Käss, M.: Experimentelle Untersuchungen von Stickoxidemissionen und Ausbrand an einer Versuchsanlage zur Kohlenstaubverbrennung. VDI-Fortschrittberichte Nr. 261, Reihe 6: Energieerzeugung, 1991

/3/ Maier, H.; Nakamura, T.; Morgan, D.J.; Smart, J.P.: Experimentelle Untersuchungen zum Einfluß der Brennstoffausmahlung auf die Bildung von Stickoxiden bei der Kohlenstaubverbrennung. VGB-Technisch-wissenschaftliche Berichte Nr. 203, 1993

/4/ Rozendaal, C.M.; Gast, C.H.; Vliet, H.N.; Hein, K.R.G.: "Kohlenstaubaufbereitung: ein Beitrag zur NO_X-Minderung". Paper to the 8th. DVV-Kolloquium, Essen 1992

A COMPARISON BETWEEN FIRING COAL-WATER SLURRY FUEL AND DRY, MICRONIZED COAL IN AN OIL-DESIGNED INDUSTRIAL WATERTUBE BOILER

Bruce G. Miller, David A. Bartley, Roger L. Poe, and Alan W. Scaroni
Energy and Fuels Research Center
The Pennsylvania State University
C211 Coal Utilization Laboratory
University Park, Pennsylvania 16802

INTRODUCTION

Penn State's Energy and Fuels Research Center is conducting proof of concept demonstrations of firing coal-water slurry fuel (CWSF) and dry, micronized coal in an oil-designed industrial watertube boiler. The objective of the program is to establish the technical and economic viability of firing coal-based fuels in package watertube boilers designed for fuel oil. Technical aspects of the demonstrations are addressed in this paper, including: evaluating systems for coal storage (hoppers for micronized coal; tanks for CWSF) and handling (conveyors, screw feeders, and pneumatic transport for micronized coal; pumps and piping for CWSF) and their integration with the burner; determining coal combustion and boiler performance; determining rates of ash deposition and erosion; monitoring emissions; and quantifying the level of boiler derating.

BOILER SYSTEM

The demonstrations are being conducted in a package watertube boiler manufactured by Tampella Power Corporation, that is of D-type design, is rated for 14,900 lb/h saturated steam (at 300 psig), and is integrated into the University's steam distribution system. The boiler was designed to fire fuel oil but the overall system has been modified to fire coal-based fuels. Figures 1 and 2 are schematic diagrams of the system showing the components and configurations firing CWSF and dry, micronized coal, respectively. Modifications were made to the original system to provide combustion air and CWSF preheating, fly ash removal from the flue gas using a baghouse, coal unloading, storage, and crushing, and either CWSF preparation (not shown in Figure 1) or dry coal micronization. The combustion chamber and convective pass have not been modified. The furnace is approximately 8 ft long by 6 ft wide, with a volume of 370 ft^3. The bulk gas residence time in the furnace is less than one second. Discussions of the equipment and program history can be found elsewhere (Miller and Scaroni, 1990; Miller and Scaroni, 1993a,b; Jennings et al., 1994).

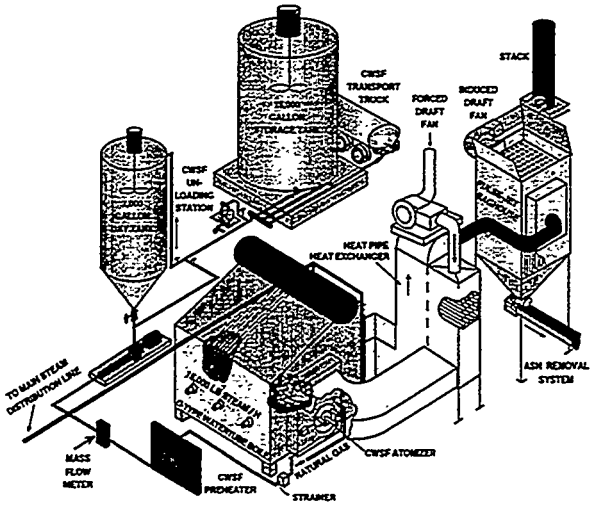

Figure 1. CWSF-FIRED BOILER SYSTEM

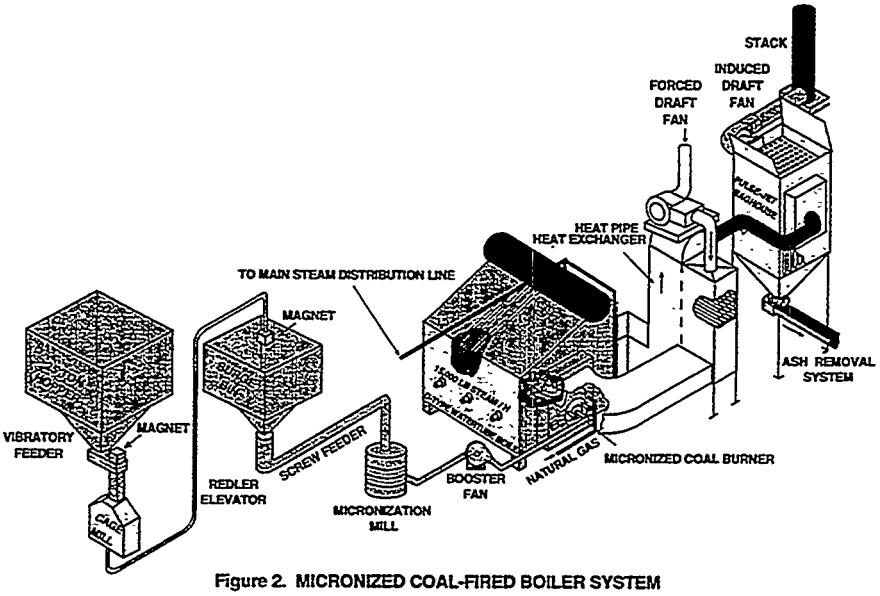

Figure 2. MICRONIZED COAL-FIRED BOILER SYSTEM

CWSF AND DRY, MICRONIZED COAL FIRING

Completed Research and Development Activities

The installation of the boiler system shown in Figure 1 was completed in 1991. This configuration was used to fire CWSF from October 1991 to December 1992. For this testing, CWSF was produced off-site and transported to Penn State. The initial CWSF testing was conducted using the fuel oil atomizer/burner system that was provided with the boiler. Because the boiler/burner system was to be used with CWSF, the only guarantee provided by the manufacturer was that the burner would have 4:1 turndown. Figure 3 is a schematic diagram of the atomizer, burner, and boiler windbox.

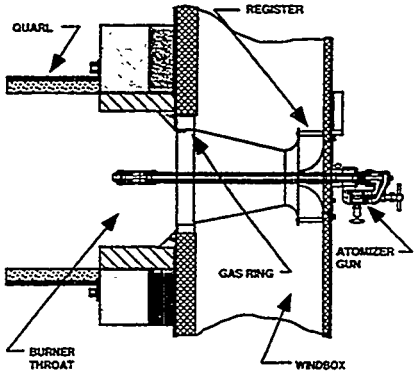

Figure 3. SCHEMATIC DIAGRAM OF THE WINDBOX, HEAVY OIL ATOMIZER, AND QUARL (Not to Scale)

A facility to produce micronized coal and house a CWSF-preparation circuit was constructed from November 1992 to June 1993. The facility and the dry, micronized coal circuit were completed in June 1993. The micronization mill (TCS, Inc.) was integrated into the firing system. The fuel oil burner was replaced with a High Efficiency Advanced Coal Combustor (HEACC, ABB Combustion Engineering Systems, Inc.) in July 1993 (Jennings et al., 1994). Burner performance goals included NO_x emissions of less than 0.6 lb/million Btu (450 ppm) @ 3%O_2 and combustion efficiency >98%. Burner testing was conducted from July 1993 to May 1994. A schematic diagram of the HEACC is given in Figure 4.

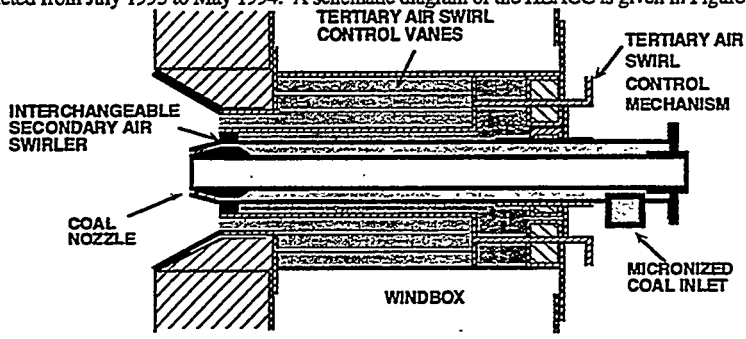

Figure 4. SCHEMATIC DIAGRAM OF THE HEACC (Not to Scale)

In May 1994, a Low-NO_x multifuel burner (Engineering and Environmental Research Corporation (EER)) that was designed to fire either CWSF or dry micronized coal was installed (Morrison, et al., 1994). The expected burner performance was: high carbon conversion; >3:1 turndown; <30% excess air; combustion air preheat temperature of <400°F; burner pressure drop of less than 8" water column; and capable of using air or steam as the atomizing medium (when firing CWSF). Figure 5 is a schematic diagram of the burner. Initial testing of the burner was with micronized coal from May through December, 1994.

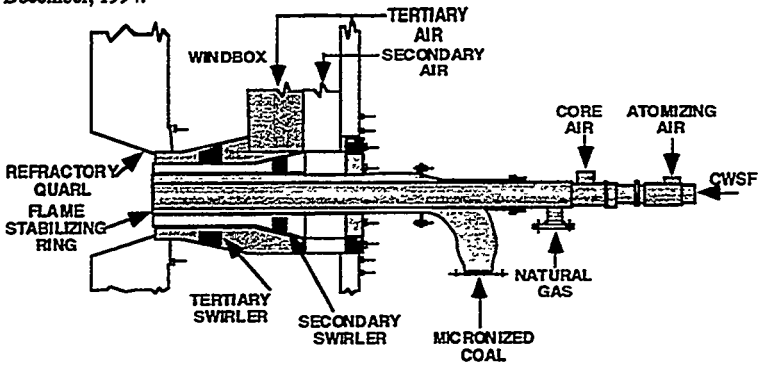

Figure 5. EER BURNER SECTIONAL VIEW (Not to Scale)

Current Research and Development Activities

Construction of the CWSF preparation circuit occurred from May 1994 to January 1995. Shakedown of the circuit and preliminary CWSF production and combustion testing using the EER burner began in January 1995 and testing will be completed in April 1995.

As a consequence of the micronized coal testing (summarized below) using the HEACC and EER burner, the dry coal handling system and soot blowing capabilities of the boiler will be modified during

April and May, 1995. After the modifications, additional micronized coal and CWSF testing will be conducted using the HEACC and EER burner.

TECHNICAL COMPARISON BETWEEN CWSF AND MICRONIZED COAL

A comparison, based on Penn State's experience, between firing CWSF and dry micronized coal in a fuel-oil designed industrial boiler is given in this section. The comparison includes integration of the fuel storage and handling systems with the burners, coal combustion and boiler efficiencies, the occurrence of deposition/erosion, emissions levels, and boiler derating.

Fuel Storage and Handling

Problems had to be overcome with both CWSF and dry micronized coal handling and transport. This section describes the problems encountered and the solutions to them, and recommendations for proper fuel storage and handling (Morrison et al., 1993).

CWSF Transport, Storage, and Handling

The initial test program used CWSF that was produced off-site and transported approximately 80 miles to Penn State. Properly formulated and prepared CWSFs were successfully transported in non-modified, readily-available tankers. The transport tankers used by Penn State were 5,600 gallon, single cavity, insulated, rear discharge, stainless-steel tankers. With each shipment, a small amount of sedimentation remained after the CWSF was transferred to the 15,000-gallon storage tank. The sedimentation was rinsed into the storage tank.

The formation of hardpack affects all aspects of CWSF handling. Difficulties in handling were experienced when off-specification (high dispersant concentration) CWSF was received. These included blockage of the tanker discharge valve, blockage of in-line strainers, and build-up of hardpack on the bottom of the tankers. Hardpack that formed in the storage tank and tanker bottoms had to be physically removed. After reformulating the CWSF, which included reducing the amount of A-23M used as a dispersant (from 1.0 to 0.7 wt.%), modifying the particle size distribution (reducing the mean particle size from 20 to 17 μm and increasing the fines concentration), and adding ammonium hydroxide as a pH modifier (to increase the pH from ~7.0 to ~9.0), hardpack formation was minimized.

Handling the CWSF in cold weather presented problems, which included partial freezing of the CWSF within the tanker discharge valve, and freezing of the exhaust manifold on a compressed air driven diaphragm pump used to transfer CWSF from the incoming tankers into the storage tanks. CWSF transfer lines were insulated and wrapped with heat tape to prevent freezing. The pumping station was enclosed and heated to prevent the pump, lines, and exhaust manifold from freezing.

The CWSF storage tanks were equipped with top-mounted agitators. The mixers are low-speed (low shear), extend to within 5 feet of the tank bottom, and have impellers that are of high-flow design. An air sparge system was installed in the 15,000-gallon storage tank but was found to be ineffective in re-entraining sedimentation. Compressed air inlets were placed prior to the tank outlet valves to re-entrain sediment in the event of valve blockage. The 15,000-gallon storage tank was insulated and heated to prevent CWSF freezing.

Recommendations for proper CWSF handling include minimizing the number of piping turns and vertical legs, installing drain valves on vertical legs, minimizing the number of flow obstructions in the piping (fittings, valves, etc.), using stainless-steel valves to combat erosion, having manual override capabilities on pneumatic valves, having water (preferably hot) purge capabilities, using ground-faulted interrupters (for personnel safety), insulating and heat tracing exposed piping, using strainers with two baskets (for on-line cleaning), using bladder-type gauges, and using high-pressure alarms or torque limiters.

Micronized Coal Handling, Pulverizing, and Transport to the Burner

One objective of the micronized coal testing was to determine the operating characteristics of a complete, integrated firing system (Jennings et al., 1994). Although all of the system components (e.g., coal hoppers, crushers, conveyers, and mill) have been used commercially, an integrated system from coal preparation to steam production has not been proven at this scale. Testing to date has established that the coal handling and transport systems require careful engineering.

Coal handling problems were encountered due to the high moisture content and small particle size of the coal delivered to the main coal hopper. Because of the relatively small quantities of low ash coal required, the coals were cleaned in a batch mode by heavy media cyclones and stored in a local coal yard. During testing in winter, snow and ice were included in the shipments. The wet coal (often with moisture content in excess of 12%) tended to bridge in the main hopper and this required manual intervention. Wet coal which clogged the cage mill (crusher) had to be extracted manually. The Redler conveyor was prone to binding and, at one point, broke when feeding wet coal. An amperage overload breaker was installed

to shut down the system when necessary so that an operator can correct the problem. With drier coal, the feed system operation is acceptable.

Bridging and ratholing of the coal in the surge bin also required constant operator attention and corrective action. Initially, coal was removed manually from the sides of the hopper and the bridge broken. Air sparge ports were installed on the sides of the hopper to reduce manual work. The sparges helped greatly, but bridging and ratholing occasionally occurred with both wet and dry coals. The sparges needed periodic monitoring because they are susceptible to wear and blow-out. The sparge air created a positive pressure in the Redler conveyor causing the dust seals to fail. A filtering system was installed in the man-hole on top of the surge bin to relieve the excess pressure and capture fine coal.

Ratholing and bridging resulted in erratic coal feed. Consequently, constant supervision was required. This inconsistent coal feed, coupled with the variability introduced by varying coal size and moisture content, made it difficult to maintain a constant feed to the burner. The moisture content was inconsistent because of drying in the heated building and by the air sparge system in the surge bin.

The boiler/burner is very sensitive to fuel/air input conditions. Fuel feed oscillations, fuel transport air pressure swings, and coal maldistribution in a single burner application are not as forgiving as in a multiburner configuration. Each of these creates instability problems in the boiler.

The operating problems encountered due to high moisture content of the fine coal and fuel transport oscillations are being addressed. The moisture content of the coal is being limited by storing it in a protected environment after cleaning. Since most of the coal feed problems occurred in the surge bin, a pyramidal bin with a length to width discharge outlet of 3:1 and a steeper angle (70 vs 60°) was designed and will be installed in April/May, 1995. In addition, the screw feeder will be replaced with a weigh-belt feeder to eliminate fuel feed oscillations. The new surge bin will be constructed out of stainless steel to eliminate scaling.

Care must be exercised in design and operation to prevent foreign material reaching the TCS mill. The mill, which is of a hammer-type design, has ceramic components which are costly to repair and replace.

Combustion Performance

CWSF Combustion (October 1991 - December 1992)

CWSFs (see Table 1 for the analysis of the coals tested in the boiler) made from coals with ash contents of less than 4.4 wt.% and sulfur contents less than 1 wt.% (on a dry basis) were fired from October 1991 to December 1992 to characterize the boiler and optimize the combustion performance. Initially, tests were performed without boiler modifications but subsequent minor, low cost modifications were made in an attempt to achieve acceptable coal combustion efficiencies. A parametric study was conducted to determine the effect of solids concentration, CWSF preheat temperature, atomization medium and pressure, CWSF spray angle, atomizer type, and minor burner modifications on combustion performance (Pisupati et al., 1993).

The initial study indicated that CWSF could not be burned in the fuel oil-designed package boiler, using the fuel oil burner provided with the boiler, without using natural gas as a support fuel. However, by optimizing the operating parameters, and making minor boiler modifications (e.g., adding a quarl in the furnace (see Figure 3) and enlarging the burner throat to reduce the combustion air velocity), the coal combustion efficiency was increased from 82 to 95% (with 15% natural gas support). The boiler efficiencies ranged from 70 to 80%. The reason for not achieving coal combustion efficiencies higher than 95% was believed to be the inability of the burner to create an effective internal recirculation zone. One goal of the program was to achieve fuel firing rates of 100% CWSF, 100% natural gas, or any combination of the two. In order to achieve this goal with the targeted coal combustion efficiency (>98%), the need for major burner modifications was identified. Therefore, a burner which has air staging capabilities was installed prior to the most recent CWSF testing.

Micronized Coal Combustion (June 1993 - December 1994)

Micronized coal testing has been conducted using the HEACC and the EER burner. The HEACC was tested over a variety of firing rates, excess air levels, combustion air damper settings, burner gun configurations, and burner swirl levels. In addition, two coals and two furnace geometries were tested. The results from the first round of testing with the HEACC have been used as the basis for modifying the burner in order to optimize combustion efficiency and NO_x emissions during additional testing to be conducted from July 1995 to November 1995.

Steady-state operation was achieved when burning 100% coal with the HEACC. All testing was conducted over one or two shifts per day. The combustion and boiler efficiencies (which are averaged each test over half hour periods), after burner optimization, ranged from 90 to 95% and from 80 to 84%, respectively, for both a Brookville seam (Pennsylvania) and a Kentucky coal. The installation of a

ceramic tunnel at the exit of the furnace to alter the gas patterns and temperature profiles in the boiler had a minor positive effect on combustion efficiency. Although combustion efficiencies of ~95% were achieved, this was below the target value of 98%. Consequently, burner modifications are planned for the next series of tests using the HEACC.

The EER burner was tested over a variety of firing rates, excess air levels, tertiary air-to-secondary air ratios, and test durations when firing dry, micronized coal. Steady-state operation was achieved with the EER burner when firing 100% coal. The majority of the testing was conducted over one or two shifts per day (6-12 hours of steady-state operation) with two tests conducted on a continuous (24 hour per day) basis. The testing was conducted using Brookville seam and Upper Freeport (Pennsylvania) coals. The combustion and boiler efficiencies ranged from 90 to 95% and from 80 to 84%, respectively, when operating over one or two shifts per day. The combustion and boiler efficiencies during the continuous testing averaged 92 and 80%, respectively, when firing at 15 million Btu/h (MM Btu/h), and 93 and 82%, respectively, when firing at 12 MM Btu/h. The results from the initial period of testing have led to some minor burner modifications which will be implemented during a second series of tests to be conducted from June 1996 to December 1996.

The maximum coal combustion efficiency (~95%) that was achieved when firing both the Brookville seam and Kentucky coals in the HEACC and the Brookville seam and Upper Freeport coals in the EER burner, is the same as that observed when cofiring the Brookville seam coal as a CWSF. Consequently, the reactivities of the Brookville seam and Kentucky coals are being determined and furnace modeling is being performed to determine if the combustion efficiency obtained is the maximum achievable for these coal reactivities, operating conditions, and furnace geometries.

Table 1. Analysis of Coals Fired in the Boiler as CWSF and Dry, Micronized Coal

Coal:	Brookville Seam[a]	Brookville Seam[b]	Kentucky[c]	Upper Freeport Seam[d]
Proximate Analysis (wt.%, dry):				
Volatile Matter	34.7 - 35.9	35.5	35.7	31.8
Ash	3.4 - 4.3	3.4	4.9	6.7
Fixed Carbon	60.5 - 61.1	61.1	59.4	61.5
(Moisture)	50.0 - 64.4	5.2	6.8	4.4
Ultimate Analysis (wt.%, dry):				
Carbon	78.5 - 83.1	79.9	77.9	79.5
Hydrogen	4.8 - 5.5	5.3	5.3	5.1
Nitrogen	1.5 - 1.6	1.6	1.5	1.5
Sulfur	0.7 - 0.9	0.7	0.8	0.4
Oxygen	7.3 - 11.1	9.6	9.6	6.8
Heating Value (Btu/lb, dry):	13,850 - 14,260	14,390	14,030	13,909
Ash Fusion Temperatures (°F, reducing)				
Initial Deform.	>3,000	2,820	2,803	N.D.[e]
Softening	>3,000	>3,000	>3,000	N.D.
Hemispherical	>3,000	>3,000	>3,000	N.D.
Fluid	>3,000	>3,000	>3,000	N.D.

[a]CWSF; range of analyses conducted on samples collected during testing performed from October 1991 to November 1992

[b]Micronized coal; April 25-29, 1994 composite

[c]Micronized coal; April 11-19, 1994 composite

[d]Micronized coal; November 21-22, 1994 composite

[e]Not determined

Deposition

CWSF Combustion

A probe was constructed and inserted into the demonstration boiler in June 1992 to obtain long-term information on convective pass deposition. Figure 6 shows the location of the probe. Probe details can be found elsewhere (Miller et al., 1993c).

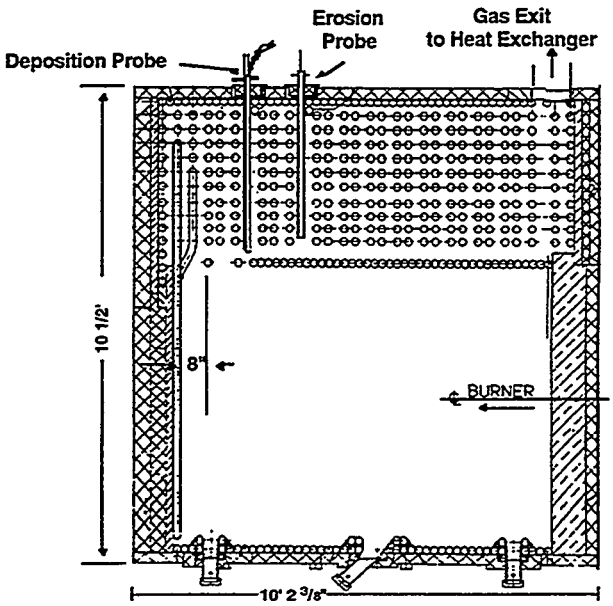

Figure 6. PLAN VIEW OF THE BOILER DEPICTING SIDEWALL PENETRATIONS INTO THE RADIANT AND CONVECTIVE SECTIONS

The probe was in place for approximately 126 hours of operation (June 1992 through August 1992) without the formation of any sintered ash deposits. A thin ash and carbon coating was collected on the probe as a result of the low combustion efficiency (84-93%) obtained during the testing, the low ash content of the CWSF, and the high fusion temperatures of the ash (initial deformation temperature >3,000°F).

Another measure of deposition in the boiler is the required frequency of sootblowing in the convective pass to maintain a boiler outlet temperature below 600°F. Sootblowing was not necessary during the test periods of 4 to 10 hours in duration. In most cases, boiler outlet temperatures were 550 to 575°F. When the convective pass was sootblown, there was no noticeable effect on the boiler outlet temperature.

There was also little buildup of ash on the boiler walls and floor. This is in contrast to what was encountered when firing the same coal in dry, micronized form, as discussed below.

Micronized Coal Combustion

Deposition was experienced when firing micronized coal with the HEACC and EER burner. The extent of deposition was dependent on the coal type and test mode (cyclic or continuous operation). Figure 7 is a typical plot of the boiler outlet temperature history for a day of operation. (Similar data for a CWSF test is included for comparison.) When the boiler outlet temperature approached 600°F, the convective section was sootblown.

The testing of the HEACC firing the Brookville seam and Kentucky coals was for two-shifts/day. During operation, ash accumulated on the furnace floor until the boiler was shutdown and cleaned out. The ash composition and fusion temperatures were similar for both coals but they behaved differently. Less accumulation was noted with the Brookville seam coal than with the Kentucky coal; however, accumulation was a concern and a system was installed on the furnace floor to re-entrain the accumulated ash. This system was successfully utilized when testing the EER burner.

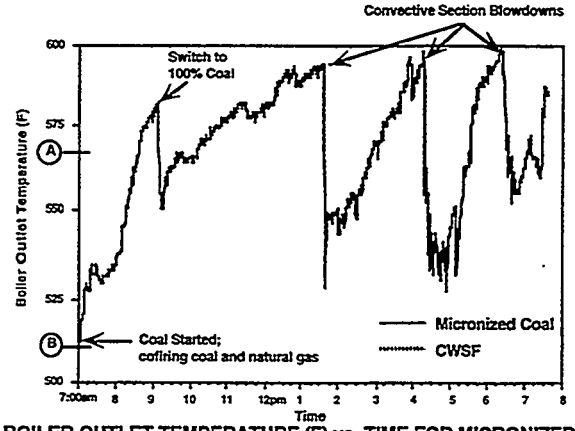

Figure 7. BOILER OUTLET TEMPERATURE (F) vs. TIME FOR MICRONIZED COAL (15 MILLION BTU/H) AND CWSF (18.5 MILLION BTU/H WITH 26% NATURAL GAS SUPPORT) TESTING

(A)- Average Boiler Outlet Temperature When Firing Natural Gas at 18.5 Million Btu/h

(B)- Average Boiler Outlet Temperature When Firing Natural Gas at 13.0 Million Btu/h

The demonstration boiler was operated on a 2-shift/day and a continuous (24 hour) basis during November and December, 1994 to evaluate the effect of ash deposition on boiler performance during long-term operation. The boiler was also operated at firing rates of 15 and 12 MM Btu/h.

No operational problems were encountered when operating the boiler on a two-shift per day basis. There was no significant deposition on the boiler walls or accumulation at the convective pass entrance, and the floor blast system entrained the majority of the ash (after a steady-state layer was deposited) that accumulated on the floor. It appears that the ash that deposited on the walls sloughed off due to the cyclic nature of the operation. Conversely, the tests conducted when operating on a continuous basis were terminated when significant accumulation occurred at the entrance to the convective pass (when firing at 15 MM Btu/h) and when refractory failure around a sight port on the side wall occurred (when firing at 12 MM Btu/h).

Table 2 summarizes the results of the two continuous tests conducted at the two firing rates. The boiler shutdown on November 22, 1994 was the first due to ash accumulation at the entrance into the convective pass. The shutdown on December 7, 1994 occurred when the sidewall (metal) warped allowing burning between the refractory rear wall and the insulation/metal skin interface.

As a consequence of the excessive ash accumulation at the convective pass entrance during continuous testing, a sootblower is being designed for this region. It will be directed towards the convective pass entrance.

Erosion

One objective of the initial CWSF testing was to determine the effect of coal ash on convective pass erosion and, ultimately, determine the maximum flue gas velocity before erosion became a concern. Erosion of carbon steel by fly ash was studied in the convective section using a specially designed probe. Details of the probe and its operation can be found elsewhere (Walsh et al., 1992; Walsh et al., 1994).

An erosion-corrosion model was developed from the experimental measurements. Calculated results indicate that the CWSF can be fired in an oil-designed boiler without incurring significant erosion damage, if the flue gas velocity in the convective section is below a critical value and the particle stream is uniform. This is illustrated in Figure 8, which shows the transition from slower oxide erosion to a combination of oxide/metal erosion (for a particle size of 87 μm and particle concentration of 2.7 g/m^3) at approximately 36 ft/s (~12 m/s). This is in excess of the convective pass velocity (when firing CWSF and natural gas at a rate of 18.6 MM Btu/h) of 12.8 ft/s (~4.2 m/s) in the demonstration boiler. Note that the erosion rate limit of 50nm/h occurs in the transition region from oxide erosion to metal erosion.

Table 2. Deposition Summary -- Two Continuous Tests

15 Million Btu/h -- 11/21 to 11/22/94	12 Million Btu/h --12/05 to 12/07/94
• 37,945 lb of coal were consumed at a rate of 1,148 lb/h for 33 h of operation.	• 53,476 lb of coal were consumed at a rate of 904 lb/h for 59 h of operation.
• The boiler outlet pressure (B.O.P.) gauge went off scale(<-2.0" W.C.) after consuming 33,927 lb of coal.	• The B.O.P. gauge went off scale after consuming 43,080 lb of coal.
• The B.O.P. started at -0.8" W.C. and began decreasing at 24,000 lb of coal consumed. There was 10,000 lb of coal consumed between the time the B.O.P. started to decrease and when the pressure went off scale. This is equivalent to 8.7 hours of operation.	• The B.O.P. started at -0.8" W.C. and began decreasing at 35,000 lb of coal consumed. There was 8,000 lb of coal consumed between the time the B.O.P. started to decrease and when the pressure went off scale. This is equivalent to 8.9 hours of operation.
• The sootblowing frequency was typically every half hour and increased to 1.5 and then 2.0 h before boiler shutdown.	• After the B.O.P. went off scale, the soot blowing frequency increased to 2.0, 2.75 2.5, and 2.0 h before the forced shutdown.
• The ID fan amperage exhibited a decrease from ~31.5 amps to 30.0 amps after consuming ~1,000 lb of coal. The amperage then slowly increased to ~32.5 over the consumption of ~27,000 lb of coal.	• The ID fan amperage was less than that observed during the 15 million Btu/h tests because of the lower volume of flue gas and was ~28 amps as compared to 30 to 32.5 amps. The amperage was relatively constant at ~28.5 with an increase to ~29.5 at the time of shut down.
• The convective pass temperature decreased from ~1,300 to 1,000°F while the B.O.P. was decreasing.	• No temperature data were collected.
• Steam production rate increased as the test progressed.	• Steam production rate remained relatively constant during the test.

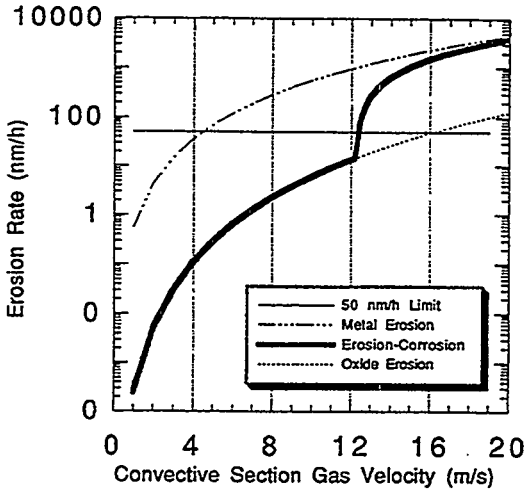

Figure 8. EROSION RATE PREDICTION FOR CWSF COMBUSTION FOR TYPICAL CONVECTIVE SECTION CONDITIONS (particle concentration 2.7 g/m^3, particle size 87 μm, particle density 1,250 kg/m^3, 30° impaction angle, 50% of the particles colliding, and 600 K metal temperature)

Emissions

CWSF Combustion

When firing CWSF, average steady-state SO_2 emissions ranged from 0.6 to 1.0 lb/MM Btu. NO_x emissions ranged from 0.7 to 1.4 lb/MM Btu and the emissions increased during the optimization program as the combustion efficiency increased. Increases in the boiler outlet temperature also accompanied increases in the combustion efficiency. Carbon monoxide emissions varied from 0.10 to 0.22 lb/MM Btu.

Micronized Coal Combustion

When firing micronized coal, SO_2 emissions ranged from 0.7 to 1.3 and from 0.6 to 1.2 lb/MM Btu during the HEACC and EER burner test programs, respectively. The NO_x emissions ranged from 0.5 to 0.9 and from 0.5 to 1.3 lb/MM Btu during the HEACC and EER burner test programs, respectively. The NO_x emissions were lower when firing micronized coal than when firing CWSF, due to the air-staging aspects of the HEACC and EER burner and the lower firing rates. Firing rates when cofiring CWSF and natural gas (15% support) were typically 18-20 MM Btu/h while firing rates for dry, micronized coal varied from 13-18 MM Btu/h.

The carbon monoxide emissions varied considerably during the micronized coal tests. This was a function of variable coal feed, maldistribution of the coal feed, and burner operation. The CO emissions ranged from 0.4 to 1.3 and from 0.3 to 3.0 lb/MM Btu (corresponding to approximately 190, 650, 120, and 1,450 ppm CO) during the HEACC and EER burner test programs, respectively. However, very high CO emissions (sometimes >4,000 ppm) were observed when coal feed variability and maldistribution were encountered (HEACC and EER burner), and during the natural gas/coal cofiring period when transiting to 100% coal firing (EER burner).

Boiler Derating

CWSF Combustion

The rated capacity of a DS-15 package boiler is 15,000 lb saturated steam/h at 300 psig; however, the design capacity was decreased to 14,900 lb steam/h (at a natural gas firing rate of ~19.8 MM Btu/h)

when two rows of tubes were removed from the convective pass (see Figure 6) to accommodate test probes. Natural gas testing conducted in January 1992 resulted in 14,700 lb steam/h produced when firing at 18.5 MM Btu/h.

Steam production during the CWSF test program ranged from ~9,600 to 15,000 lb/h while cofiring CWSF and natural gas at firing rates from 15.0 to 19.5 MM Btu/h, and no definite trends were evident when comparing steam production with boiler firing rate, CWSF solids content, CWSF firing rate, coal combustion efficiency, or level of natural gas support. The mean steam production when firing CWSF was 12,185 lb/h or ~83% of design capacity, the standard deviation was 1,747 lb steam/h, and the median steam production was 12,239 lb/h. This represents a boiler derating of 17%. Boiler derating was approximately 16 and 14% for tests conducted with firing rates of 18 to 19 MM Btu/h and greater than 19 MM Btu/h, respectively.

Micronized Coal Combustion

Steam production during the micronized coal test program using the HEACC ranged from ~11,800 to 15,600 lb/h at firing rates from 15.0 to 18.0 MM Btu/h, with most of the firing rates ranging from 15.0 to 15.5 MM Btu/h. The mean steam production was 13,262 lb/h or 90% of design capacity and the standard deviation was 1,209 lb steam/h. This represents a boiler derating of 10%.

Likewise, steam production during the micronized coal test program using the EER burner ranged from ~9,700 to 15,500 lb/h at firing rates from 15.0 to 18.0 MM Btu/h with most of the firing rates ranging from 15.0 to 16.5 MM Btu/h. The mean steam production, for all tests in which the steam flow was measured, was 12,368 lb/h or 84% of design capacity and the standard deviation was 1,218 lb steam/h. This represents a boiler derating of 16%. The higher boiler derating with the EER burner is attributed to slightly lower combustion efficiencies, because the burner was not fully optimized. As previously mentioned, additional testing is planned with a slightly modified EER burner.

Summary

Special considerations are necessary when transporting, storing, and handling coal-based fuels that are being utilized in industrial boilers that have been designed for fuel oil. The challenge for handling CWSF is to maintain the coal in suspension and minimize flow perturbations. The challenge for dry, micronized coal is to maintain constant coal flow through the storage and pulverizing systems to the burner. This is especially crucial in a one-burner boiler system.

The maximum combustion efficiency achieved in the retrofitted industrial boiler, whether firing CWSF or micronized coal, was 95%. Burner modifications and computer modeling are in progress in an attempt to increase the combustion efficiency to the target value of 98%.

Erosion of the convective pass has not been significant. Likewise, deposition during cyclic testing has been manageable. However, firing micronized coal on a continuous basis (24 hours per day for several days) has resulted in significant ash accumulation at the entrance to the convective pass. Sootblower designs for keeping the convective pass entrance open are being reviewed.

Sulfur dioxide emissions were similar when firing CWSF and micronized coal. This is as expected since they are a function of the sulfur content in the coal and the combustion efficiency. Nitrogen oxides emissions were lower when firing dry, micronized coal than when firing CWSF because of the air-staging designs of the dry, micronized coal burners and the lower firing rates. NO_x emissions were 1.4 lb/MM Btu when cofiring CWSF and natural gas (15% support) at a total firing rate of 19.6 MMBtu/h with a coal combustion efficiency of 95%. Targeted NO_x emissions of <0.6 lb/MM Btu were achieved when firing dry, micronized coal at firing rates of 12-15 MMBtu/h and combustion efficiencies of 90-94%. At 95% combustion efficiency, NO_x emissions were 0.7 and 1.3 lb/MM Btu in the HEACC and EER burner at firing rates of 17.6 and 16.4 MM Btu/h, respectively. On average, the CO emissions were higher with micronized coal than with CWSF. This was the result of coal feed variability and unoptimized burners.

Derating of the boiler was observed when firing the coal-based fuels. Steam production was approximately 16% less than design capacity when cofiring natural gas and CWSF, and approximately 10 and 16% less when firing dry, micronized coal in the HEACC and EER burner, respectively.

ACKNOWLEDGMENTS

The authors acknowledge the support of the Commonwealth of Pennsylvania and the U.S. Department of Energy, Pittsburgh Energy Technology Center. Financial support for this work stems from Cooperative Agreements No. DE-FC22-89PC88697 and DE-FC22-92PC92162, and from Agreement No. DE-AC22-91PC91160. John Winslow and Douglas Gyorke (U.S. Department of Energy, Pittsburgh Energy Technology Center), Richard Borio and Mike Rini (Combustion Engineering Inc.), and the staff of the Energy and Fuels Research Center are acknowledged for their support of this work.

REFERENCES

Jennings, P.L., R.W. Borio, B.G. Miller, A.W. Scaroni, and J.G. McGowan, "Installation and Initial Testing of Micronized Coal in a Gas/Oil-Designed Package Boiler," *19th Intern. Conf. on Coal Util. and Fuel Systems*," Coal and Slurry Technology Association in Cooperation with the U.S. Department of Energy's Pittsburgh Energy Technology Center, p. 63 (March 22-24, 1994).

Miller, B.G., and A.W. Scaroni, "Superclean Coal-Water Slurry Combustion Testing in an Oil-Fired Boiler," *6th Annual Coal Prep., Util., and Environ. Control Cont. Conf.*, U.S. Department of Energy, Pittsburgh, Pennsylvania, p.81 (August 6-9, 1990).

Miller, B.G., and A.W. Scaroni, "Superclean Coal-Water Slurry Combustion Testing in an Oil-Fired Boiler," *9th Annual Coal Prep., Util., and Environ. Control Cont. Conf.*, U.S. Department of Energy, Pittsburgh, Pennsylvania, p. 120 (July 19-22, 1993a).

Miller, B.G., and A.W. Scaroni, "Development of Coal-Based Technologies for Department of Defense Facilities," *9th Annual Coal Prep., Util., and Environ. Control Cont. Conf.*, U.S. Department of Energy, Pittsburgh, Pennsylvania, p. 564 (July 19-22, 1993b).

Miller, B.G., S.V. Pisupati, R.L. Poe, J.L. Morrison, J. Xie, P.M. Walsh, R.T. Wincek, D.A. Clark, and A.W. Scaroni, "Superclean Coal-Water Slurry Combustion Testing in an Oil-Designed Boiler," Semiannual Technical Progress Report for the Period 08/15/1992 to 02/15/1993, U.S. Department of Energy, Pittsburgh Energy Technology Center, Pittsburgh, Pennsylvania, DE-FC22-89PC88697 (March 12, 1993c).

Morrison, D.K., R.L. Frato, T.M. Sommer, B.G. Miller, and A.W. Scaroni, "System Design to Convert a Package Boiler to Fire Coal-Based Fuels, "*19th Intern. Conf. on Coal Util. and Fuel Systems*," Coal and Slurry Technology Association in Cooperation with the U.S. Department of Energy's Pittsburgh Energy Technology Center, p. 51 (March 22-24, 1994).

Morrison, J.L., B.G. Miller, and A.W. Scaroni, "Preparing and Handling Coal-Water Slurry Fuels: Potential Problems and Solutions," *18th Intern. Conf. on Coal Util. and Fuel Systems,* " Coal and Slurry Technology Association in Cooperation with the U.S. Department of Energy's Pittsburgh Energy Technology Center, p. 361 (April 26-29, 1993).

Pisupati, S.V., S.A. Britton, B.G. Miller, and A.W. Scaroni, "Combustion Performance of Coal-Water Slurry Fuel in an Off-The-Shelf 15,000 lb Steam/h Fuel Oil-Designed Industrial Boiler," *18th Intern. Conf. on Coal Util. and Fuel Systems,* " Coal and Slurry Technology Association in Cooperation with the U.S. Department of Energy's Pittsburgh Energy Technology Center, p. 349 (April 26-29, 1993).

Walsh, P.M., J. Xie, J.T. Elston, B.G. Miller, and A.W. Scaroni, "Erosion of Carbon Steel and Deposition of Particles Under the Influence of a High Velocity Jet Containing Fly Ash From Coal-Water Slurry Combustion," *17th Intern. Conf. on Coal and Slurry Tech.*, Coal and Slurry Technology Association in Cooperation with the U.S. Department of Energy's Pittsburgh Energy Technology Center, p. 561 (April 28-May 1, 1992).

Walsh, P.M., J. Xie, R.L. Poe, B.G. Miller, and A.W. Scaroni, "Erosion of Fly Ash and Deposition of Ash on Carbon Steel in the Convective Section of an Industrial Boiler," Corrosion, Vol. 50, No. 1, p. 82 (January, 1994).

ENHANCEMENT OF SULFUR DIOXIDE CAPTURE BY LIMESTONE SORBENTS IN THE PRESENCE OF AN ACOUSTIC FIELD

Rajesh Nair and Savas Yavuzkurt*
Center for Gas Turbines and Power
Department of Mechanical Engineering
The Pennsylvania State University, University Park, PA 16802

ABSTRACT

The effect of high intensity acoustic fields on sulfur capture during pulverized coal combustion is investigated. A two-dimensional, steady, axisymmetric code, PCGC-2 (Pulverized Coal Gasification and Combustion-2 Dimensional) developed over ten years at Brigham Young University, was used to simulate the combustion of pulverized coal. The effects of increased heat and mass transfer to a burning particle in the presence of an acoustic field were modeled by modifications made in the code which were obtained from previous studies. The code was also used to predict SO_2 levels in the furnace during combustion. A comprehensive single particle model to capture sulfur dioxide using limestone sorbent was developed. Following previous approaches, the particle was modeled as a sphere formed of overlapping grains. Calcination, sintering and sulfation processes occur simultaneously during sulfur capture by limestone. Thermal decomposition of calcium carbonate (calcination) is described by a shrinking core model for a spherical particle. Decomposition begins on the surface and proceeds inwardly in a symmetrical fashion, and the diameter of the unreacted core decreases. At the interface of the two phases, heat is absorbed and CO_2 diffuses out during reaction. The particle is assumed isothermal. Sintering which is melting and sticking of individual grains in the particle is modeled by moving the grain centers in the particle closer to each other, thereby decreasing the porosity and the specific surface area of the particle. The reduction in the porosity and specific surface area causes a decrease in the rate of sulfation. A rate equation is used to model the sintering phenomenon. Structural changes occurring in the particle during sulfation were of primary concern, since sulfation depends directly on sorbent structure. Processes controlling sulfation are external heat and mass transfer, pore diffusion, diffusion through the product layer ($CaSO_4$), sintering and calcination. However the principal forces governing the rate of SO_2 capture by the sorbent seem to be pore diffusion, product-layer diffusion and sintering. This model has been incorporated into the PCGC-2 combustion code, in order to test for influence of acoustic fields on the sulfur capture. A direct result of the inclusion of acoustics is the increase in the heat and mass transfer coefficients, and thereby an increase in the gas-phase (bulk) diffusion of sulfur dioxide into the particle. For larger particle sizes of the order of 100 μm, which is the range at which acoustic fields and pore diffusion show significant effects, it is shown that an increase in sulfur capture (~10-12%) results since pore diffusion includes contributions from both gas-phase diffusion and Knudsen diffusion.

NOMENCLATURE

a	pore radius (m)
c	concentration of SO_2 (kmol/m^3)
k_1	calcination rate constant using the shrinking core model (kg/(m^{2}s))
Nu	particle Nusselt number
p_{CO_2}	partial pressure of carbon dioxide in gas phase (kPa)
p_{H_2O}	partial pressure of water vapor in gas phase (kPa)
r_c	radius of unreacted core of particle (for calcination) (m)
Sh	particle Sherwood number
S_m	surface area per unit mass of particle (m^2/kg)
S_r	diffusion surface area at radius r (m^2)
T	gas temperature (K)
V_c	volume of unreacted core (m^3)
x	extent of calcination
ε	porosity of particle

*Corresponding author

INTRODUCTION

Coal comprises about 75% of the world fossil fuel reserves, with America contributing 25% of the world's coal resources. The increase of oil prices worldwide coupled with the realization that the world's oil resources are being fast depleted has led to an increasing use of coal and coal-based fuels in the past decade. Trends of energy usage reveal that by the turn of the century, nearly 55% of the total power production in the U.S. will be through fossil fuels (coal contributing to 28%), followed by natural gas, nuclear power, and the rest made up of hydroelectric, solar and geothermal sources[1]. Such an increased use of coal will necessarily cause pollutant emissions to increase. Some of many such emissions from coal-fired utility boilers are sulfur oxides (SO_2+SO_3), which have been found to be precursors of acid rain. Natural emissions of sulfur have remained essentially constant, while emissions from anthropogenic sources keep increasing. The necessity of reducing the emission levels of these acid rain precursors has been instrumental in developing SO_2 control technologies for retrofit applications. Possible strategies for SO_2 control can be classified according to the stage of implementation, namely, before (physical beneficiation), during (atmospheric fluidized bed combustion or limestone sorbent injection multistage burning) and after combustion (wet flue gas desulfurization or dry flue gas desulfurization). Wet scrubber systems have been in use for some years, but they are subject to drawbacks like corrosion, pressure drop through scrubbers and crystal deposits in the equipment. A promising approach to reducing these emissions involves the injection of dry pulverized sorbent (limestone, dolomite, calcium hydrate or dolostone) into the combustion chamber. The major limitation in this technique is however, the high temperatures attained during combustion and the resulting sintering of the sorbent. The design of multistage combustors has helped to alleviate this problem somewhat, and the technology has become more promising. The injected sorbent is rapidly heated by hot gases and decomposes forming lime and carbon dioxide. The lime thus produced reacts with SO_2 and excess O_2 in the combustion gases to form $CaSO_4$. Fundamental studies of the sulfation reaction of CaO derived from limestone with SO_2 have been done since the early 1970s. Borgwardt[3] did pioneering work in flash calcination and sintering, and studies on sulfation of CaO were carried out by Borgwardt and Bruce[4], Borgwardt et al.[5] among others. Models describing the calcination, sintering and sulfation processes have been developed by Milne et al.[6] They included effects of pore diffusion, diffusion through the product layer, sintering, and heat and mass transfer. Since pore diffusion is an important limitation in the sulfation of large sorbent particles (~100 μm), increasing mass transfer of SO_2 to the particle surface could very well increase the extent of sulfation.

Studies of pulverized coal combustion show that char combustion is the limiting factor in the overall burnout of coal in practical furnaces. This is so mainly because in the later stages of combustion, the coal particle/agglomerate gets entrained in the bulk flow, and as a result the effective Nusselt and Sherwood numbers reduce to the pure conduction values of 2.0. Imposing a high intensity acoustic field over the region of interest causes a large and rapid fluctuation in the gas velocity, while the particles on account of their inertia do not get entrained, thereby, the gas-particle slip velocity is greatly enhanced. As a result, the rate of heat and mass transfer to the particle remains quite high. Theoretical investigations of acoustic enhancement of heat and mass transfer in the case of oscillating flow with and without a steady velocity were carried out by Ha[9]. Ha and Yavuzkurt[10] also developed correlations for the space and time averaged Nusselt and Sherwood numbers under the influence of an acoustic field imposed on a steady flow using a 2-dimensional unsteady formulation. The current paper focuses on the effects of an acoustic field on SO_2 capture by limestone sorbents of different sizes and porosities. A comprehensive sulfation model based on the results of Milne et al.[7] has been used. The model has also been incorporated into the PCGC-2 code to study the effects of acoustics on sulfur capture in a pulverized coal combustor.

MODELING OF THE SULFATION PROCESS

The comprehensive mathematical model developed by Milne et al.[7] has been used in order to predict the percentage of sulfur dioxide capture by limestone sorbents. Dry sorbent injection in pulverized coal

boilers occurs at temperatures ranging from 1100-1500 K and the residence times range from 0.5-3.0 seconds. The sorbent therefore initially calcines before undergoing sulfation. The porous carbonate (or hydrate) decomposes to a highly porous CaO solid of the same volume. Rapid initial sulfation of the newly formed CaO can occur in a high temperature reactor in the presence of SO_2. The processes of calcination, sintering and sulfation occur simultaneously in a combustor. The following sections provide some particulars of each process. For more details refer to Milne et al.[6]-[8]

Calcination

The calcination process is described by a shrinking core model for a spherical particle. The particle is assumed to be isothermal, since the Biot number is small. The classical shrinking core model for any decomposition reaction is based on the assumption that the rate of change of volume of the unreacted solid is proportional to the surface area of the unreacted spherical core. While this assumption may not be true especially at high heating rates, it is useful as a simple approximation of the process of calcination. Decomposition begins on the surface and proceeds inward symmetrically. Highly porous calcium oxide forms on the surface, and the radius of the unreacted core decreases as the reaction progresses. At the reaction interface, heat is absorbed and CO_2 diffuses out during the calcination reaction.

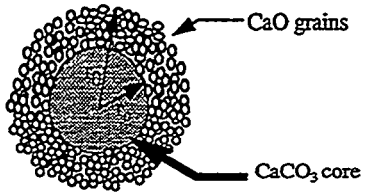

FIGURE 1. Illustration of the shrinking core model (Milne et al.[6])

Mathematically, the shrinking core model can be represented as

$$\frac{dV}{dt}_c = -k_1\left(4\pi r_c^2\right) \tag{1}$$

However, as shown in, a calculation of the values of k_1, using the calcination rate data from Borgwardt shows that the rate constant is not independent of the surface area. The decomposition process, therefore is more complicated than indicated by the shrinking core model applied at the particle grain level. Hence an empirically modified form of the shrinking core model at the particle level, which fit the experimental data was used by Milne et al.[6], namely

$$x = 1-\left(1-\frac{k}{d_0^{0.6}}t\right)^3 \tag{2}$$

where x is the extent of calcination, k is a modified rate constant with properly adjusted units, d_0 is the initial diameter of the particle. The equation for k was the same as that used by Milne et al.[6] i.e.,

$$k = 10.303exp\,(-10980/T) \tag{3}$$

The value of the exponent, 0.6 was later adjusted to 0.55 to fit experimental data from Hu et al.[14] better.

Sintering

The sintering model proposed by Lindner and Simonsson[11] which approximated the calcine structure as a system of overlapping grains (Figure 2) was used. The surface area and volume of a system of overlapping grains with n contacts per grain, r and r_i being the initial radius of the grain and the distance from the centre of the grain to the plane of contact respectively, were deduced from geometric considerations[11]. Sintering influences both surface area and porosity. The sintering model used here to describe the loss of surface area is the one formulated by Milne et al.[7] as an empirical equation. Equation (4) accounts for the loss of surface area due to the presence of both water vapor and carbon dioxide, both of which are known to influence the phenomenon. Another assumption used is that the change in porosity is proportional to the change in surface area. While this is not necessarily true, it has been used by a number of researchers in the past.

$$\frac{dS_m}{dt} = -2450\left(1 + 50.7p_{H_2O}^{0.17} + 10.3p_{CO_2}^{0.67}\right)exp\left(\frac{29600}{T}\right)(S_m - 5000)^2 \qquad (4)$$

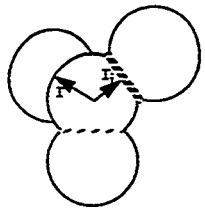

FIGURE 2. Illustration of the overlapping grain model ([11])

Sulfation

The process of sulfation is a complicated phenomenon, with structural changes occurring due to the increased molar volume of the product, $CaSO_4$ in comparison to that of CaO. The resulting swelling of the grain causes pore closure and hinders sulfation due to increased product layer thickness. Product layer diffusion, pore diffusion and external mass transfer (bulk gas phase diffusion) all play a part in sulfation. Diffusion through the product layer is modeled by assuming a spherical grain of CaO. Using a quasi-steady-state approximation and assuming constant product layer diffusivity, we get simply,

$$\frac{d}{dr}\left(S_r\frac{dc}{dr}\right) = 0 \qquad (5)$$

Sulfation of the exposed CaO grain surface causes a monolayer of product (CaSO4) to be formed, the process being considered instantaneous compared to the time scale of the transport processes. After formation of the monolayer, product layer diffusion is assumed to be limiting for the local rate of sulfation at the grain level. Details of the boundary conditions used and the formulation of the method used in solving this equation can be found in Milne et al.[7]. The product layer diffusivity was expressed as the following Arrhenius type expression[7]

$$D_s = 4.10 \times 10^{-9} exp\left(\frac{12820}{T}\right) \qquad (6)$$

The rate of sulfation of porous CaO is also limited by transport of SO_2 to the interior of the particle. Using a quasi-steady-state approximation, the differential equation for SO_2 diffusing through and reacting simultaneously in a porous sphere is given by

$$\frac{d}{dr}\left(D_e r^2 \frac{dc}{dr}\right) + Gr^2 = 0 \tag{7}$$

where G is the rate of consumption of SO_2 per particle volume and D_e the effective pore diffusivity. The particle was now divided into shells of constant effective pore diffusivity, and the differential equation was integrated with the appropriate boundary conditions, thereby giving the SO_2 concentration profile in the particle. The effective pore diffusivity was calculated as

$$D_e = \frac{\varepsilon}{\tau}\left(\frac{1}{D_m} + \frac{1}{D_K}\right)^{-1}, \text{where, } D_K = 97a\left(T/M_{SO_2}\right)^{1/2} \tag{8}$$

D_K is the Knudsen diffusivity which is proportional to the pore radius, a given by $a = 2\varepsilon/S$, and M_{SO_2} is the molecular weight of SO_2. The tortuosity, τ is assumed to be 1.47. Bulk diffusion, D_m is important for very large pores, and is calculated as the effective binary diffusivity of SO_2 in a multicomponent gas mixture as described in Bird et al.[12]

For large particles (~100 μm), the rate of transport of SO_2 from the bulk gas phase to the surface of the particle becomes an important factor in capture by the sorbent. At very low particle Reynolds numbers (cases of low gas velocity, very small particles or complete entrainment of particles), the Sherwood and the Nusselt numbers reduce to 2. However, it is not so for high gas-particle slip velocities. The influence of bulk flow on the flux of SO_2 to the particle surface was shown by Bird et al.[12] to depend also on blowing of CO_2 from the particle surface. The formulae for the binary diffusivity of each species in a mixture of gases, the bulk diffusivity, viscosity and thermal conductivity and the values of the constants needed for their calculation are also taken from Bird et al.[12]

IMPLEMENTATION OF ACOUSTIC FIELDS

As described in Rawson[13], in a traveling wave acoustic field with a sound pressure of P_{rms} and acoustic impedance $\rho_g c_{sound}$, ρ_g being the density of the medium, and c_{sound} the speed of sound, the acoustic velocity amplitude is given by

$$U_1 = \frac{\sqrt{2}P_{rms}}{\rho_g(\gamma R T_g)^{0.5}}, \text{where, } P_{rms} = 10^A, \text{and } A = (L_p - 94)/20 \tag{9}$$

L_p being the sound intensity in dB. When the Reynolds number of the flow over the particle is small, the entrainment factor η can be obtained by equating the particle drag and inertial forces for a smooth sphere as shown by Rawson[13].

$$\eta = \frac{1}{\left(1 + \omega^2\tau^2\right)^{1/2}}, \tau = \frac{\rho_p D^2}{18\mu} \tag{10}$$

where τ is the particle relaxation time, and ω is the angular frequency of the acoustic wave.

In order to implement the acoustic field in the sulfation model, correlations developed by Ha[9] using an unsteady, two dimensional computer program for the heat and mass transfer over a spherical particle in the presence of an acoustic field were used. Since the sorbent particles are assumed to be more or less entrained in the gas flow, the relative velocity U_0 between the gas and the particle is close to zero. From Ha[9], the dimensionless space and time averaged, quasi-steady heat and mass transfer coefficients, normalized by their steady flow values, can be expressed as a function of the ratio ξ ($=U_1/U_0$)

$$\frac{Nu_t-2}{Nu_0-2}\left(or \quad \frac{Sh_t-2}{Sh_0-2}\right) = F(\xi) \tag{11}$$

where, F is given by (Ha[9], Ha and Yavuzkurt[10])

$$\begin{aligned} F &= 1.0+9.608\times10^{-3}\xi-0.109608\xi^2 \quad for \quad 0\le\xi\le1 \\ F &= 0.7628\xi^{0.5}+0.1372 \quad for \quad \xi>1 \end{aligned} \tag{12}$$

where Nu_0 and Sh_0 are given by the following equations.

$$Nu_0 = 2.0+0.65Re^{1/2}Pr^{1/3},\ Sh_0 = 2.0+0.65Re^{1/2}Sc^{1/3} \tag{13}$$

RESULTS AND DISCUSSION

Calcination And Sulfation

The model was validated by comparing to data from experiments by Hu et al.[14]. These experiments were conducted in an entrained flow reactor consisting of a preheater, a side-heated sorbent injector, and a vertical reactor at temperatures of 1000 °C and 1100 °C. Comparisons are shown for only one kind of stone, both for calcination and sulfation. Particle sizes used had mass mean diameters of 45, 63 and 89 μm. The sorbent feed rate was adjusted to achieve a molar Ca/S feed ratio of 2.0. The SO_2 concentration in the reactor was 2000 ppm.

To compare calcination results (Figure 3), the sulfation model was turned off and only the calcination and sintering models were used. The initial calcination rate shows a rapid increase and then levels off later. The discrepancy between the model and the experimental results observed in the initial stages is because no provision was made for the decrease in reactor inlet temperature that inevitably follows when the sorbent entraining air mixes with the preheated air at the top of the reactor. The resulting lower inlet gas temperature causes a delay for the particles (more so for the larger ones) to reach calcination temperatures. Therefore in the initial stages (~<300 ms) of calcination model predictions are about 100-80% higher than the experimental results, whereas when the temperature in the reactor reaches the constant value used in the modeling (1273 K at ~500 ms) the experimental and predicted results are within 10% of each other. In the modified shrinking core model used, the particle diameter dependency was reduced from 0.6 to 0.55 in order to fit the data better.

Sulfation results (Figure 4) show a strong influence of particle size. The delay in onset of sulfation observed in the larger particles is associated with pore diffusion resistances and the time required for significant calcination to occur. Comparisons with experimental data show that the model predicts sulfation extents 100-80% higher than those obtained experimentally in the initial stages due to lower temperatures of the reactor and resulting lower calcination rates as explained above. However, in the later stages, the prediction is within 10% of that observed experimentally as is also seen in the calcination results.

Influence Of Acoustics On Sulfation

To implement the correlations for increased heat and mass transfer in the presence of an acoustic field superimposed on a steady flow, it was assumed that the sorbent particles were traveling with terminal velocity (~0.5 m/s) w.r.t to the entraining gas. A simple Stokes force balance provided an estimate of the terminal velocity. Results for sulfation under the influence of an acoustic field are shown for large particles. The extent of sulfation of small particles did not change by imposing an acoustic field. But for larger particles, the changes are manifest. The increase in sulfation is also seen to be a strong function of the porosity of the particle (Figure 5). Up to an 11% increase is seen in the case of the highest porosity, namely ε=0.5. If these large particles agglomerate, then a further increase in the rate of sulfation with increasing intensity of acoustic field is observed. Here 50 and 100 μm particles are assumed to form a 200 μm agglomerate (Figure 6). An increase of 4% and 12% is seen for the agglomerate consisting of 50 and 100 μm particles respectively. Since product layer diffusion is a controlling resistance at the grain level, for ~10 μm size particles, the SO_2 concentration profile within the particle is not very steep (since pore diffusion is not limiting). Therefore increasing the mass transfer does not influence sulfation. However, in cases of large (~100 μm) particles, significant pore diffusion limitations cause the interior concentration to fall rapidly. Since the outer shells which get calcined also get rapidly deactivated, increasing the mass transfer allows the SO_2 to penetrate to the particle interior, where it can be taken up by fresh calcine. Also, a lower rate of calcination aids in the phenomenon, because then the grains do not sinter and no reduction in the surface area occurs, thereby allowing for better eventual capture. The same reason holds for the particle agglomerates.

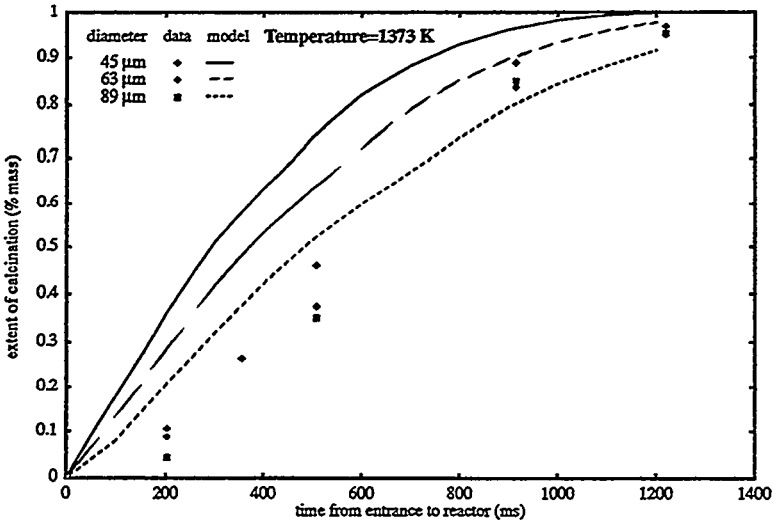

FIGURE 3. Comparison of calcination rates with data, Linden Hall sorbent, Hu et al. [14]

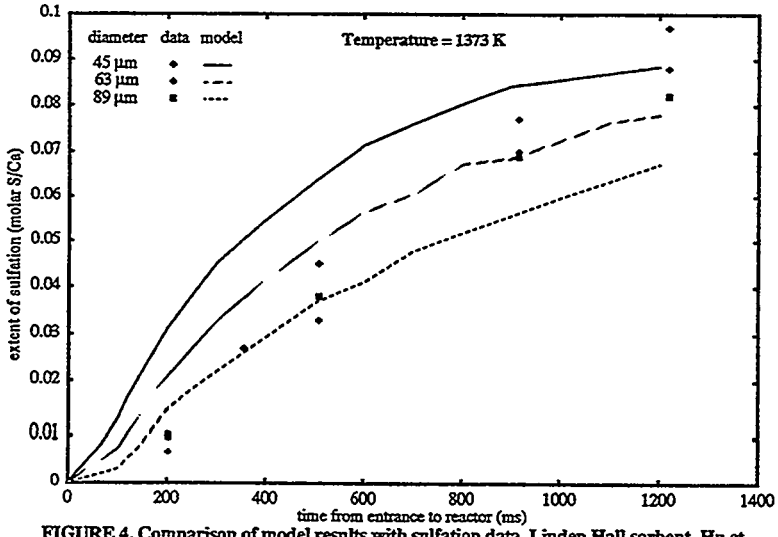

FIGURE 4. Comparison of model results with sulfation data, Linden Hall sorbent, Hu et al.[14]

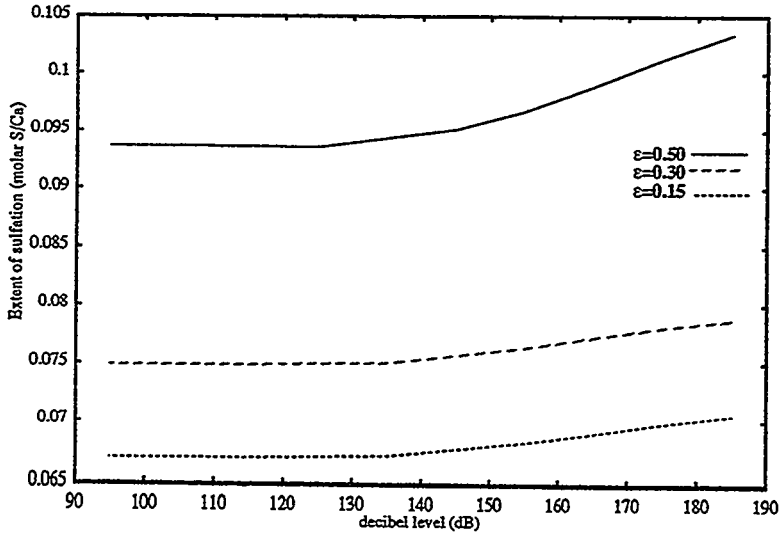

FIGURE 5. Extent of sulfation of 100 µm particle with increasing sound intensity

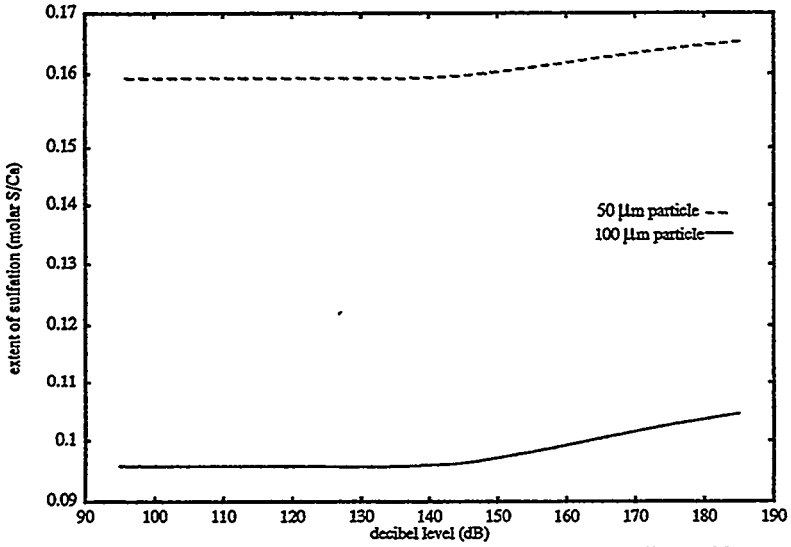

FIGURE 6. Extent of sulfation of 200 µm agglomerate composed of smaller particles

Implementation Of Sulfation Model In PCGC-2

The SO_2/sorbent model discussed earlier has been incorporated into a comprehensive two dimensional, axisymmetric, pulverized coal combustion code (PCGC-2[15]). The conditions of operation considered were fuel lean, and in normal boiler operating conditions with excess air, almost all the fuel sulfur is converted to SO_2 with small quantities of SO_3. Fuel rich species like COS and H_2S exist only in the regions of rapid devolatilization of coal. Gas phase reactions of the sulfur species to form SO_2 are assumed to be fast, giving rise to what is commonly called the "local instantaneous equilibrium" assumption in PCGC-2. As in other species calculated in PCGC-2, sulfur is assumed to be released from the coal at a rate proportional to the total coal mass loss and is partitioned between SO_2 and H_2S according to the chemical equilibrium concentration of each. Presently, interconversion of SO_2 to H_2S and vice versa is not allowed. The effects of sorbent particles on gas velocity, radiation fluxes and concentrations of major species are assumed to be small since the particles are light, follow the motion of the gas and the sorbent loading itself is quite small. As a result, the sorbent model can be completely decoupled from the main combustion code, and hence requires less overall time for convergence.

The entire procedure can be summarized as follows. First the coal particle/gas flow is solved without the sorbent particles. Second, the Eulerian number density of the particles are calculated. This is to calculate a "turbulent particle diffusivity" which is used in the next step while tracking the coordinates of the reacting sorbent particles through the combustor in a Lagrangian fashion. Source (in this case, sink) terms are obtained for the SO_2 species. Lastly the continuity equation for the SO_2 species is solved using the source+sink terms calculated from the equilibrium assumption (used during the calculation of the combustion flow field) and step 3 respectively. The last two steps are repeated till a converged solution for the SO_2 species equation is obtained. The concentration of SO_2 in the combustor in the absence of sorbent particles calculated using the equilibrium assumption compared favorably to data obtained from MTCI Inc (~711

ppm). An average exit concentration of ~580 ppm (Figure 7) is seen for the conditions at which the program was run (9.9% excess air fuel lean at a sound intensity level of 180 dB). The SO_2 concentration field at the combustor exit with and without sorbent injection is also shown (Figure 8), and the corresponding reduction is clearly seen.

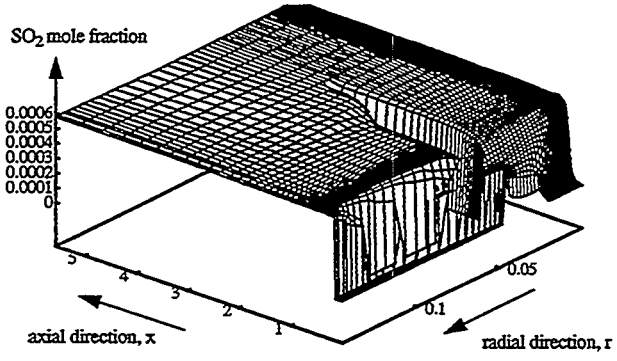

FIGURE 7. SO_2 concentrations in the combustor

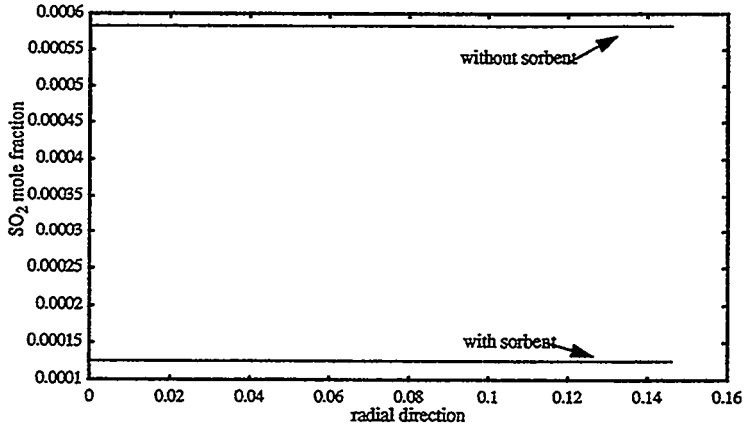

FIGURE 8. SO_2 concentrations at the exit of the combustor with and without sorbent

CONCLUSIONS

A comprehensive sulfation model based has been incorporated into PCGC-2, a steady, two-dimensional, axisymmetric combustion code. The sulfation model compared well(within 10%) with experimental results for the case of no acoustic field both for calcination and sulfation.. Model results for cases with acoustics predict an increase of ~12% in the sulfur capture by limestone sorbent for large particles (~100 μm) at high values (~180 dB) of the sound intensity level while no increase was seen for small particles (~10 μm). Preliminary results from the PCGC-2 program after incorporating the sorbent model show good agreement (within 20%) with test combustor data from MTCI Inc.

Acknowledgment: This work has been partially sponsored by the DOE/METC and MTCI Inc. of Columbia, Maryland under sub-contract No. 10038-04, Mod.3. Their support is greatly appreciated.

REFERENCES

1 *Power to the People*, A Survey of Energy, The Economist, June 18-24, 1994.

2 Slack, A.V. and Hollinden, G.A., *Sulfur Dioxide Removal from Waste Gases*, Pollution Technology Review No. 21, p. 47, (1975).

3 Borgwardt, R.H., *Environ. Sci. Technol.*, 4:59-, (1970).

4 Borgwardt, R.H., Bruce, K.R., *AIChE J.*, 32:239-, (1986).

5 Borgwardt, R.H., Bruce, K.R., and Blake, J., *Ind. Eng. Chem. Res.*, 26:1993-, (1987).

6 Milne, C.R., Silcox, G.D., Pershing, D.W., and Kirchgessner, D.A., *Ind. Eng. Chem. Res.*, 29:139-149, (1990).

7 Milne, C.R., Silcox, G.D., Pershing, D.W., and Kirchgessner, D.A., *Ind. Eng. Chem. Res.*, 29:2192-2201, (1990).

8 Milne, C.R., Silcox, G.D., Pershing, D.W., and Kirchgessner, D.A., *Ind. Eng. Chem. Res.*, 29:2201-, (1990).

9 Ha, M.Y., *A Theoretical Study of augmentation of particle combustion via acoustic enhancement of heat and mass transfer*, Ph.D. Thesis, The Pennsylvania State University, Pennsylvania (1990).

10 Ha, M.Y., and Yavuzkurt, S., *Int. J. Heat Mass Transfer*, 36: 949-959, (1993).

11 Lindner, B., and Simonsson, D., *Chem. Eng. Sci.*, 36:1519-1527, (1981).

12 Bird, R.B., Stewart, W.E., and Lightfoot, E.N., *Transport Phenomena*, Wiley, New York, 1960.

13 Rawson, S.A., *An Experimental Investigation of the influence of high intensity acoustics on heat and mass transfer rates from spheres as related to coal-water slurry fuel combustion enhancement*, M.S. Thesis, The Pennsylvania State University, Pennsylvania (1988).

14 Hu, N., Liu, Y., Miller, S.F., and Scaroni, A.W., "Experimental Investigation of High-Temperature, Short residence-time Calcination and Sulfation of Limestone and Dolostone sorbents," Private communication, (1994).

15 Smoot, L.D., Smith, P.J., and Brewster, D.B., "Pulverized Coal Gasification and Combustion, Users' Manual", Revised version, 1987.

DEVELOPMENT OF METAL MELTING SYSTEM USING OXY-COAL COMBUSTION

Nobuaki Kobayashi

Tech. Div., Yamanashi Lab.,

Nippon Sanso Corp., Yamanashi, Japan

INTRODUCTION

Recently, "Clean Coal Technology" has become increasingly important world-wide from the viewpoint of environmental pollution problems as well as concerning economical energy consumption. In Japan, various research activities are being progressed in response to this situation by Center for Coal Utilization, Japan (CCUJ) as the research center. As for the subject of coal combustion, new combustion technique in application to metal melting is being studied for clean and effective utilization of coal, with the technique of effective combustion in boilers for generator and of preventive measures against environmental disruption. At present, a large quantity of scrap metals (steel, copper and aluminum) is recycled to remelt with electricity. Direct use of coal to remelting instead of electricity, which is generated mainly by use of a great deal of oil and coal, can reduce possible consumption of energy resources remarkably. Figure 1 shows an example of electricity consumption in electric arc furnace (EAF) generally used for steel melting. In late years, it has been reduced by development in new melting method and improvement of operation conditions, but used to approximately 400 kWh/T. Taking into account efficiency of conversion from oil or coal to electricity in generation, the thermal efficiency is short with less than approximately 30%, even 45% with the direct use of fuel-air combustion processes. To solve these problems, associated with the drastic reduction of carbon dioxide, a new technique regarding the utilization of coal has been desperately needed.

Further the quantity of supply of metal scrap in Japan has increased year by year and this tendency is predicted to continue in future. The quantity of total supply including obsolete and process scrap in the year of 2010 is estimated to reach up to sixty-eight million tons by increase of approximately eighteen million tons from present state. Metal recycling technology is becoming increasingly important in point of effective use of metal resources and environmental integrity from waste out of use.

In this paper, the new method, that metal scrap can be effectively melted without pollution of atmosphere with pulverized coal combustion by burner using preheated oxygen, is described. After fundamental confirmation that the use of preheated oxygen has the good effect on combustion and melting, this burner is applicable to melting furnace of 1 ton scale to examine optimum conditions of melting metals.

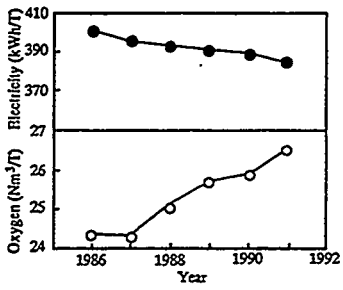

Figure 1 Changes on energy consumption

CONCEPT OF NEW SYSTEM ON METAL MELTING

This technique can be mainly characterized by the following two factors shown in Figure 2. One is a new burner using preheated oxygen for combustion of pulverized coal. It is well known that, in case of oxygen combustion of liquid or gas fuel, higher flame temperature of approximately 2500 degrees is easily obtained than in that of air combustion. Even in case of combustion of coal,

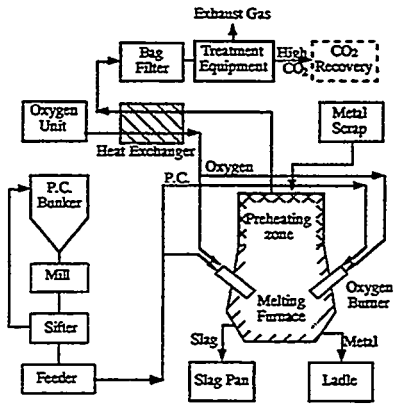

Figure 2 Schematic flow chart

high temperature of flame and efficiency equivalent to those in combustion of liquid or gas fuel, are easily obtained by new burner using preheated oxygen to 1073K. Furthermore, those have the advantage of melting metal with high melting point. The other is a melting system composed of melting furnace for recycled metals (steel, copper and aluminum) and recovery equipment for concentrated carbon dioxide in the exhaust gas. The dimensions of the furnace which function as a preheater, the operational conditions of burner combustion and gas-stirring of melt are also optimized for high efficiency of heat transfer from flame of burner to metal. More than 50 to 60% of thermal efficiency can be designed at the practical furnace. Thermal efficiency used is defined to following equation.

$$\text{(thermal efficiency)}=\frac{\text{(sensible heat of metal)}}{\text{(latent heat of fuel)}}$$

COMBUSTION CHARACTERISTICS OF OXY-COAL BURNER

Burner Design

Outline of burner construction is shown in Figure 3. Pulverized coal from a center nozzle is strongly mixed with oxygen gas injected into ahead combustion room. For preheater of oxygen gas, either indirect heating type or direct one can be possibly used. Indirect type heater generates high temperature oxygen by heat exchanger using process gas exhausted from melting furnace. Direct type heater is useful chiefly in operation by the batch in which oxygen temperature is needed to rise rapidly. The preheating equipment, small amount of gas fuel burning in, is installed inside the burner. Fundamental characteristics of this burner flame and the effect of preheated oxygen on combustion and melting ability were examined.

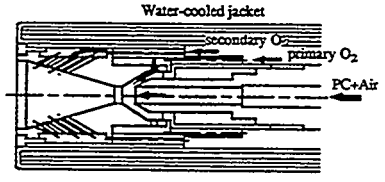

Figure 3 Schematic diagram of burner nozzle

Fundamentals of Pulverized Coal Combustion

Combustion rate of pulverized coal particles was fundamentally measured to understand quantitatively the effect of preheated oxygen up to 1223K at maximum using drop furnace shown in Figure 4. The oxygen concentration in combustion gas was also changed from 40 to 100%. The reaction furnace is 990 mm high with 55 mm inside diameter. Pulverized coal particles were dropped into the furnace through the water-cooled lance. Oxygen gas was preheated with an electric heater and then introduced into the reaction furnace. Particles at various combustion stages were sampled by a water-cooled probe which was inserted from the bottom and moved up and down in the furnace. Combustion rate can be calculated from reaction time and fractional unburned ratio which was obtained according to ash ratio by analysis of particles before and after reaction. Test conditions and properties of pulverized coal are shown in Table 1.

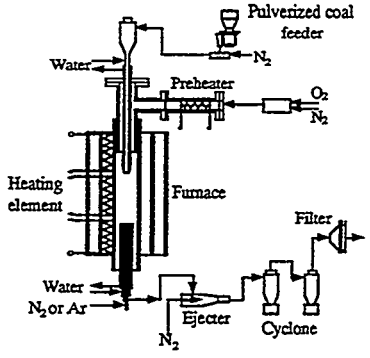

Figure 4 Schematic diagram of apparatus

Table 1 Properties of P.C. and test conditions

Proximate analysis	Fixed Carbon	51.0 %
	Volatile matter	34.8 %
	Ash	14.2 %
Gas temperature		973～1223 K
P.C. feed rate		1.8 g/hr
Oxygen flow rate		1.5 Nm³/hr

Relationship between fractional unburned ratio and reaction time are shown in Figure 5. The coefficient of reaction rate calculated is shown in Figure 6. Combustion rate is obtained to increase linearly in proportion to oxygen temperature up to 1173K. Fundamental experiment to confirm effect of preheating of oxygen under combustion by burner is carried out as follows.

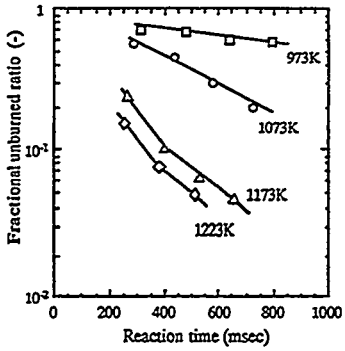

Figure 5 Relationship between fractional unburned ratio and reaction time

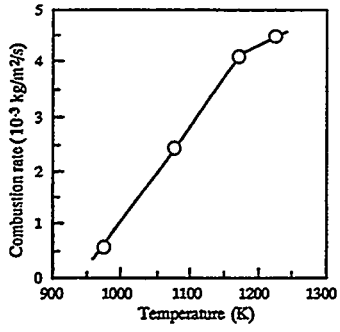

Figure 6 Relationship between reaction rate and oxygen temperature

Fundamental Tests on Combustion Characteristics of New Burner

Tests were carried out by use of the burner with capacity of pulverized coal 150 kg/hr. Table 2 shows an example of characteristics of pulverized coal used. Water-cooled furnace used for combustion puts the side with dimension of 1.1 m inner diameter and 5.5 m length. Burned ratio was measured from powder sampled by the same method as above mentioned. Flame temperature was representative by particle temperature measured by two-color pyrometer.

Relationship between oxygen temperature and burned ratio is shown in Figure 7. The higher temperature of oxygen, the higher rate of combustion is possible. Burned ratio of approximately 70% was obtained at distance of 0.5 m by preheating of oxygen up to 873K. Distribution of flame temperature is shown in Figure 8. Higher temperature of flame at distance within 0.7 m was obtained by use of preheated oxygen, compared with atmospheric temperature of oxygen. On pulverized coal combustion with preheated oxygen, higher efficiency and higher flame temperature can be easily obtained.

Table 2 Properties of pulverized coal

Proximate analysis (dry)	Fixed Carbon	59.5 %
	Volatile matter	34.4 %
	Ash	6.1 %
Ultimate analysis (d.a.f)	Carbon	76.0 %
	Hydrogen	4.7 %
	Oxygen	11.0 %
	Nitrogen	1.4 %
	Sulfer	0.8 %

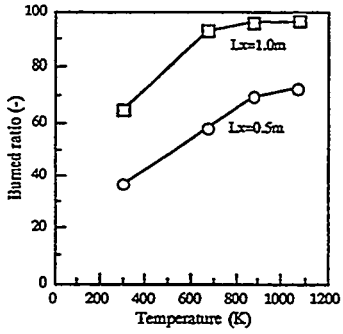

Figure 7 Relatioship between burned ratio and oxygen temperature

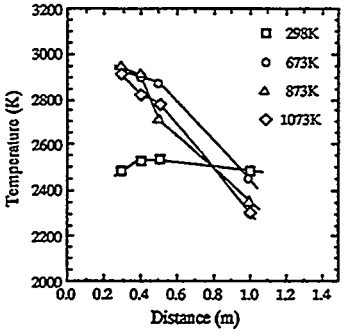

Figure 8 Distribution of flame temperature

Fundamental Tests on Direct Melting by Burner Flame

The schematic diagram of apparatus is shown in Figure 9. Metal rod of 20 mm diameter was

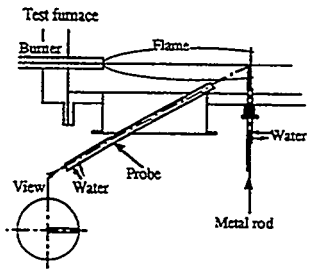

Figure 9 Schematic diagram of metal melting test

Table 3 Metal melting test condition

P.C. burner		
P.C. flow rate	(kg/hr)	150
Carrier N_2	(Nm^3/hr)	20
O_2 flow rate	(Nm^3/hr)	225
O_2 preheat temp.	(K)	298~1073
Oil burner		
Oil flow rate	(L/hr)	120
O_2 flow rate	(Nm^3/hr)	240

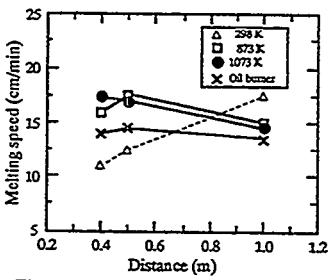

Figure 10 Relationship between distance from burner and melting speed

inserted into the center of furnace in right-angled to flame axis. Speed of insertion which was considered to be melting speed was continuously controlled as the top of rod regulated to be the center of flame according to melting speed of metal rod. Burner system used for pulverized coal with capacity of 150 kg/hr has a function of indirect preheating of oxygen above 873K. Oil burner with almost equivalent capacity of calorific value was also used comparing with this burner in the conditions as shown in Table 3.

In Figure 10, melting speed of steel rod is shown to distance from burner nozzle. In the case of higher temperature of oxygen, a point of maximum melting speed had a tendency to approach toward burner side. Melting speed at distance 0.4 m was more than 1.5 times as large as that by use of oxygen without preheating. Melting speed in coal burner using preheated oxygen more than 873K is equivalent to that in kerosene burner. From the fundamental investigation above mentioned, pulverized coal burner with preheated oxygen is estimated to be useful for metal melting. The temperature of oxygen in melting at distance 0.5 m will not need beyond approximately 873K.

MELTING CHARACTERISTICS IN 1 TON METAL MELTING

Procedure

By melting tests of 1 ton scale, mainly in use of steel, optimum conditions for high heat efficiency and high yield of metals were investigated. Dimension of furnace is thought to influence heat efficiency as well as combustion condition of burner. Firstly effect of faculty of preheating supplemented with melting furnace is examined and subsequently optimization of burner arrangement and conditions, for example distance between burner and heated material, is also examined. The effect of prevention of direct oxidation and reduction of iron slag by carbon addition on yield of iron is studied due to mechanism of iron loss estimated to be slag formation by oxidation. Oxygen ratio in combustion by burner and amount of carbonaceous materials as initial charge were changed. Schematic

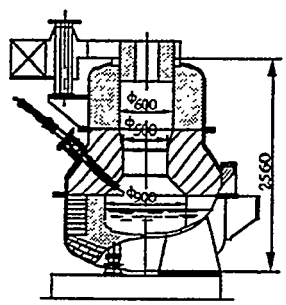

Figure 11 Schematic diagram of apparatus

Table 4 Experimental conditions

Raw materials	
Scrap (ton)	1
Pig iron (kg)	80
coke (kg)	5
Flux (kg)	60
P.C. burner condition	
P.C. flow rate(kg/hr)	90
Carrier gas (Nm^3/hr)	27
O_2 flow rate(Nm^3/hr)	120
O_2 preheat temp.(K)	873
Bottom blown N_2 (Nm^3/hr)	6

diagram of apparatus is shown in Figure 11 and in the conditions as shown in Table 4. Investigation on furnace dimension and burner condition was carried out mainly by kerosene and optimized conditions were applicable to the case of pulverized coal. Pulverized coal in use was Datong coal with a grain of approximately 200 mesh under. Burner of pulverized coal had the capacity of 30 kg/hr with indirect type of oxygen heating up to 873K.

Melting Behavior

After preheating of furnace refractory to fixed temperature, all of metal scrap and flux were added from upper part of furnace. Direct melting by burner flame of metal scrap in lower part of furnace was taken place and simultaneously preheating of charged scrap progressed by heat exchange with rising gas exhausted from upper part of furnace. Metal scrap was heated up to be softened, melted and fell down. This period till all falling down is called step 1 in the following. Falling scrap is continued to be heated and melted down by direct heating of metal surface. This period is called step 2. In last step 3, metal melted down is heated to tap temperature (1903K in case of steel) in raising of temperature approximately 100 degrees. All melt of metal and slag were evacuated off from tapping runner. This serial behavior is schematically shown in Figure 12. Typical change at every steps on composition, temperature and heat efficiency are shown in Figure 13. In step 1, heat efficiency is reached to more than 70%, because heat loss by sensible heat of exhaust gas is remarkably reduced by effective heat exchange in upper part of furnace. In step 2 and 3 after falling down of charged scrap, heat loss of exhaust gas increases a little.

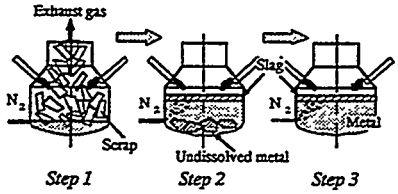

Figure 12 Schematic diagrams of melting steps

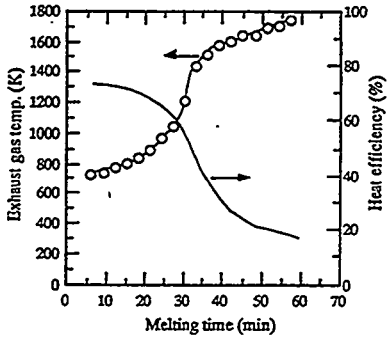

Figure 13 Changes of exhaust gas temperature and heat efficiency

Effect of burner condition on thermal efficiency

Heat efficiency within entire period, heat loss of exhaust gas in step 1, and the rate of heating in step 3 are shown in Figure 14. Highest heat efficiency can be achieved in the case of lowest position of burner and largest angle to horizontal section. This result is considered to depend on effective preheating of charged metal in step 1 and heating of melt in step 3.

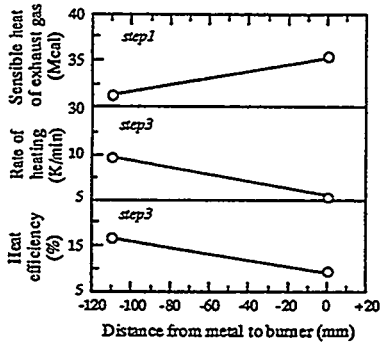

Figure 14 Heat efficiency, heat loss of exhaust gas and heating rate

Iron yield

Amount of iron loss almost agreed with iron content in slag formed by oxidation. In case of lowering excess oxygen ratio in burner combustion, oxidation speed of iron is possible to decrease but total amount of iron oxidation can not decrease in consequence of extension of treating time.

Figure 15 shows the result in case of increase of carbonaceous material for initial addition. Iron content in slag and iron loss are decreased according to increase of final carbon content in steel melt. If final carbon is more than 0.07%, iron content in slag is possible to be less than 20%. When slag volume is 50 kg/T, iron loss corresponds to less than 1% of total charged iron.

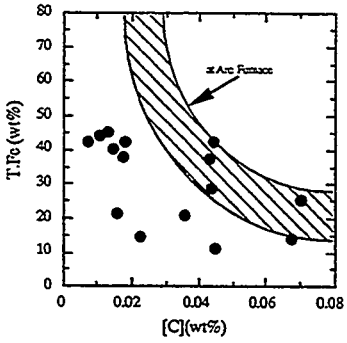

Figure 15 Relationship T. Fe and [C]

Thermal efficiency and yield by oxy-fuel burner using pulverized coal

Based on above mentioned result, oxy-coal burner by use of preheated oxygen is applicable to melting tests of 1 ton scale furnace with optimum dimension and burner conditions. The heat efficiency and iron yield in condition of heat input 173 Mcal/hr to 242 is shown in Figure 16. High heat efficiency close to 50% and high iron yield above 93% can be achieved equivalent to the result obtained by kerosene burner.

An example of metal composition before tapping is shown in Table 5. Sulfur and nitrogen content are comparatively low, because absorption into melt during burner combustion is trifling due to good combustion in flame and to good control of atmosphere absent from air. Phosphorus, manganese and chromium are also possible to be reduced by slag control. But copper content which depends on content in raw material is relatively high.

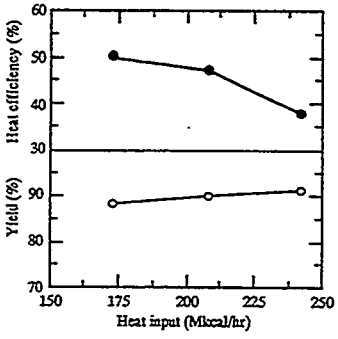

Figure 16 Yield and heat efficiency in P.C. combustion

Table 5 Metal composition

C	Si	Mn	S	P	N
0.01	<0.01	0.02	0.02	0.003	0.005

Behavior of exhaust gas

Cleanness of exhaust gas in use of pulverized coal is very important. Behavior of NOx and SOx during melting are examined and analyzed. In Figure 17 typical changes on NOx and SOx content in exhaust gas is shown in the condition of rate of pulverized coal 35 kg/hr and excess oxygen ratio unity. NOx content in conversion into dry base is shown to be almost 10 ppm below within 30 minutes from beginning of melting and then to be increasing approximately 200 ppm to more than 800 ppm. These results are considered to be due to influence of high temperature of atmosphere for the absorption reaction. Technology on combustion control is very important same as selection of carrier gas with less nitrogen and faculty of airtight furnace and so on. SOx content remains in low value of around 130 ppm except for final period of melting.

Recovery of carbon dioxide is possible as above mentioned. Nitrogen content, which is main component except carbon dioxide, can be reduced down to 6 % less.

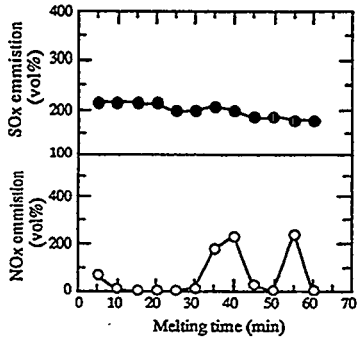

Figure 17 Changes of NOx and SOx

Result of thermal efficiency and yield in melting of copper and aluminum

Based on result in melting of iron above mentioned, optimum condition of high thermal efficiency and metal yield are respectively

examined experimentally. Outline of experimental result is following. Experimental conditions is shown in Table 6 and thermal efficiency and yield in Figure 18. Thermal efficiency and yield are as high as those of iron melting.

Table 6 Experimental conditions

Raw materials		
	AL-ingot (ton/ch)	0.4
	Cu-scrap (ton/ch)	1.0
P.C. burner condition		
	P.C. feed rate(kg/hr)	90
	Carrier gas (Nm^3/hr)	27
	O_2 flow rate(Nm^3/hr)	120
	O_2 preheat temp.(K)	873

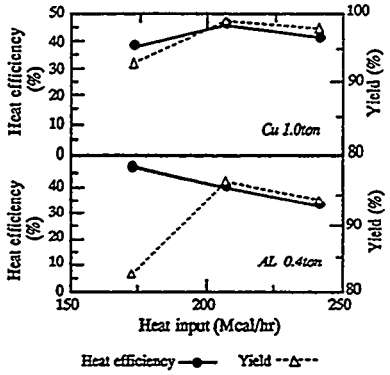

Table 7 Comparison of energy and main consumption data of different processes based on 100% steel scrap

	EAF	EOF	NSP
Electric power (kWh/ton)	380-480		
Coal/coke (kg/ton)	10-15	110	85
Natural gas (Nm^3/ton)	4		
Oil (L/ton)	3	10	
Oxygen (Nm^3/ton)	0-35	170	125
Yield (%)	90-92	89-90	93
Heat efficiency (%)	55	32	60

Comparison with other processes for melting of steel scrap

As melting processes of steel scrap, various kinds of new processes are proposed besides Electric Arc Furnace as present main process. Among those processes, Energy Optimizing Furnace (EOF) has been applicable to actual production. Consumption unit of electricity and other fuel and so on are shown together with brief comparison of both processes in Table 8. New process described in this paper has attractive features in lower consumption, flexibility of operation and cheap equipment.

CONCLUSION

New oxy-coal burner with preheater of oxygen, can be applicable to metal melting system. Technology on effective melting possible to high thermal efficiency and yield can be developed and responded to preventive measures against environmental disruption. The scale-up and improved tests have been carried out.

REFERENCES

1.The iron steel institute of Japan , *Recent Progress of Steelmaking Technology in Electric Arc Furnace (3rd Edition)*, 1993 .
2.R.Weber,D.Nose,L.morsoletto H.C Pfeifer , *Larevue de metallurgie-CIT*, 1994 , p439-444

THE EFFECTS OF BENEFICIATION ON ASH FORMATION IN A PILOT-SCALE COMBUSTOR

T.M. Strobel and J.P. Hurley
Energy & Environmental Research Center
University of North Dakota
and
O.K. Chow and A.A. Levasseur
ABB Power Plant Laboratories
Combustion Engineering Inc.

INTRODUCTION

Ash formed during coal combustion in a utility boiler can deposit and impede heat transfer, thus decreasing the efficiency of the system. Coal cleaning is used to decrease the amount of mineral matter in coal, which may minimize deposition problems. In order to study the effects of coal cleaning on coal combustion, the U.S. Department of Energy Pittsburgh Energy Technology Center has contracted with Combustion Engineering Inc. for a multi-year project to determine the combustion characteristics of beneficiated coal-based fuels. The specific objectives of the program are 1) to develop an engineering database that will provide detailed information on the properties of approximately fifteen beneficiated coal-based fuels (BCFs) influencing combustion, ash deposition, ash erosion, particulate collection, and emissions; and 2) to apply this technical database to predict the performance and economic impacts of firing the BCFs in various commercial boiler designs. The University of North Dakota Energy & Environmental Research Center (EERC) is providing sample analysis for this program.

This paper focuses on the effect of beneficiation on fly ash particle size, chemical composition, and deposition of Upper Freeport, Pittsburgh No. 8, and Illinois No. 5 beneficiated products produced by the selective microagglomerate process (1). These products were tested in ABB Power Plant Laboratories Fireside Performance Test Facility (FPTF) at 3.0×10^6 to 4.0×10^6 Btu/hr under standard and staged low-NO_x firing conditions.

The fuels, in-flame solids collected at various elevations in the FPTF, and fly ashes were characterized for bulk chemistry, mineralogy, ash particle size and chemical composition distributions. These samples were chosen to follow mineral transformations during combustion and to provide information about the changes in ash particle size and composition caused by beneficiation. Bulk ash particulate and deposit compositions were determined by x-ray fluorescence (XRF) and crystalline phases by x-ray diffraction (XRD). Computer-controlled scanning electron microscopy (CCSEM) was used to quantify the composition and size distributions of coal minerals and fly ash particles with sectioned diameters between 1 and 100 μm (2). The CCSEM provides detailed information on size and composition of individual particles that can be useful for interpreting ash behavior during combustion.

RESULTS

Upper Freeport Fuels

The microagglomerate beneficiation process reduced the Upper Freeport coal ash loadings on a calorific value basis by approximately 29% (from 6.3 to 4.5 lb/10^6Btu). However, with the exception of sodium enrichment which probably was retained from coal precleaning, the chemical composition of the product ash was relatively unchanged from that of the feed coal (Table 1).

TABLE 1

Normalized Compositions of the Upper Freeport[a] Feed and Product Fuels

Oxide, wt%	Feed[a]	Product
SiO_2	46.5	44.5
Al_2O_3	24.0	24.0
Fe_2O_3	21.4	20.9
TiO_2	1.2	1.4
P_2O_5	0.3	0.5
CaO	1.4	1.7
MgO	1.0	1.0
Na_2O	0.4	1.4
K_2O	2.3	2.4
SO_3	1.2	1.3
Ash Loading, lb/10^6 Btu	6.3	4.5

[a]Upper Freeport coal was from the Sheesley Pit Mine, Jefferson County, PA, P&N Coal Company. The coal was precleaned at CQ Inc.

The results from CCSEM analysis show that the cleaning process did not dramatically change the size distribution of the mineral particles in the product fuel. The feed fuel contains 80 wt% of its mineral particles in the less-than 10-μm size range, and the product contains 90 wt% in the same range.

Figure 2 shows the relative quantities of the major types of mineral particles detected by CCSEM in the two fuels. Both the feed and product contain similar percentages of quartz, kaolinite, and potassium-alumino-silicates. The iron-containing phases were not preferentially removed during cleaning. The pyrite content in the product was slightly higher, probably as a result of the less efficient removal of this mineral by the beneficiation process. The unknown, or unclassified, analyses in both fuels are mixtures of pyrite, clay, and sulfur-containing species. The similar chemical compositions between the feed and beneficiated microagglemerate product are due to the fact that most of the mineral phases present in Upper Freeport are included in the fuel particles (Figure 3). The beneficiation process was not as effective removing included mineral grains than minerals excluded in fuel particles.

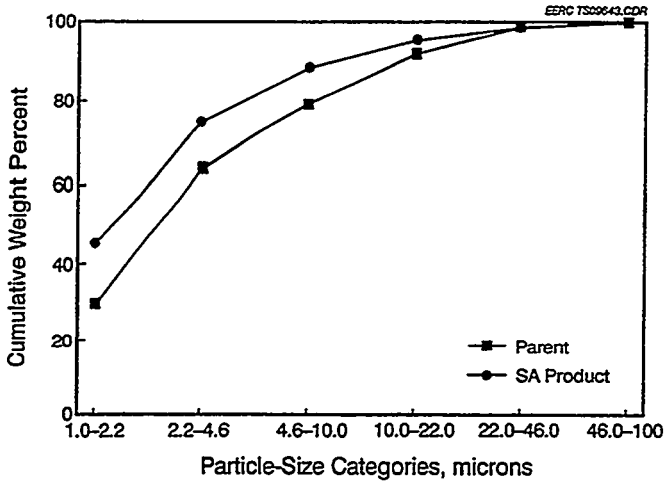

Figure 1. Cumulative size distributions of the inorganic particles in the Upper Freeport feed and product fuels.

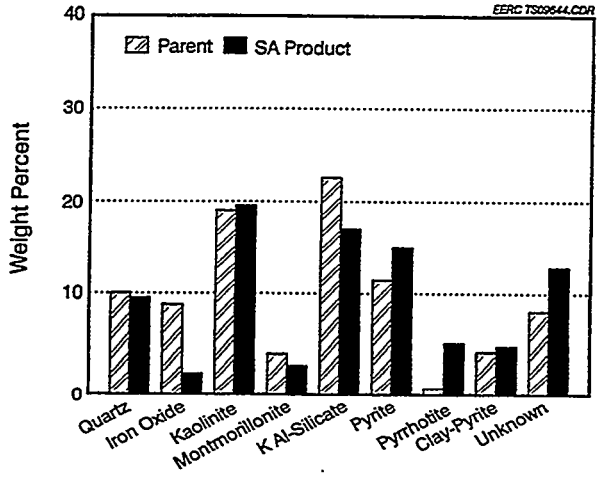

Figure 2. Composition distributions of the inorganic particles in the Upper Freeport feed and product fuels.

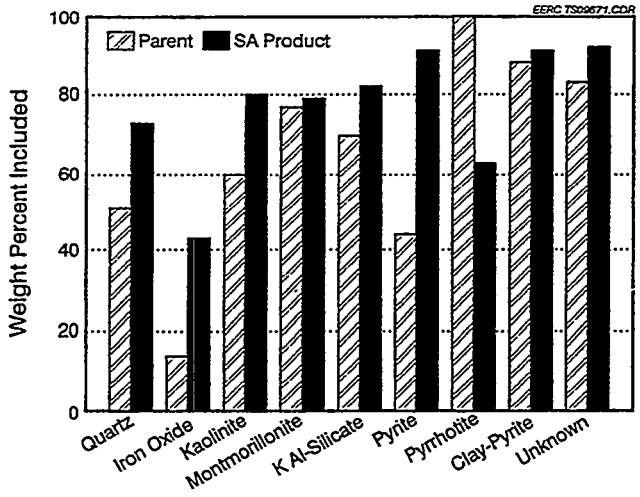

Figure 3. Composition distributions of the inorganic particles in the Upper Freeport feed and product fuels that are included in fuel particles.

The physical and chemical characteristics of the furnace particulate and deposit samples generated between staged or standard firing conditions were generally similar. The results from the 3.6 × 10^6 Btu/h staged and standard firings are presented for discussion purposes.

The cumulative size distributions of the parent and product ashes from the 3.6 × 10^6 Btu/h staged and standard firing combustion test runs in the FPTF are shown in Figures 4 and 5. In general, the furnace particulate samples show increases in the size of the particles compared to their respective fuel mineral particles, indicating some coalescence between mineral particles has occurred under either staged or standard firing conditions.

The chemical composition of the minerals in the feed and product fuels changed during the combustion process. The results can be illustrated by the particulate samples collected at the FPTF furnace outlet plan during staged and standard firing conditions. Most of the pyrite constituents in both fuels were oxidized and interacted with alumino-silicate to form iron-alumino-silicates during combustion. The main mineral phases present in the two particulate samples include quartz, kaolinite,

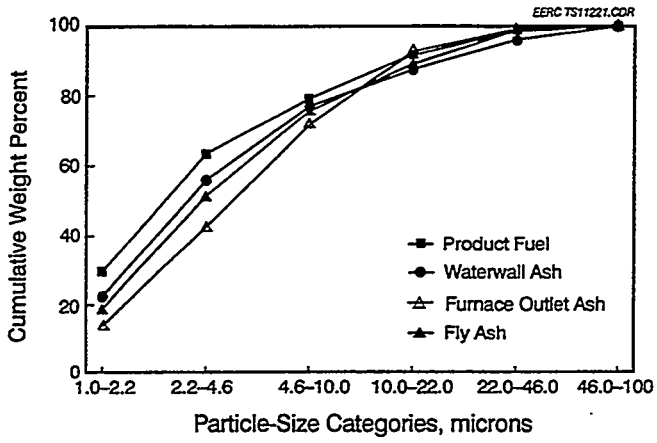

Figure 4. Cumulative size distributions of the inorganic particles in the Upper Freeport feed fuel and ashes.

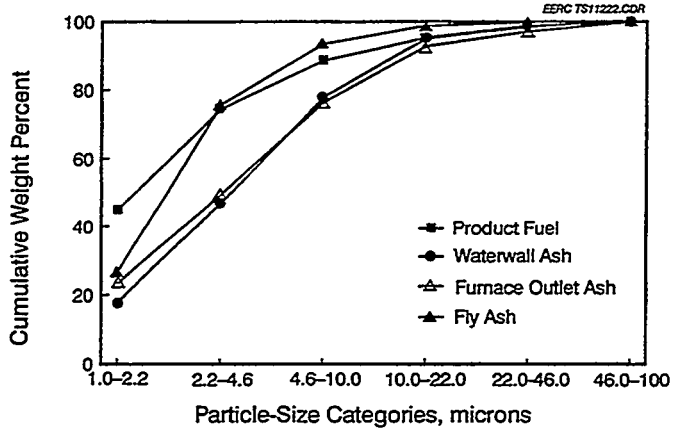

Figure 5. Cumulative size distributions of the inorganic particles in the Upper Freeport product fuel and ashes.

potassium–alumino-silicates, iron–alumino-silicates and unknown (Figures 6 and 7). The major crystalline phase in the ashes is quartz (SiO_2), and minor phases include iron-rich spinels ($Mg[Al,Fe]_2O_4$), mullite ($Al_6Si_2O_{13}$), and hematite (Fe_2O_3).

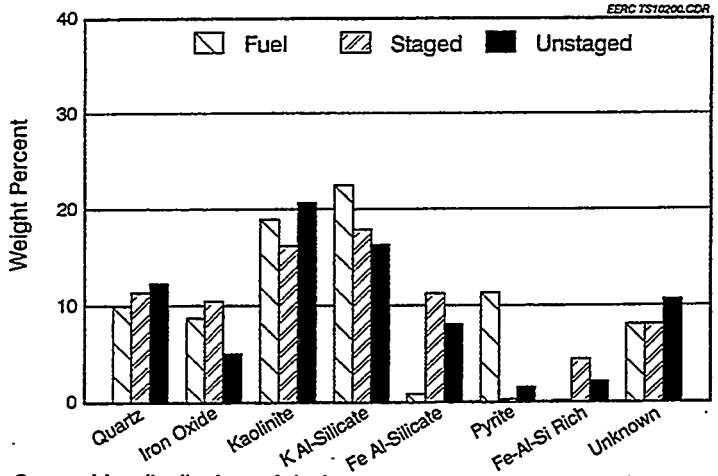

Figure 6. Composition distributions of the inorganic particles in the Upper Freeport feed fuel and particulate collected at the FPTF furnace outlet.

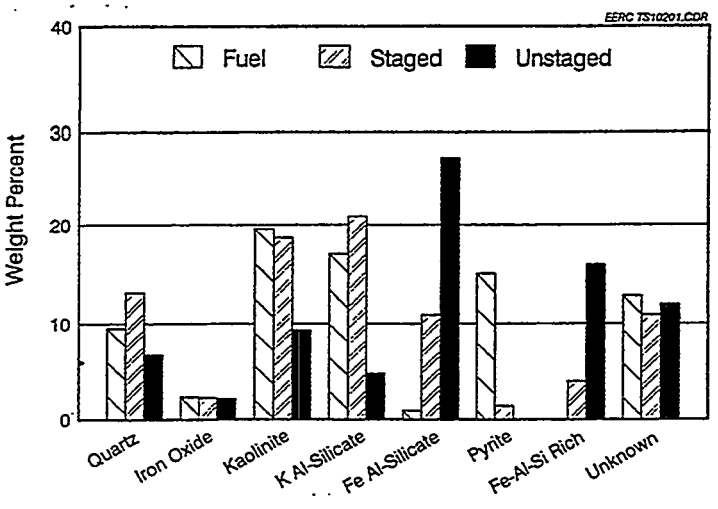

Figure 7. Composition distributions of the inorganic particles in the Upper Freeport micro-agglomerate fuel and particulate collected at the FPTF furnace outlet.

The relative fluidity or viscosity of deposits is an important characteristic that affects sintering rates and removability of deposits. Figure 8 shows the viscosity distributions of the amorphous material in the deposits that formed on the waterwall panel. The data were acquired from SEMPC analyses used to determine the composition distributions of the deposits. The composition distributions were then used to calculate a viscosity distribution of the amorphous material, with an algorithm developed by Kalmanovitch and Frank (3). The temperature used in the calculations is an average gas temperature of 1650°C (3000°F) at the level of the waterwall panel during many FPTF runs. The distributions indicate that the product deposits have a slightly lower viscosity distribution than the feed coal deposits for the illustrated viscosity ranges. At the FPTF gas temperature of 1650°C (3000°F), iron would be present as ferrous iron (Fe^{2+}) and would act as a fluxing agent (4). However, the slight difference in viscosity did not affect the overall FPTF combustion test results, as the cleanability of the waterwall deposits was similar between the feed and product fuels at either staged or standard firing conditions (5, 6).

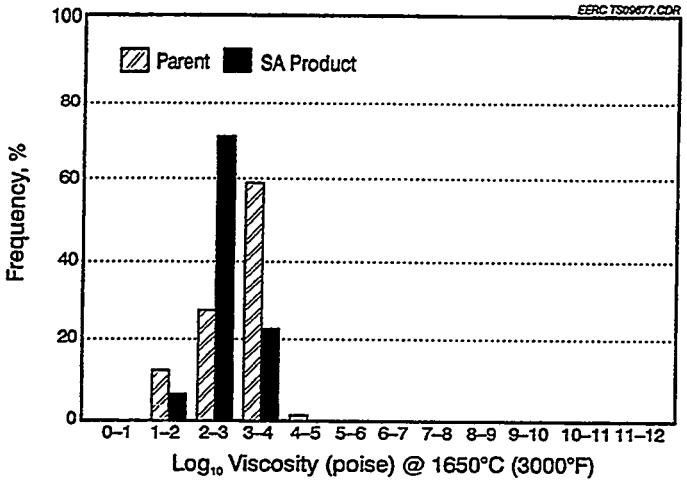

Figure 8. Calculated viscosity distributions in the waterwall deposits generated from the Upper Freeport feed and Product fuels at staged firing conditions

In summary, the parent and product ashes from the 3.6×10^6 Btu/hr staged and standard firings have similar particle-size and composition distributions, with minor variations. The major mineral phases present are quartz, kaolinite, potassium-alumino-silicate, and iron–alumino-silicate, with only slight variations in the relative amounts between the firing modes.

Pittsburgh No. 8 Fuels

The microagglomerate beneficiation process reduced the Pittsburgh No. 8 feed coal ash loadings by approximately 15%. Comparison between the feed coal ash and product ash shows the oxide bulk chemistries are similar between the two fuels (Table 2). The relatively higher iron content in the product ash is attributed to the less efficient removal of this species, compared with other minerals, by the beneficiation process.

TABLE 2

Normalized Compositions of the Pittsburgh No. 8 Feed and Product Fuel Ashes

Oxide, wt%	Feed[a]	Product
SiO_2	44.3	41.8
Al_2O_3	24.6	24.5
Fe_2O_3	19.2	23.5
TiO_2	1.2	1.3
P_2O_5	0.5	0.4
CaO	3.5	2.7
MgO	1.0	1.0
Na_2O	0.5	0.9
K_2O	1.3	1.3
SO_3	3.7	2.3
Ash Loading, lb/10^6Btu	4.6	3.9

[a]Pittsburgh No. 8 coal was from the Emerald Mine, Greene County, PA, Cyprus Coal Company. The coal was precleaned at the mine.

CCSEM analysis performed on the Pittsburgh No. 8 beneficiated fuel shows the fuel contains 90 wt% of its mineral particles in the <10-μm size range. The main mineral phases present are quartz, kaolinite, potassium-alumino-silicate, pyrite, and unknown particles. Most of the inorganic minerals in the fuel are included, or locked, within the fuel particles, which suggests that they have a greater chance than excluded mineral grains of interacting with each other during the combustion process and forming ash particles that usually have a lower melting temperature than that of the original mineral grains.

The type of firing, staged or standard, did not dramatically change the particle-size distribution or the composition of the minerals in the Pittsburgh No. 8 particulate samples. Figures 9 and 10 illustrate the composition distributions for the fuel and ash minerals for the two firing conditions. In both cases, the amount of kaolinite decreases from the fuel to the ashes, and iron–alumino-silicates increase. Pyrite also decreases from the fuel to the ashes, indicating oxidation of pyrite and subsequent interaction with alumino-silicates to form iron–alumino-silicates. The unclassified phases in the ashes are mainly mixtures of iron–alumino-silicates with calcium- or sulfur-rich inclusions.

Although the CCSEM analysis did not detect major differences between the particulate samples, reducing atmosphere at staged firing will have an effect on the oxidation state of iron. Iron in the reduced state acts as a fluxing agent, which may cause high-iron particles to become sticky, developing furnace deposits that are more difficult to remove by sootblowing, as was demonstrated by the FPTF combustion testing (5).

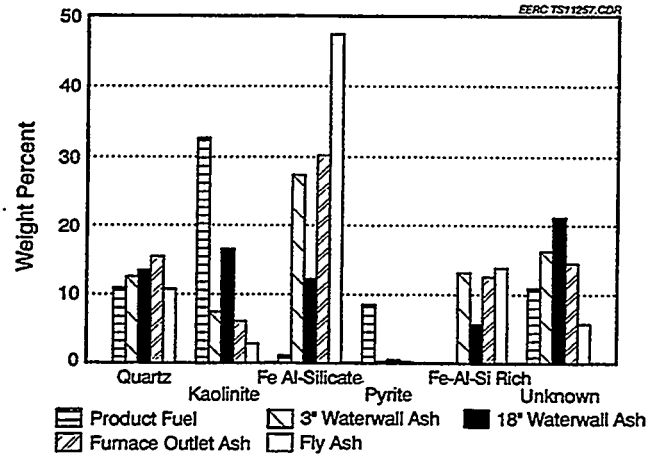

Figure 9. Composition distributions of the inorganic particles in the Pittsburgh No.8 product fuel and ashes from staged firing.

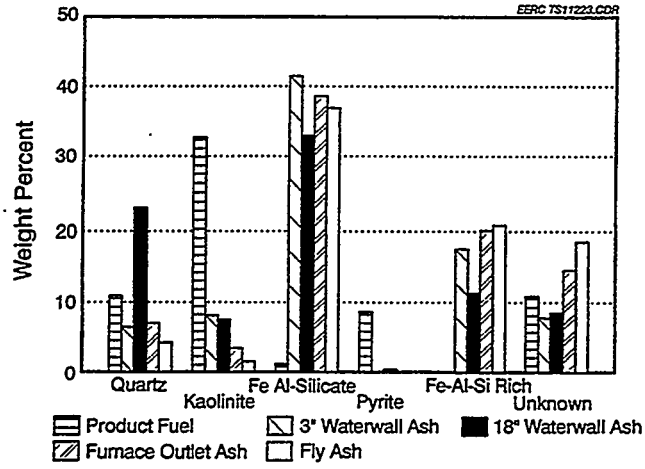

Figure 10. Composition distributions of the inorganic particles in the Pittsburgh No. 8 product fuel and ashes from standard firing

Illinois No. 5 Fuel

The ash content and normalized ash composition of the Illinois No. 5 feed and product fuels are shown in Table 3. The ash loading showed a dramatic decrease from the feed to the product fuel ash. The significant difference is due to the fact that the Illinois No. 5 feed coal was not precleaned, while the Upper Freeport and Pittsburgh No. 8 feed coals were precleaned prior to the microagglomerate beneficiation process. The chemical compositions show preferential removal of silicate minerals by the beneficiation process. The silicon content was reduced while the iron content was relatively enriched from the feed to the product ash.

TABLE 3

Normalized Compositions of the Illinois No. 5 Feed and Product Fuel Ashes

Oxide, wt %	Feed[a]	Product
SiO_2	52.9	44
Al_2O_3	21.2	20
Fe_2O_3	11.8	24
TiO_2	1.1	2
P_2O_5	0.5	1
CaO	3.1	2
MgO	1.7	2
Na_2O	0.8	1
K_2O	3.2	2
SO_3	3.4	1
Ash Loading, lb/10^6Btu	20.3	4.0

[a]Illinois No. 5 coal was from the Wabash Mine, Wabash County, IL, AMAX Coal Company. The coal was not precleaned.

CCSEM analysis conducted on the beneficiated product indicate the major mineral phases present include quartz, kaolinite, potassium-alumino-silicates, pyrite and unknown. The unknown particles in the fuel are clay–pyrite mixtures with high concentrations of potassium. As with the Upper Freeport and the Pittsburgh No. 8 fuels, most of the inorganic minerals in the fuel are included, or locked, within the fuel particles suggesting that they have a greater chance to interact with each other during the combustion process.

The main mineral phases determined by CCSEM in the staged and standard particulate ashes are illustrated in Figures 11 and 12. For both firing conditions, the data show a trend of decreasing potassium-alumino-silicates and increasing iron-alumino-silicate and potassium-iron-alumino-silicate phases from the waterwall and furnace outlet in-flame solids to the fly ashes.

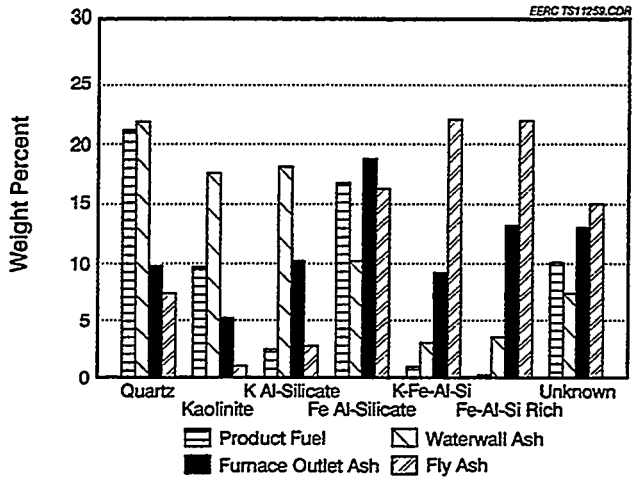

Figure 11. Composition distributions of the inorganic particles in the Illinois No. 5 product fuel and ashes from staged firing.

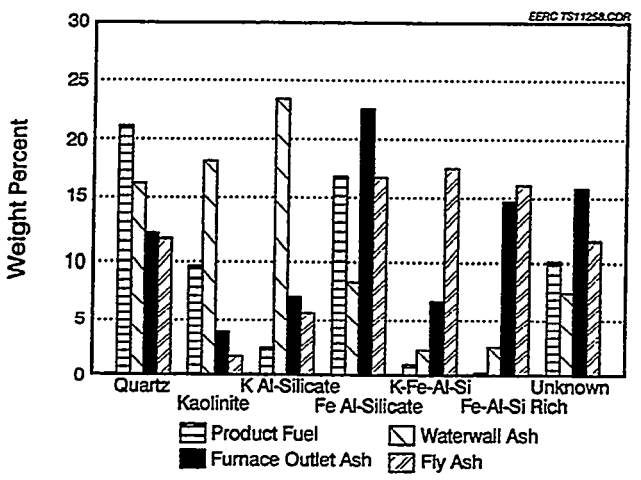

Figure 12. Composition distributions of the inorganic particles in the Illinois No. 5 product fuel and ashes from standard firing.

CONCLUSIONS

The effect of microagglomerate beneficiation process was fuel dependent. The process reduced ash loadings on a calorific value basis at various levels depending on the feed coal. The chemical composition of the minerals in Upper Freeport product was relatively unchange, while the Pittsburgh No. 8, and Illinois No. 5 products show preferential removal of silicate minerals and enrichment in iron contents. The relative increases in iron contents are probably due to their less efficient removal compared to the other mineral species.

CCSEM analysis conducted on the furnace particulate and fly ash samples from staged and standard firings of a given fuel were similar. The major changes included oxidation of pyrite and subsequent interactions with alumino-silicate species. However, as demonstrated from the combustion test results of these fuels, the reducing atmosphere associated with staged firing generated more difficult to remove waterwall deposits. Iron in the reduced state can act as a fluxing agent to develop low viscosity deposits that are more difficult to remove by sootblowing.

REFERENCES

1. Engineering Development of Selective Agglomeration, final report, March 1993 US DOE Contract No. DE-AC22-89PC88879.

2. Zygarlicke, C.J.; Steadman, E.N. "Advanced SEM Techniques in the Study of Coal Minerals," *The International Journal of Scanning Electron Microscopy*, **1990**, 4 (3), 579–590.

3. Kalmanovitch, D.P.; Frank, M. "An Effective Model of Viscosity for Ash Deposition Phenomena," In *Mineral Matter and Ash Deposition from Coal;* Engineering Foundation, 1988.

4. Nowok, J.W.; Hurley, J.P.; Stanley, D.C. "Local Structure of a Lignitic Coal Ash Slag and Its Effect on Viscosity," *Energy & Fuels* **1993**, *7*, 1135–1140.

5. Chow, O.K.; Griffith, B.; Levasseur, A.A. Hargrove, M.J. "Evaluation of Beneficiated Coal Microagglomerates in Various Fuel Forms," Presented at the 19th International Conference on Coal Utilization and Fuel Systems, Clearwater, FL, 1994.

6. Chow, O.K.; Hargrove, M.J.; Levasseur, A.A. "Combustion Characterization of Beneficiated Coal-Based Fuels," Presented at the 10th Annual Coal Preparation, Utilization, and Environmental Control Contractors' Conference, Pittsburgh, PA, 1994.

SO_2 AND NO_x CONTROL IN A PULVERIZED COAL-FIRED VORTEX COMBUSTOR

Jianrong Chen and Sen Nieh
Department of Mechanical Engineering
The Catholic University of America
620 Michigan Avenue, N.E.
Washington, DC 20064
Tel: 202-319-5170 Fax: 202-319-4499

ABSTRACT

This paper presents the major results of the emission levels of NO_x and SO_2 controlled respectively by staged air feeding and limestone injection in a pulverized coal-fired vortex combustor. Results showed that the strong swirl in the combustor formed by the progressive injection of secondary air along the combustor height gives a uniformly low combustion gas temperature around 900 °C and a progressively changing environment from reducing to oxidizing along the combustor height, which collectively results in a low NO_x formation and emission. It is found that the NO_x emission is 40% lower with staged secondary air injection than that in one stage combustion. SO_2 emission can also be effectively reduced by limestone injection due to the intense gas-solid mixing in the stable circulating suspension layers of particles in the combustor. At Ca/S molar ratio of 2.0, the desulfurization efficiency reached 75%.

INTRODUCTION

Increasingly stringent standards for pollutants (NO_x, SO_2, and particulate) emission from coal combustion have led to the introduction of many pollutant-controlling measures. These measures fall into three major categories [1]: 1) advanced combustion measures; 2) flue gas treatment techniques; 3) deep cleaning of coal. Flue gas treatment has been extensively studied and several effective measures have been developed [1]. However, because of its increased cost and

additional complexity of the combustion system, more attention has been put on the *clean coal combustion technology* in recent years [2,3], by which the pollutants formation may effectively be controlled *during* the combustion process. During this clean coal combustion technology program, many advanced coal combustors were developed.

An innovative coal-fired combustion device, vortex combustor, was successfully developed at the Catholic University of America [4,5] for small and medium scale industrial boiler and furnace applications to overcome some deficiencies of conventional pulverized coal-fired combustion systems, such as low combustion efficiency, low firing intensity, and high pollutants emission. This vortex combustor features a gas-tight vertical annular combustion chamber and a coaxial center exhaust tube, and is characterized by a low temperature combustion environment and a strong swirl produced by progressive tangential air injection.

In order to explore its performance in NO_x and SO_2 emission abatement, theoretical analyses and experimental studies have been carried out on a 0.1 MW exploratory model and a 0.6 MW proof-of-concept model. During combustion tests on both models, two types of coal, Polish "Jaworzno" high sulfur content coal and West Virginia Bituminous, were burned under different operating conditions. The pulverized coal is pneumatically fed into the combustor bottom, while combustion air is tangentially injected into the annular combustion chamber through one, two, or multiple arrays of air nozzles located at some strategic levels. Staged combustion with different secondary air injecting mode was evaluated for the suppression of NO_x formation. To achieve a high sulfur retention during combustion, limestone is injected into the combustor along with the pulverized coal. Temperature distribution, flue gas composition, and flyash properties were measured during the combustion tests.

EXPERIMENTAL

The vortex combustion test system used in this study is schematically shown in Figure 1. It consists of a vortex combustor and its associated auxiliary subsystems for fuel supply, air supply, startup, heat removal, flue gas exhaust, and instrumentation.

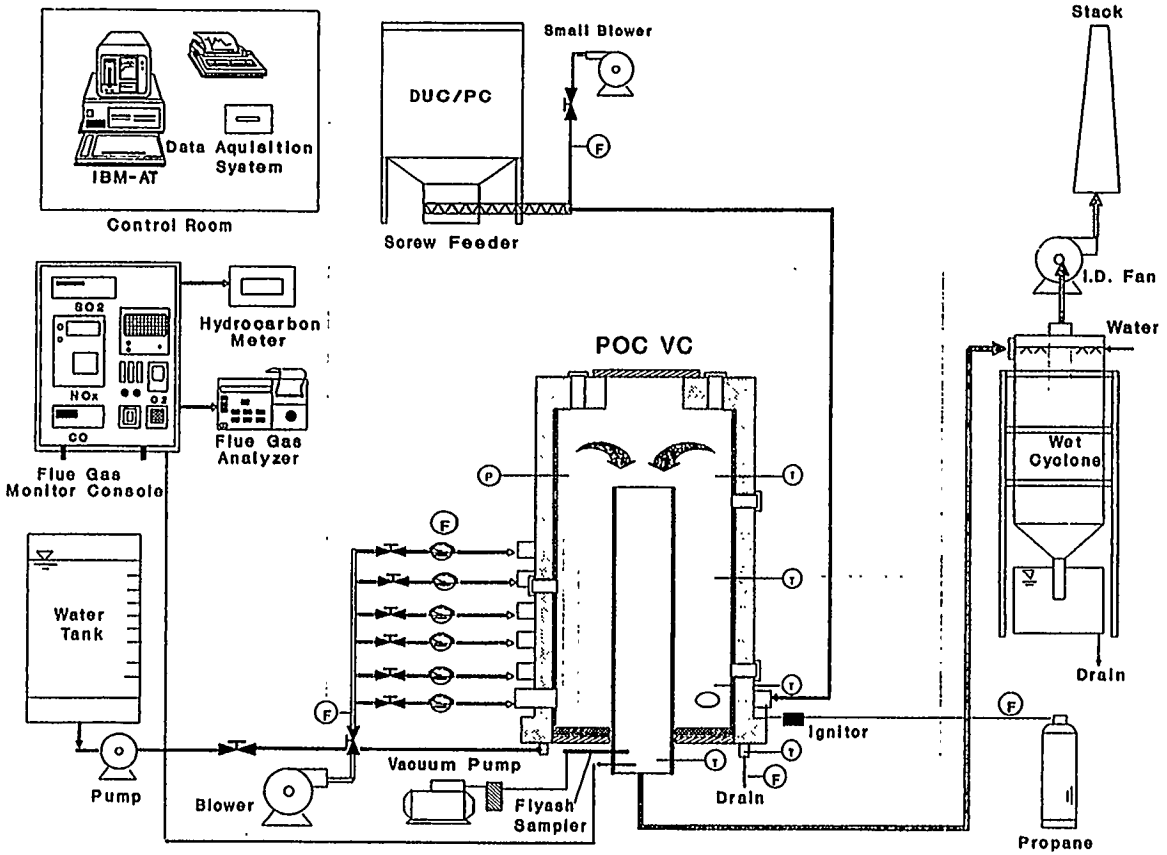

Figure 1 Schematic diagram of the proof-of-concept model test setup

Coal is injected to the combustor bottom along with the primary air provided from a high pressure blower, and the secondary air is injected tangentially into the annular combustion chamber at different heights of the combustor to form a staged combustion in a strong swirling, recirculating, and developing turbulent flow environment. Flue gas is exhausted downwards from the center tube to the stack via a cyclone dust collector. A computer-assisted data acquisition system was used to accelerate the data-taking process, and four groups of instrumentation were used for the measurements in the experiments: temperature, flow, combustion, and pollution.

The vortex combustor test models used in this system are a 0.1 MW exploratory model and a 0.6 MW proof-of-concept model. Two types of coal were burned in the combustion tests: Polish "Jaworzno" high sulfur content coal and ultra-fine West Virginia Bituminous. Their properties are listed in Table 1.

Table 1 Properties of tested coals

	Polish Jaworzno Coal	West Virginia Coal
Proximate Analysis: (% wt)		
Moisture	5.0	0.72
Volatile Matter	29.6	34.80
Fixed Carbon	45.6	63.00
Ash	19.8	1.48
Heating Value (kJ/kg)	23,635	34,290
Ultimate Analysis: (% wt)		
Carbon	57.60	86.83
Hydrogen	3.93	5.14
Nitrogen	1.07	1.54
Oxygen	9.37	3.64
Sulfur	3.23	0.63

RESULTS AND DISCUSSIONS

Studies [1,6] have proven that *thermal* NO_x formation is mainly dependent on the combustion temperature and the oxygen concentration in high temperature regions

(T > 1500 °K), while *fuel* NO_x formation, although not well understood, is controlled basically by the nitrogen content of the fuel and the degree to which the fuel is mixed with air particularly during the early stages of combustion when the bound nitrogen is liberated from the fuel. From this point of view, NO_x formation/emission may be suppressed by modifying the conditions for combustion, such as the stoichiometry and the combustion temperature. These modifications can be achieved by modification of the burner itself or externally through modification of the air or fuel flow to the combustion chamber [7], which include such measures as low excess air, low temperature, staged air injection, and staged fuel injection (reburning). The vortex combustor, with staged combustion in a low temperature environment as its feature, is expected to be effective in the suppression of NO_x formation.

Gas temperature distributions in the combustion chamber are measured at different operating conditions and are shown in Figure 2. Figure 3 shows the numerical results of the axial distribution of the *thermal* NO_x concentration at these conditions. In the numerical calculation for thermal NO_x formation, the Zeldovich reaction mechanism was used [8]. It could be found that most NO_x is produced in the lower part of the combustion chamber, and that its emission is largely dependent on the formation rate at early stage of combustion. The effect of staged secondary air injection can be clearly seen from Figure 3(a). If large portion of secondary air is provided to the bottom of the combustor (90% at level a, 10% at level b), NO_x formation in this region is very large, which is obviously caused by the larger oxygen concentration and the higher temperature (*hot spot* at the combustor bottom as shown in Figure 2) in this region. This high formation rate in this region results in a high NO_x emission at the combustor exit. However, by using a staged air injection, such as 45% at level a, 30% at level b, 15% at level c, and 10% at level d, because of the more uniformly-distributed gas temperature (1100 ± 100 °C) in the combustion chamber and the lower oxygen concentration at the earlier combustion stage, the NO_x formation is greatly abated, and its peak value is only about 1/3 of the case mentioned above. As a result, the NO_x emission is about 40% lower. Figure 3(b) shows the effect of the overall excess air on NO_x formation, where the air distribution (injecting mode) is kept unchanged. As expected, larger excess air brings about a faster NO_x formation and a

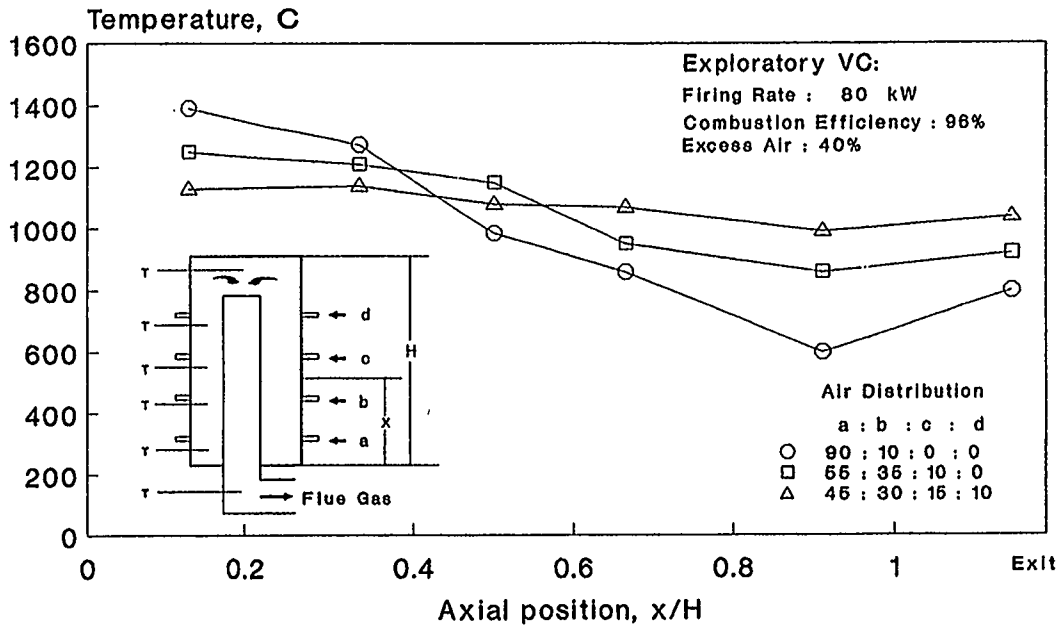

Figure 2 Illustration of temperature controllability in vortex combustors

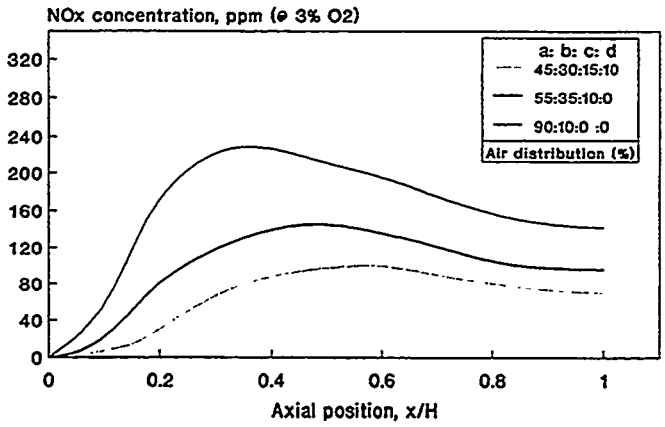

(a) Effect of secondary air injection

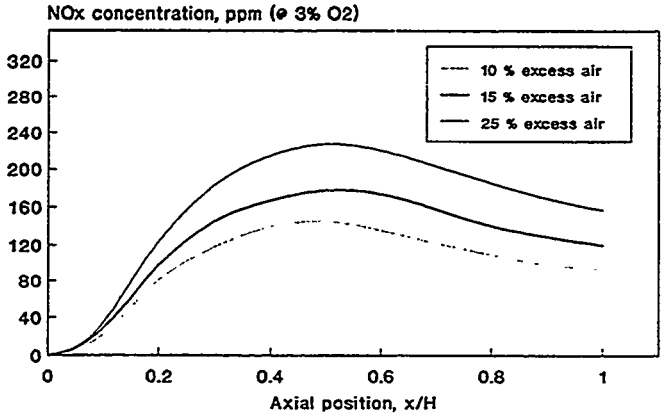

(b) Effect of excess air

Figure 3 Effect of excess air and staged-secondary air injection on NOx formation

higher NO_x emission. unfortunately, the excess air coefficient cannot be set too low, otherwise it will hurt the combustion performance and result in a high CO emission and a low combustion efficiency. Consequently, it cannot be used as an effective measure to control NO_x emission.

Figure 4 shows some measured results of NO_x emission from the exploratory hot model burning pulverized West Virginia bituminous at different combustion temperatures. During combustion tests, the total excess air and air injecting mode were kept unchanged, and the different combustion temperature was obtained either by changing heat removal rate or by changing fuel feeding rate. It is seen that, besides the local temperature distribution (*hot spots*), the averaged gas temperature in the combustion chamber also has a large effect on NO_x emission. A low and uniform combustion temperature is critically important for NO_x reduction. However, in most pulverized-coal-fired entrained-bed combustors, the combustion temperature is usually high (~1600 °K at the core, required by combustion performance), which makes the *in-furnace* NO_x abatement difficult.

A comparison between Figures 3 and 4 shows that the measured NO_x emission is higher than the calculated. One of the reasons is believed to be the ignorance of *fuel* NO_x in the numerical modelling. This also indicates that, for coal combustion, *fuel* NO_x plays an important role in composing the NO_x emission.

Sulfur dioxide emission is largely dependent on the sulfur content of the burned coal, if no other measures such as sorbent addition are adopted. To evaluate the ability of sulfur retention in the vortex combustor by means of a sorbent addition, a higher sulfur content coal, Polish "Jaworzno" coal, was used in the combustion experiments on the exploratory hot model. Properties of the Polish coal are listed in Table 1. During the combustion tests, pulverized limestone with a mean diameter of 126 μm was premixed and injected into the combustor together with the pulverized Polish coal. The feeding rate of limestone was pre-determined according to the selected Ca/S molar ratio.

Combustion tests show that SO_2 emission from the vortex combustor can be effectively reduced by the well-known limestone injection technique. The measured results are shown in Figure 5(a) [9]. It is seen that the SO_2 emission is as high as

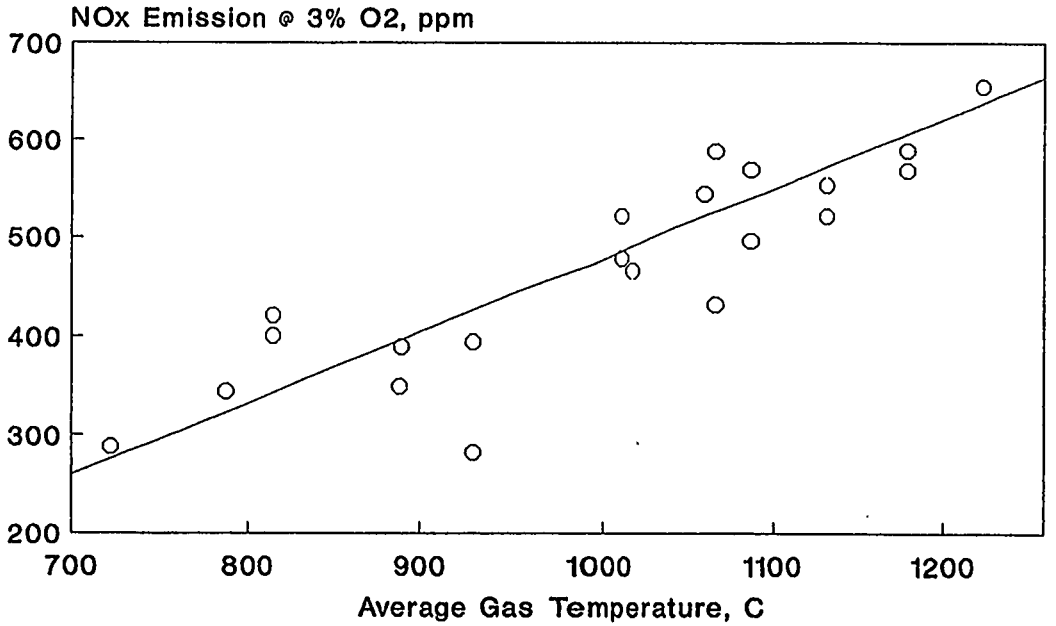

Figure 4 Effect of average combustion temperature on NOx emission

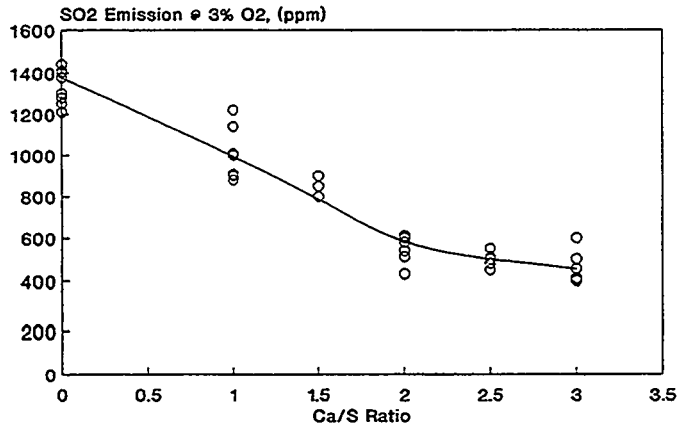

(a) SO_2 emission

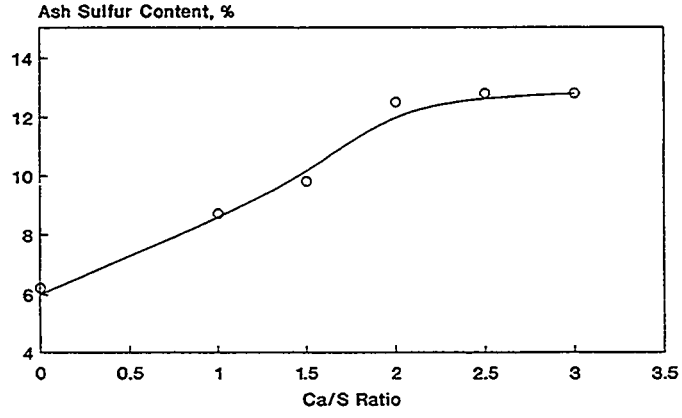

(b) Ash sulfur content

Figure 5 Measured results of SO_2 emission and sulfur content of ash

1400 ppm under ordinary operating conditions where no limestone is used. However, along with an addition of the pulverized limestone, the SO_2 emission will be greatly reduced as the limestone feeding rate increases, and can be as low as 500 ppm when the Ca/S molar ratio reaches 2.0. When further increasing the limestone feeding rate, this effect becomes weakened. The analytical results of sulfur content in the ash samples collected under different Ca/S ratios are shown in Figure 5(b), where the values of sulfur content in ash are converted to the base of the original ash content of the coal. The ability of sulfur retention in the vortex combustor can be clearly seen. With an addition of limestone, most sulfur in coal will be burned, fixed, and retented in a solid form, and removed with ash disposal. The efficiency of desulfurization reached 70% or higher when the Ca/S molar ratio is 2.0 or larger.

The mechanism governing the process of desulfurization by limestone adoption can be expressed by the following two reactions:

Calcination reaction: $CaCO_{3(s)} + \text{heat} \rightarrow CaO_{(s)} + CO_{2(g)} \uparrow$

Desulfurization reaction: $CaO_{(s)} + SO_{2(g)} + \frac{1}{2}O_{2(g)} \rightarrow CaSO_{4(s)} \downarrow$

These two reactions can only effectively take place if there is enough reaction time, moderate temperature level (~1200 °K), and strong gas-solid turbulent mixing. Considering the vortex combustor in terms of its suitable temperature level, strong turbulent mixing, and its special features in controlling particle (including limestone) behavior, the high sulfur retention efficiency obtained via limestone injection is not a surprise. Limestone particles, after being injected into the combustion chamber, will be kept dynamically in the combustor for an extended period of time to get calcinated in the decomposition reaction, similar to the situation in fluidized beds. Because of their relatively larger sizes and weights compared with those of the pulverized coal, the calcinated lime particles will be trapped in the combustion chamber and form several stable *suspension layers* in the upper part of the combustion chamber. Therefore, the flue gases, containing SO_2 that is produced during coal pyrolysis, have to go through these layers. In the meantime, the temperature level in the combustion chamber is maintained below 1300 °K, which is favorable for the desulfurization

reaction. All these factors make it possible to achieve an efficient sulfur retention in the vortex combustor by means of sorbent addition.

CONCLUSIONS

Test results show that the vortex combustor exhibits a good combustion performance for pulverized coal, during which NO_x formation may be effectively abated by the progressive injection of secondary air along the combustor, and SO_2 emission can also be reduced by the limestone addition technique. It is found that the NO_x emission is 40% lower with staged secondary air injection than that in one stage combustion. At Ca/S molar ratio of 2.0, a desulfurization efficiency of 70% was reached.

ACKNOWLEDGEMENT

This work was supported jointly by Pittsburgh Energy Technology Center, and Germantown Headquarters, U.S. Department of Energy. Their support is gratefully acknowledged.

REFERENCES

[1] Sloss, L.L., A.K. Hjalmarsson, H.N. Soud, and L.M. Campbell, et al, Nitrogen Oxides Control Technology, Fact Book, Noyes Data Corporation, Park Ridge, New Jersey, 1991.

[2] "Advanced Combustion Systems and Technology Development", PRDA No: DE-RA22-86PC90259, Pittsburgh Energy Technology Center, U.S. Department of Energy, 1986.

[3] "Advanced Environmental Control Technologies for Coal-Based Power Systems, Phases I & II", PRDA No: DE-RA22-94PC92291, Pittsburgh Energy Technology Center, U.S. Department of Energy, 1994.

[4] Nieh, S., and T.T. Fu, "Development of a Non-slagging Vortex Combustor (VC) for Space/Water Heating Applications", Proc. 5th Int. Coal Conference, Pittsburgh, 9/1988.

[5] Nieh, S. and T.T. Fu, "Annular Vortex Combustion", U.S. Patent No. 5,123,361, 6/1992.

[6] Desoete, G., "Overall Reaction Rates of NO and N_2 Formation from Fuel Nitrogen", 15th Symp. (Int.) on Combustion, 1974.

[7] Desoete, G., "Overall Kinetics of Nitric Oxide Formation in Flames", Survey Paper, Flame Chemistry Panel Meeting of the IFRF, 1974.

[8] Chen, J., "Multiphase Flow and Pulverized Coal Burning in A Vortex Combustor", Ph.D. Dissertation, The Catholic University of America, 1994.

[9] Nieh, S., J. Chen, and X. Cao, "Combustion Tests of Polish Coals in a Commercial-Scale Vortex Combustor", Proc. 10th Int. Coal Conference, Pittsburgh, Sept. 1993.

Predicting the Performance of NO_x Reduction by Gas Reburning

Bruce W. Li
Senior Research Engineer

David Moyeda
Manager, Process Design & Evaluation

Roy Payne
Senior Vice President

Energy and Environmental Research Corporation
18 Mason, Irvine, California 92718

ABSTRACT

The supplemental use of natural gas in a reburning mode has been developed as a retrofit technology for the control of NO_x emissions from coal–fired utility boilers. The technique involves combustion staging, achieved through the injection of natural gas at an elevation above the main burner zone, followed by the subsequent use of overfire air to complete burnout. The fundamentals of the reburning process are well understood, and a large body of data exists concerning controlling parameters and their relative impacts on NO_x reduction. In recent demonstrations of the technology on full–scale utility boilers, NO_x reduction levels up to 70% have been achieved.

As a result of recent full–scale boiler demonstrations, much of the understanding gained at laboratory and pilot experimental scales has been verified, refined, and incorporated into various computational models. These models can be used to evaluate the performance achievable by the application of gas reburning to a specific coal–fired utility boiler, or to assess options for optimizing the performance of an installed system. This paper describes how computational tools were used to evaluate the reduction in NO_x emissions from a 33 MW_e cyclone–fired boiler retrofit with gas reburning. The two primary computer tools in this study were a two–dimensional furnace combustion and heat transfer code, and a one–dimensional chemical kinetics code equipped with a detailed hydrocarbon and nitrogen reaction mechanism.

The approach used to model the performance of the gas reburning system on the 33 MW_e cyclone–fired boiler is described and the results of a sensitivity analysis of the various process parameters on the reburning system performance are discussed. The key parameters evaluated in this study included the operating stoichiometries of the cyclone furnace, reburning zone, and burnout zone and the reburning fuel jet mixing time.

INTRODUCTION

In response to increasing regulatory pressure world wide, operators of coal–fired utility boilers are considering the use of a wide range of technologies for reducing NO_x emissions. Gas reburning is one technology which can be used to control NO_x emissions from coal–fired utility boilers (Pratapas and Bluestein, 1994). Reburning is a combustion modification technology which removes NO_x from combustion products by using fuel as the reducing agent. Full–scale

demonstrations of this technology have shown that the emissions reduction achievable are higher than those typically attainable with other technologies, such as low-NO_x burners and selective non-catalytic reduction, and that it is applicable to all types of firing configurations, such as wall-, tangential-, and cyclone-fired boilers.

Application of gas reburning to a coal-fired boiler conceptually divides the furnace into three zones: primary zone, reburning zone, and burnout zone. In the primary zone, the normal firing system is used to fire the bulk of the fuel, typically 80 to 90 percent of the total heat release, at an excess air level which is close to or slightly below normal operation. The reburning fuel is injected downstream of the primary zone to create a slightly fuel-rich "reburning" zone. The reburning fuel provides the remainder, normally 10 to 20 percent, of the total heat input. In this zone, hydrocarbon radicals generated during breakdown of the reburning fuel reduce nitric oxide formed in the primary zone to molecular nitrogen, N_2. In the burnout zone, combustion air is added to complete fuel burn out and to bring the boiler back to a normal operating excess air level. A number of small-scale studies have provided insight into the parameters which control the effectiveness of the reburning process (Greene et al., 1986; Overmoe et al., 1986).

In considering the application of gas reburning to a particular boiler or in evaluating the performance of an existing gas reburning system, it is desirable to predict the performance achievable with gas reburning. In this regard, the reburning process lends itself more easily to computational modelling than do other combustion modification techniques. This paper describes one approach to predicting the performance of gas reburning for coal-fired utility boiler applications where the critical processes—fluid mechanics, radiative heat transfer, and chemistry—are treated in a semi-coupled fashion. In this approach, a zoned heat transfer model is used to describe the time-temperature profile of flue gas in the boiler furnace. The fluid mechanics used in the zone model are prescribed from a physical model or from a computational fluid dynamics model. The results of the heat transfer model are then used to develop a chemical kinetics model which simulates the key gas-reburning processes including: mixing rates of reburning fuel and overfire air, reaction chemistry in the reburning zone, and combustion in the burnout zone.

In the study described in this paper, the above modelling approach was applied to a 33 MW_e cyclone-fired boiler. This boiler was the subject of a field demonstration of gas reburning technology (Folsom et al., 1994). The objectives of this study were to verify the gas-reburning modelling technique by comparing model results with full-scale field data, and to use the models to assess the impacts of key process parameters on the NO_x control performance of the technology. The process parameters evaluated in this study included: cyclone (primary zone) stoichiometry (SR_1), reburning zone stoichiometry (SR_2), burnout zone stoichiometry (SR_3), quantity of flue gas recirculation (FGR), and entrainment of overfire air into the reburning zone. In this paper, reburning zone stoichiometry is defined as the ratio of the total air supplied to the cyclone furnace and reburning zone to the total stoichiometric air requirements of the primary and reburning fuels.

The following two sections present a brief description of the two computer models used in the study, followed by an overview of the modelling approach. The subsequent section discusses the results of a sensitivity analysis of the impacts of key gas-reburning process parameters on the NO_x reduction performance of the process. This paper concludes with recommendations for optimizing the operation of the gas-reburning system on the cyclone-fired boiler.

MODEL DESCRIPTION

For this study, the NO_x reduction achievable with gas reburning was simulated by two computer models: a furnace heat transfer model and a chemical kinetics model. The models are decoupled, but operate with coupled input and output. This section provides an overview of the two computer codes, and their individual roles in the NO_x performance evaluation. More detailed descriptions of

the computational techniques employed can be found elsewhere (Payne et al. 1988; Wu et al. 1990 and 1991; Li et al. 1993)

Furnace Heat Transfer Model

A two–dimensional furnace combustion and heat transfer model was applied to evaluate the thermal characteristics in the radiation–dominated boiler furnace. A key element of this model is the radiation submodel for calculating radiative heat exchange between all volume and surface zones in the boiler furnace. This submodel is based on a semi–stochastic method derived from pure Monte–Carlo techniques, uses the four weighted gray gas approach, and considers radiative species of CO_2 , H_2O, ash, char, and soot as non–gray components. The heat transfer model calculates radiative heat exchange between upper–furnace radiant heat transfer surface and the lower–furnace flame zone. The code is decoupled from the solution of the momentum conservation equation. For this study, the flow field was prescribed based on the results of isothermal flow modelling.

The heat transfer model has submodels to handle coal devolatilization, as well as char and volatile combustion. Coal particles are divided into ten different size classes, and are devolatilized according to a one–step Arrhenius rate law. Volatile packets are assigned statistically distributed lifetimes, and each packet reacts completely at the end of its assigned lifetime. Char oxidation is described by a global rate equation which considers diffusion and chemical reaction rates.

The geometry and set up of the heat transfer model for the 33 MW_e cyclone–fired boiler are shown in Figure 1. Figure 1–a illustrates how the boiler furnace was divided into 21 layers in the direction of the gas flow. Figure 1–b illustrates how the three–dimensional boiler is represented in the two–dimensional model as an axisymmetric cylindrical grid. This geometric transformation was performed while maintaining the heat transfer similarity between the model and the actual boiler. Seventy percent of the coal ash content was assumed to be captured in the cyclone furnace, while the rest of ash content was treated as fly ash. Char reactivity parameters (activation energy and frequency factor) for the char combustion model were specified based on the rank of the coal fired in this boiler.

Chemical Kinetics Model

The chemical kinetics model was developed to evaluate the impact of various control techniques on furnace NO_x emissions. The model is particularly suited for evaluation of the potential NO_x reductions associated with the application of gas reburning technology to coal–fired utility boilers. The key input parameters used in the analysis include the flue gas analysis and initial NO_x emissions from the primary combustion zone, furnace gas temperature profiles, residence time distributions, local stoichiometries upstream and downstream of the reburning fuel injection zone, reburning fuel and overfire air local mixing rates, and injection locations.

A basic part of the NO_x model is a package of detailed fuel/air chemistry modules which includes 43 species and 201 elementary reaction steps. Gas phase species important for NO_x formation and destruction from fuel bound nitrogen, such as NH_3, HCN, NO_x, and N_2O, are all included. A one–dimensional flame/reaction model is used to perform the chemical kinetics calculations (Kau et al. 1987).

In the kinetics model set–up for evaluating the application of gas reburning to the cyclone–fired boiler, distinctive zones in the furnace were identified and represented by a series of four plug flow reactors as shown in Figure 2. This figure also shows the correspondence of the zones to various furnace regions identified from a physical flow model study of the boiler. The zone arrangement follows the NO_x destruction path from the reburn–fuel mixing zone, through a post–mixing zone

where reaction occurs and where the furnace bulk flue gas mixes with overfire air entrained into the reburning zone, through a zone where overfire air is mixed into the flue gas, and then into a zone where the combustion products are quenched in the radiative/convective section of the upper furnace.

APPROACH

The study was carried out through the application of the computational models to a range of actual and potential boiler and reburning system operating conditions. The boiler heat transfer model was first applied to predict the temperature field resulting from various modes of operation. The resulting temperature data were subsequently incorporated into the chemical kinetics model to predict the impact on NO_x emissions. The parameters which were evaluated in this study were the primary, reburning, and overfire air zone stoichiometries, the entrainment of overfire air into the reburning zone, and the reburning fuel jet mixing time.

Due to the simplification and assumptions made in the modelling approach, the thermal model was first calibrated against boiler design and field measurement data to assure that the model was correctly simulating the thermal characteristics in the furnace. Calibration of the boiler thermal model was accomplished through application of the model to known boiler operating conditions at full load (33 MW_e). The mean gas temperatures predicted by the heat transfer model up to the upper-furnace superheater section are shown in Figure 3. Figure 4 compares the measured and predicted heat absorptions for the primary superheater (PSH), secondary superheater (SSH), and furnace water-walls including radiant platens and wing walls. Overall, the calibration was considered adequate since the predicted heat absorption in each section was within five percent of the measured values. Once the thermal model was calibrated, a series of cases were then run to assess the impact of gas reburning with various gas heat inputs on the mean gas temperature distribution, while cyclone and burnout stoichiometries were maintained at 1.09 and 1.22, respectively. The time-temperature profiles predicted by heat transfer model were then input into the kinetic model for prediction of reburning NO_x control performance.

In the kinetics model set-up, the mixing times of the reburning and overfire air jets were specified using empirical correlations for jet trajectory and entrainment based upon the reburning system design specifications. NO_x performance predictions were developed assuming that the reburning fuel followed a range of time-temperature histories with flow paths representing: perfect mixing of the reburning fuel and flue gas, mixing of the reburning fuel through the center of the boiler, and mixing of the reburning fuel along the cooler water-wall surfaces. Each of these paths represented jet mixing patterns which were observed from an isothermal flow model study of the boiler. Time-temperature histories for each path were determined based upon the results of the furnace heat transfer model. Figure 5 shows an example of time-temperature profiles for the case where the reburning fuel corresponds to 25 percent of the total heat input. These profiles represent potential paths which a packet of flue gas may thermally experience in the boiler furnace.

The initial NO_x concentration entering the reburning zone was based on the thermal load and operating stoichiometry of the cyclone burners. Typically, recycled flue gas is added to the reburning fuel nozzle for enhancing its mixing characteristics. Since the oxygen added to the reburning jet is insignificant compared to the available oxygen from the primary combustion products, the reburning zone stoichiometry was calculated without accounting for the oxygen in the recycled flue gas.

REBURNING PERFORMANCE PREDICTIONS

This section presents the results of an analysis of the impacts of process parameters on the performance of the reburning system. The parameters investigated include: primary, reburning, and overfire air zone stoichiometries, the entrainment of overfire air into the reburning zone, and the reburning fuel jet mixing time.

Reburning Zone Stoichiometry

Figure 6 compares model predictions to field data for operation of the gas reburning system at full load as a function of the reburning zone stoichiometry. The prediction band represents the variation in performance observed for the various reburning fuel mixing paths. Two sets of model predictions were performed: one set in which overfire entrained into the reburning zone was taken into account, and one set with an otherwise identical temperature field where the entrained overfire air was neglected. The amount of overfire air entrained into the reburning zone was estimated from the physical flow model study. The assumed and actual gas addition rate, expressed as a percent of total fuel heat input, are also plotted in Figure 6 as a function of the reburning zone stoichiometry.

As shown in Figure 6, good agreement between the model predictions and the field data was achieved. Entrainment of overfire air into the reburning zone increases the effective reburning zone stoichiometry at a given gas addition rate, resulting in higher NO_x emissions. The impact of overfire air entrainment is highest for gas heat inputs between 10 to 20 percent. At gas heat inputs more than 20 percent, the impact of overfire air entrainment becomes less significant.

Cyclone (Primary Zone) Stoichiometry

Figure 7 shows the impact of the cyclone operating stoichiometry on NO_x emissions at 33 MW_e as a function of the reburning zone stoichiometry. As the cyclone operating stoichiometry is reduced, less reburning fuel is required to reach a specific reburning zone stoichiometry. Therefore, reducing the cyclone stoichiometry reduces the costs associated with operating the gas reburning system, without adversely impacting the NO_x control performance. The model predictions indicate that NO_x reduction depends primarily on the reburning zone stoichiometry and is almost independent of the cyclone zone stoichiometry. This point is also illustrated in Figure 8, where the results shown in Figure 7 are graphed in terms of overall NO_x reduction.

Burnout Stoichiometry

Figure 9 shows the impact of the burnout zone stoichiometry on NO_x reduction at 33 MW_e with 25 percent gas heat input and a cyclone stoichiometric ratio of 1.15. The burnout zone stoichiometry is adjusted by controlling the overfire air flow rate. The model predictions indicate that increasing the burnout stoichiometry may slightly increase the NO_x emissions due to an increase of the overfire air entrainment into the reburning zone. However, the impact on overall performance is relatively small, which appears to be in agreement with the field results.

Mixing Impacts

Recirculation of flue gas to the reburning nozzles was used to promote mixing of the natural gas with the flue gases exiting the cyclone furnace. Figure 10 compares the predicted and observed impact of flue gas recirculation on reburning performance. In this figure, the quantity of recycled flue gas was varied from 2 to 10 percent of total flue gas at 33 MW_e with 25 percent gas heat input. The cyclone and burnout stoichiometries were set at 1.15 and 1.22, respectively. By increasing the amount of recycled flue gas, and hence the reburning fuel jet mixing time, some improvement in NO_x reduction would be expected.

SUMMARY

Computational models were used to evaluate gas–reburning performance on a 33 MW_e cyclone–fired boiler. The models were first calibrated against baseline operating conditions. A sensitivity study was then performed to evaluate the impacts of various process parameters on the effectiveness of gas reburning. The parameters evaluated included the various zone stoichiometries, and the mixing characteristics of the reburning fuel jets. The results of the model predictions indicate that:

- Good agreement between the model predictions and field data was obtained using the modelling approach outlined in this paper.
- For this application, the NO_x reduction with gas reburning depends on the reburning zone stoichiometry and is almost independent of the cyclone zone stoichiometry.
- Decreasing the cyclone stoichiometry reduces the requirement of natural gas to achieve the optimal reburning stoichiometry, resulting in a decrease in the cost of operating the reburning system.
- Increasing the reburning fuel jet mixing time, by increasing the amount of flue gas recycled to the nozzles or by modifying the nozzle design, should improve the NO_x control effectiveness.

Overall, the results of this study demonstrate that coupling of a detailed chemistry model with a simplified mixing model based on the results of thermal and physical models of the full–scale system can predict the general performance trends observed in full–scale systems. Therefore, models such as these can be used to design and evaluate full–scale reburning systems. To more accurately predict full–scale performance, computational models which couple chemistry with turbulent mixing are needed.

REFERENCES

Folsom, B., et al. *Demonstration of Gas Reburning–Sorbent Injection on a Cyclone–Fired Boiler.* Presented at the Third Annual Clean Coal Conference, Chicago, Illinois, September 6–8, 1994.

Greene, S.B., et al. *Bench Scale Process Evaluation of Reburning for In–Furnace NO_x Reduction.* ASME Journal of Engineering for Gas Turbines and Power, Volume 108, pp. 450–454, 1986.

Kau, C.J., et al. *Fundamental Combustion Research Applied to Pollution Formation, Volume IV—Engineering Analysis.* EPA–600/7–87–027, 1987.

Li, B.W., et al. *Use of Computer Models for Reburning/Cofiring Boiler Performance Evaluations.* ASME FACT Volume 17, Cofiring and NO_x Control, A.K. Gupta et al., editors, 1993.

Overmoe, B.J., et al. *Pilot Scale Evaluation of NO_x Control from Pulverized Coal Combustion by Reburning.* Proceedings of the 1985 Joint Symposium on Stationary Combustion NO_x Control, Volume 1; Utility Boilers, Applications, Electric Power Research Institute, Palo Alto, California, 1986.

Payne, R., et al. *Three–Dimensional Model Evaluation of Time/Temperature Histories of Combustion Products in a Coal Fired Utility Boiler.* Presented at the Fall Meeting of the CEA Thermal and Nuclear Section, Saskatoon, Saskatchewan, 1988.

Pratapas, J. and J. Bluestein. *Natural Gas Reburn: Cost Effective NO_x Control.* Power Engineering, pp. 47–50, May 1994.

Wu, K.T., et al. *Application of Engineering Computer Models and Modeling Techniques for Evaluating Boiler Thermal Performance and Emissions Control Processes.* ASME International Joint Power Generation Conference, Boston, Massachusetts, 1990.

Wu, K.T., et al. *Development and Application of a Gas Reburning Process Model for the Design of Boiler NO_x Reductions.* ASME International Joint Power Generation Conference, San Diego, California, 1991.

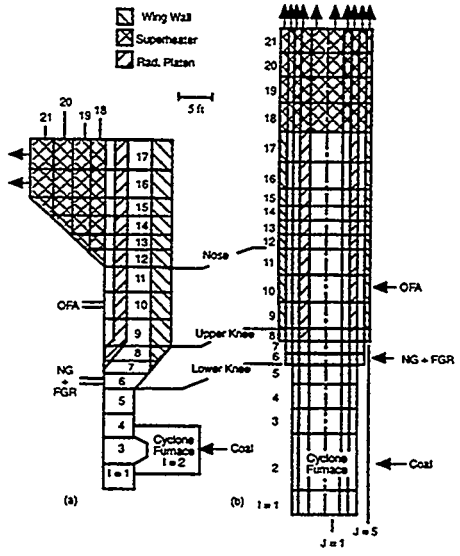

Figure 1. (a) Schematic of actual geometry, showing division into layers. (b) Two-dimensional cylindrical grids for computation.

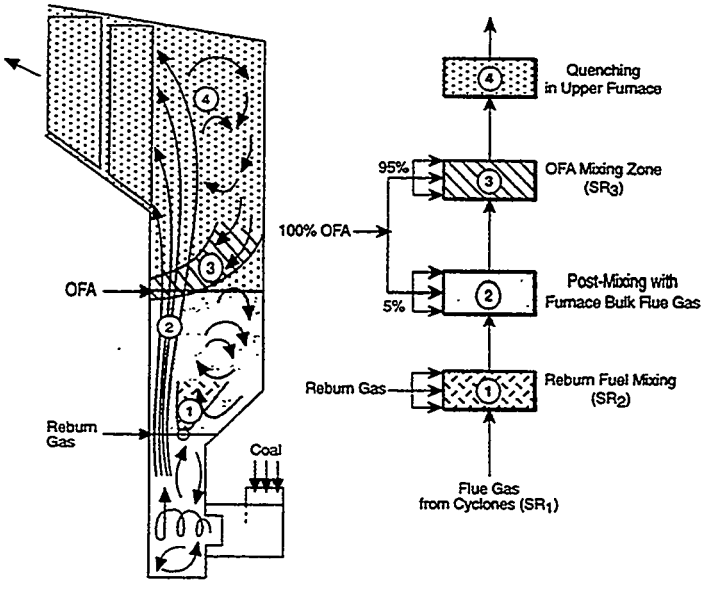

Figure 2. Distinct zones simulated by the kinetics model.

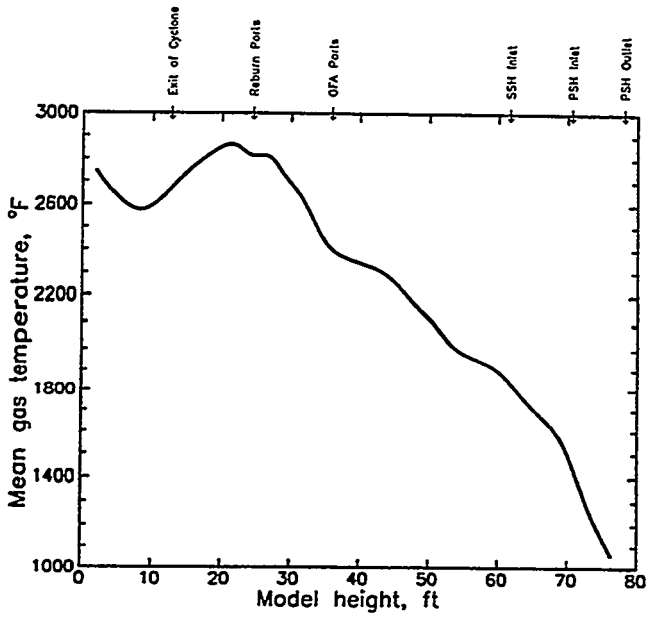

Figure 3. Furnace mean gas temperatures along model height for the calibration case.

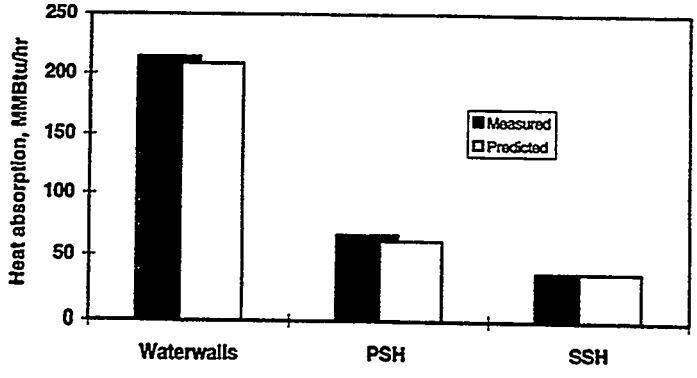

Figure 4. Comparison of predicted heat absorptions with measured data.

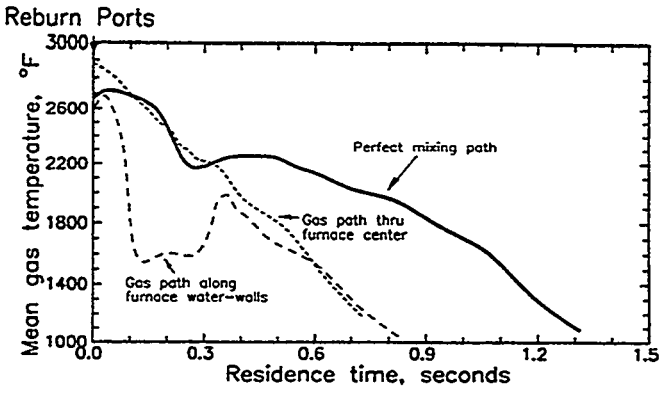

Figure 5. Time-temperature profiles for 25% gas-reburn case with various mixing paths.

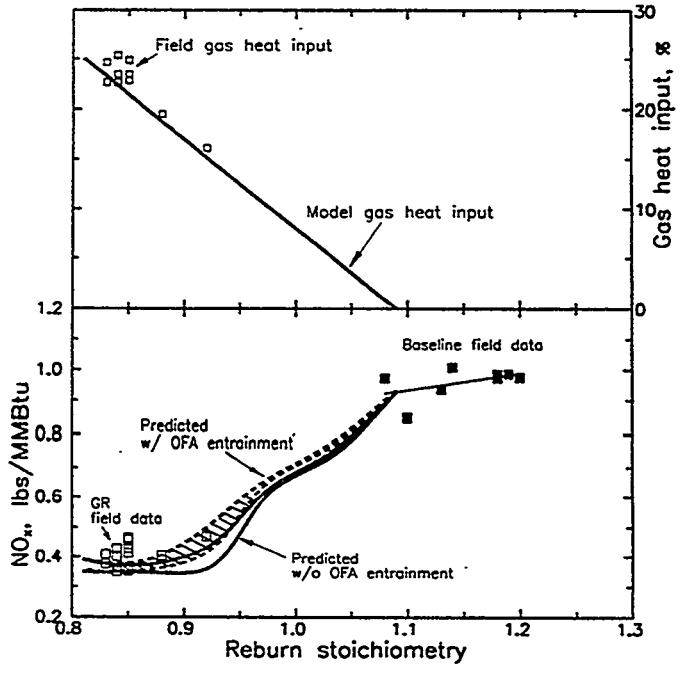

Figure 6. Impact of OFA entrained into reburn zone on NO_x emissions at 33 MW_e and comparison with field data. (SR_3 = 1.22)

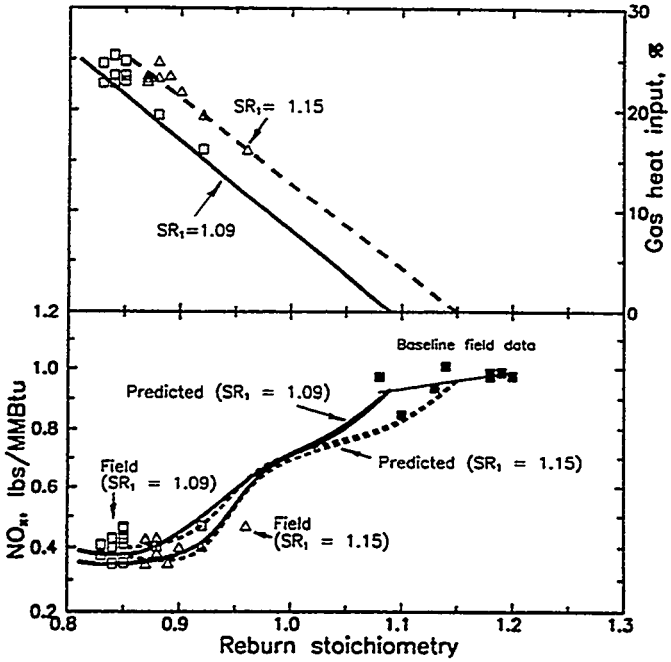

Figure 7. Impact of cyclone stoichiometry (SR_1) on NO_x reduction at 33 MW_e with SR_3 = 1.22.

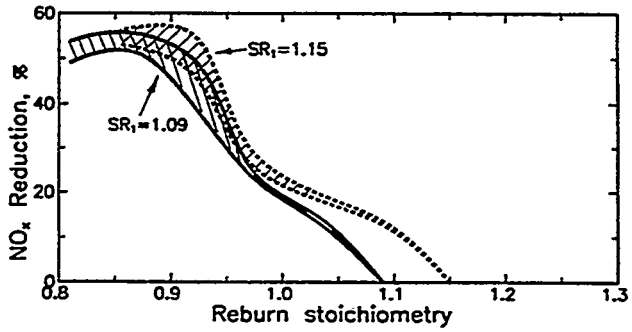

Figure 8. Impact of cyclone stoichiometry on NO_x reduction (adjusted baseline emissions) at 33 MW_e.

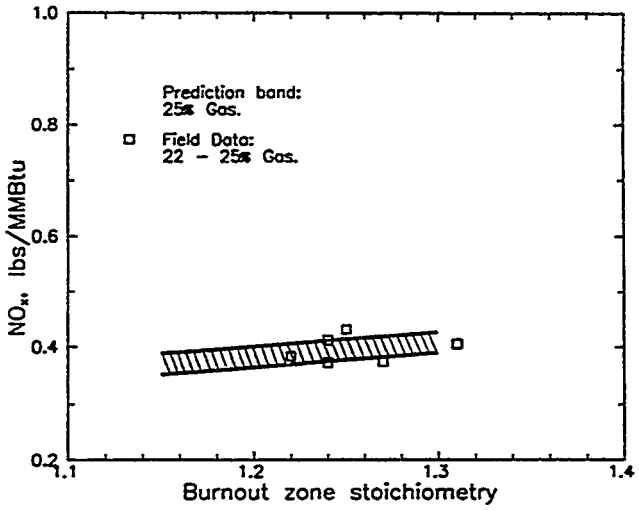

Figure 9. Impact of burnout stoichiometry (SR_3) on NO_x emissions for 33 MW_e and SR_1 = 1.15.

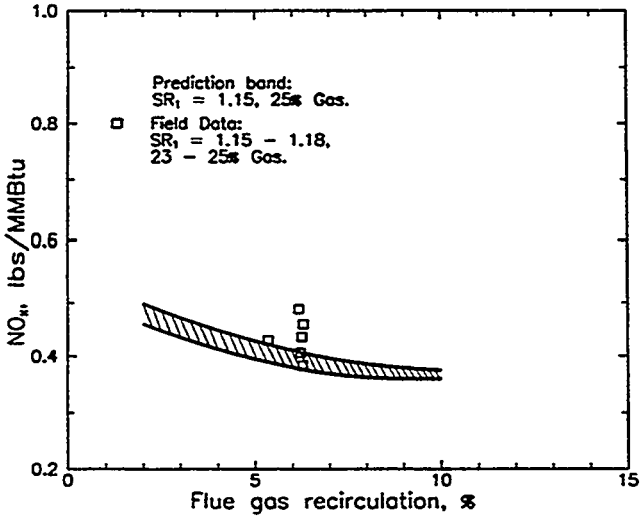

Figure 10. Impact of reburn nozzle FGR amount on NO_x emissions at 33 MW_e.

The Coal-Water Slurry Combustion Test on the 3MW Hot-Water Boiler in Shengli Oil Field, *Yao Qiang, Cao Xinyu, Liu Jianzhong, Huang Zhenyu, Zhao Xiang, Zhou Junhu, Wu Xiaorong, Ge Linfu and Cen Kefa, Institute for Thermal Power Engineering, Zhejiang University; and Hangzhou, Tang Yishi and Wu Liou Yan, ShanDong Petroleum Administrative Bureau in China, PEOPLE'S REPUBLIC OF CHINA*

This paper was received after pagination and is located on Page 739 of these Proceedings.

Greenhouse gas emissions and coal utilization

Irene M Smith, Deborah M B Adams, Charlotta Nilsson*
IEA Coal Research, 10-18 Putney Hill, London, SW15 6AA, UK.

ABSTRACT

Greenhouse gas emissions from coal are primarily CO_2 with some CH_4 and N_2O. CO_2 emissions from coal utilization amount to about one third of the CO_2 emissions from human activities. It is unclear exactly how sources of CO_2 may be accounted for among known sinks in the global carbon cycle. Different mechanisms for balancing the carbon budget affect projections of future CO_2 concentrations in the atmosphere resulting from CO_2 emissions. CH_4 emissions from coal production and use amount to about 8% of CH_4 emissions and N_2O emissions from coal combustion for about 5% of N_2O emissions (both related to emissions from human activities). These emissions need to be expressed in common terms so that the total greenhouse effect of a mixture of emissions may be estimated for each source. It is demonstrated that methods currently used to express these emissions in common terms, as global warming potentials, are inadequate and may underestimate the contributions from CH_4 and N_2O emissions relative to CO_2. Nevertheless, CO_2 is the most important greenhouse gas from coal. The most reliable estimates of global greenhouse gas emissions from coal are used to obtain an approximation of coal's contribution to the greenhouse effect of around 20%, half of this from coal-fired power generation.

The prevention of the formation of greenhouse gases from coal-fired power generation ideally requires in-depth knowledge of all energy use and greenhouse gas emissions over the complete fuel cycle. There are indirect emissions from the energy use in mining, beneficiation, storage and transport of the coal, in addition to other emissions of greenhouse gases such as CH_4 leakage from mining and post-mining operations. Progress towards such rigorous treatment is currently in its infancy. Hence, recent information is reviewed on abatement and control of CO_2 emissions from coal-fired power generation. CO_2 emissions can be reduced by increasing the efficiency of power generation. Advanced power generation has the potential to reduce the emissions by about 20-30% compared to the global net plant efficiency average of 36% (LHV). Cogeneration of heat and power offers a means of recovering heat from the steam cycle and further improving the total plant efficiency. It seems possible to reduce CO_2 emissions by about 60% by efficiency improvements. For greater CO_2 reductions, there are capture and disposal technologies which generally incur considerable energy penalties and costs. The CO_2 capture methods include absorption using amines, adsorption, cryogenics and membrane separation. For CO_2 disposal the largest potential sink is the ocean, with a potential capacity of 73 million $GtCO_2$. Other potential sinks with an estimated capacity of 150 - 520 $GtCO_2$ are aquifers, natural gas fields, oil fields, and forestry. However, there is still a lack of data on the various options.

* currently at EnerChem AB, Lund, Sweden.

INTRODUCTION

The most important greenhouse gas in the atmosphere is water vapour, which causes about two thirds of the total greenhouse effect. The second most important gas is carbon dioxide (CO_2), causing approximately 30%, then methane (CH_4), chlorofluorocarbons (CFC), nitrous oxide (N_2O) and ozone (O_3) together cause some 3% of the greenhouse effect. These gases may seem minor but increases in emissions of CO_2, CH_4, CFC, N_2O and O_3 enhance the greenhouse effect, resulting in increased evaporation of water vapour which amplifies the warming (IPCC, 1990; Lelieveld and others, 1993; Shine and Sinha, 1991).

Over the last few years international research has intensified in an attempt to improve understanding of all aspects of the greenhouse issue. The Intergovernmental Panel on Climate Change (IPCC), set up by the World Meteorological Organization and the United Nations Environment Programme, produced a scientific assessment of the issue in 1990 and revised it in 1992. A second scientific assessment is currently being prepared for publication in March 1995. An important part of the work of the IPCC together with the Organisation for Economic Cooperation and Development is to produce guidelines for national greenhouse gas inventories. All information which can contribute to an understanding of greenhouse gas emissions needs to be made more widely available to those concerned with coal and energy policy.

Coal research has already resulted in considerable improvements in power station efficiencies by use of increased steam pressure and temperature, and of steam reheat. There are many new abatement technologies which will continue to reduce greenhouse gas emissions from coal by improving conversion efficiency or reducing energy consumption. As a last resort, there are established practices to capture acid gases from the flue gas of power plants. A few commercial operations include CO_2 capture using amines in an absorption process. Other methods of CO_2 capture under development include adsorption, cryogenics and membranes. The potential and permanence of the storage sites to be used for disposal are important issues for all the options: aquifers, depleted oil and gas fields, oceans and biomass.

This paper is drawn from a *Perspectives* report from IEA Coal Research by Smith and others (1994) which updates the more detailed review by Smith and Thambimuthu (1991).

GLOBAL GREENHOUSE GAS EMISSIONS

Emissions of CO_2 from fossil fuels in 1990 are estimated by Marland and others (1994) using data from the UN Statistical Office as follows:

	GtC/y
Coals and peat	2.39
Oil industry	2.54
Gas industry	1.00
Total	*5.93*

There are uncertainties in accounting for all the CO_2 emissions which do not remain in the atmosphere. The carbon cycle is not balanced. The total sources from human activities of 6.1-9.1 GtC/y exceeded the total known sinks by 0.2-3 GtC/y during the 1980s (IPCC, 1992). Studies by Tans and others (1990) and Takahashi and others (1992) suggested that other carbon sinks on land in the Northern hemisphere were absorbing the excess CO_2 and the oceans were only taking up 1 GtC/y. Authors such as Brown and others (1992), Harrison and others (1993) and Dai and Fung (1993) support this view

and conclude that improved forest management and enhanced photosynthesis (fertilisation) due to increased CO_2 concentrations may contribute a major sink. On the other hand, Houghton (1993) considers that accommodation of such large amounts of carbon in vegetation is unlikely and uptake in soils cannot be estimated with sufficient accuracy to test the hypothesis.

The low oceanic uptake of carbon proposed by Tans and others (1990) has been revised by other authors who have suggested that transport of carbon to the oceans by rivers (Sarmiento and Sundquist, 1992; Siegenthaler and Sarmiento, 1993), and within the oceans (Broecker and Peng, 1992) may be removing the excess. Allowing about 0.8 GtC/y for riverine transport results in a total oceanic uptake of 1.8 GtC/y. This is similar to the value of 2.1 GtC/y obtained from isotopic studies by Quay and others (1992) although the uncertainties in current isotopic data are too large to confirm such estimates (Broecker and Peng, 1993). It has recently been suggested that radiocarbon data indicate an oceanic CO_2 sink which may be up to 25% smaller than the 2 GtC/y estimated (Hesshaimer and others, 1994; Joos, 1994).

None of these studies can do more than infer the carbon sinks. Direct observations are required to confirm their magnitude. The unexplained imbalance in the carbon cycle does not provide a firm foundation for forecasting CO_2 budgets in future from projected energy and land use emissions (Sundquist, 1993). Carbon cycle models with a balanced carbon budget have been used to examine how different mechanisms for closing the uncertainties in the carbon budget affect projections of future CO_2 concentrations (Rotmans and Den Elzen, 1993; Wigley, 1993). A balanced carbon cycle resulted in lower future CO_2 concentrations in the atmosphere than projected by the IPCC.

Fossil sources of CH_4 are estimated from isotopic studies to comprise about 20% of total CH_4 emissions, that is about 100 Mt/y or (70-120 Mt/y) (IPCC, 1992). Most of the estimates for CH_4 emissions from coal mining were found by Smith and Sloss (1992) to rely on very general assumptions as regards the properties of coal and coal mines. No simple methodology involving global extrapolations of CH_4 emissions from coal mined in specific areas is valid worldwide. The estimate of 25 Mt/y for global CH_4 emissions from coal mining in 1990 by the CIAB (1992) appears to be the most reasonable because it was calculated from the greatest amount of reliable data, from eight of the ten main coal-producing countries (Australia, China, the former Czechoslovakia, Germany, Poland, the UK, the USA and the former USSR). Subtracting 1 Mt/y for the CH_4 which was captured and used by industry results in 24 Mt/y for global CH_4 emissions from coal mining in 1990.

CH_4 emissions from coal use are generally regarded as insignificant but inefficient combustion does emit CH_4. Data are lacking on CH_4 emissions in non-OECD countries such as China and Eastern Europe where large quantities of coal are used inefficiently. However, a rough calculation (Smith and Sloss, 1992) using a wide range of emission factors indicates that at least 1-5 Mt/y are probably emitted worldwide from use of hard and brown coal. Berdowski and others (1993) also estimated about 5 Mt/y for global CH_4 emissions from coal combustion and metallurgical uses of coal.

Emissions of N_2O from coal use form part of the 0.1 - 0.3 Mt(N)/y attributed to stationary combustion. They were divided by De Soete and Sharp (1991) as: 0.24 ± 0.09 Mt(N)/y for coal; 0.089 ± 0.075 Mt(N)/y for fuel oil; and 0.025 ± 0.005 Mt(N)/y for natural gas. The estimate for coal assumes that all coal is currently burnt in conventional and not fluidised bed combustion (FBC) systems. Khalil and Rasmussen (1992) cited other studies from 1990 onwards which suggest that N_2O emissions from coal combustion would amount to a maximum of 0.2 Mt(N)/y. Khalil and Rasmussen also extrapolated data from plume experiments and estimated coal-fired power plants emitted 0.05 Mt(N)/y. Takeshita and others (1993) assumed a 3% share of coal use for FBC and 97% for conventional boilers and used emission factors from measurements on commercial plants in many countries. Their estimate for N_2O

emissions from global use of hard and brown coal ranged from 0.1 - 0.2 Mt(N)/y, in agreement with Khalil and Rasmussen.

CONTRIBUTIONS TO THE GREENHOUSE EFFECT

A mixture of greenhouse gas emissions from a given source at a given time cannot be compared with those from other sources without expressing the emissions in common terms. Actual temperature response or realised warming might appear to be most readily understood by policy makers. However, the model calculations required to convert emissions to temperature response depend on a further set of assumptions about the climate and thus introduce additional uncertainties. The least complicated common parameter is known as the radiative forcing of a gas. This is the perturbation of the balance between the radiative fluxes into and out of the earth-atmosphere system. The effect of each gas is usually expressed in terms of that of the equivalent CO_2 concentration.

The relative contributions (%) of trace gases to the greenhouse effect may be estimated from an increase in the concentration of each gas in the atmosphere and their greenhouse effects or potency relative to that of CO_2. Global warming potentials take account of the differing times that gases remain in the atmosphere, their greenhouse effect whilst in the atmosphere and the time period over which climatic changes are of concern. The IPCC global warming potentials are summarised in Table 1 and the IPCC (1990, 1992), Wuebbles and Edmonds (1991) and Harvey (1993) include a detailed discussion. There are difficulties in the determination of realistic global warming potentials. These relate to the indirect effects of emissions which need to be quantified in addition to the direct effects of greenhouse gas emissions and to use of CO_2 as reference gas.

The indirect effects of CH_4 emissions (the production of CO_2, stratospheric water vapour and tropospheric O_3 from CH_4 oxidation) are probably similar in magnitude to the direct effect. Other trace gases: CO, NO_x and NMHC, are more difficult to assess because the concentrations vary spatially as well as with time (IPCC, 1992). Hence a single global warming potential is not applicable to emissions in different regions.

Use of CO_2 as the reference gas introduces major uncertainties because of difficulties in evaluating the global carbon budget. A carbon cycle model involving only an oceanic sink to describe CO_2 uptake is likely to overestimate concentrations of CO_2. This leads to an underestimate of the global warming potentials of other greenhouse gases. The IPCC (1992) point out that increased concentrations of CO_2 in the atmosphere in future would lead to saturation of CO_2 absorption of radiation. This results in higher global warming potentials for other greenhouse gases than the values in Table 1, for example 15 for CH_4 when integrated over 100 y (Wuebbles and others, 1992). However, Caldeira and Kasting

Table 1 **Global warming potentials (by weight) relative to that of CO_2 over different time horizons (IPCC, 1992)**

	Estimated lifetime, y	Integration time horizon, y			sign of 'indirect' effect
		20	100	500	
CO_2	~120	1	1	1	none
CH_4 - direct only	10.5	35	11	4	positive
N_2O	132	260	270	170	uncertain
CFC-11	55	4500	3400	1400	negative
CFC-12	116	7100	7100	4100	negative

(1993) find that the effect of increased CO_2 concentrations would be compensated by the higher concentrations of dissolved carbon in the surface of the ocean which reduce the absorption of CO_2 from the atmosphere into the ocean.

The effect of using a balanced carbon cycle model on global warming potentials was investigated by Wuebbles and others (1992) and Rotmans and Den Elzen (1992) who otherwise used the assumptions in the IPCC (1992) study. Both studies resulted in increased IPCC global warming potentials for the non-CO_2 greenhouse gases, for example 13 and 40 for CH_4 over a 100 y time horizon. In addition, Rotmans and Den Elzen calculated transient global warming potentials. These take into account the delayed response of the climatic system due to the thermal inertia of the oceans. The values for CH_4 are higher at 45 (over 100 y).

Several authors are moving away from use of CO_2 as a reference gas. Wuebbles and Edmonds (1991) suggest that future global warming potentials should be defined as absolute measures of the potential for each greenhouse gas to affect climate - a trend shown by Schwartz (1993) and Zetterberg (1993) who use radiative forcing directly.

Wallis and Lucas (1994) point out that the IPCC global warming potentials are based on the actual increase in the concentrations of greenhouse gases rather than their rate of increase which is of greater environmental concern. They propose that discounted greenhouse costs should replace global warming potentials. A 3-4% discount rate would be roughly equivalent to the 30 y time horizon used in the global warming potentials. Preliminary results indicate that the use of discounted greenhouse costs related to rate of increase of the concentration of greenhouse gas would increase the importance of short-lived gases such as CH_4 compared with CO_2.

The many shortcomings of the IPCC (1992) global warming potentials discussed above must cast doubts as to their current usefulness in analysing greenhouse gas emissions and especially in formulating energy policy. However, global warming potentials are being used to express emissions in common terms for the purpose of quantifying the contributions of different sources to the enhanced greenhouse effect.

The contribution of global coal use to the enhanced greenhouse effect is evaluated from CO_2 emissions in 1990 (Marland and others, 1994) for the low and high estimates of the contribution from deforestation and land use adopted by the IPCC (*see* Table 2). The range in estimates for emissions from deforestation and land use gives rise to the ranges in percentage contributions in Table 2. The calculation is made for both the effect over 1 year (IPCC, 1990) based on increased concentrations during the 1980s and for the global warming potential over a time horizon of 100 y, using the weighting factors in Table 1. Taking a mean value for deforestation and land use, coal is responsible for about 17% of the enhanced greenhouse effect due to CO_2 emissions over one year and 23% for the integration over a time horizon of 100 y.

An approximate estimate for emissions of CH_4 and N_2O from coal is included in Table 2. The integration over 100 y excludes the indirect effects of CH_4 and therefore overestimates the role of CO_2. From these data it may be concluded that coal contributes 16-21% of the enhanced greenhouse effect over one year and 21-27% over a 100 y time horizon. Worldwide, power generation accounts for about half of all the coal used (Daniel, 1991). Hence the greenhouse effect from coal-fired power generation is about 11% of the total due to human activities. This contribution may be reduced by abatement and control technologies.

Table 2 **Contributions to the enhanced greenhouse effect in 1990**
(IPCC, 1990, 1992; Marland and others, 1994; Smith and Sloss, 1992; Takeshita and others, 1993)

Carbon dioxide	CO_2 emissions		Greenhouse effect, %	
	Gt C/y	%	over 1 y	over 100 y
Coal	2.4	36-28	20-15	26-20
Oil	2.5	38-29	21-16	27-21
Gas	1.0	15-12	8.2-6.3	11-8
Cement manufacture	0.2	2	1.3-1.0	1.7-1.3
Deforestation and land use	0.6-2.6	9-30	5-16	7-22
Total CO_2	*6.7-8.7*	*100*	*55*	*72*
Methane	CH_4 emissions			
	Mt/y	%		
Coal	25-29	7-8	1.0-1.2	0.7-0.8
Total CH_4	*360*	*100*	*15*	*10*
Nitrous oxide	N_2O emissions			
	Mt(N)/y	%		
Coal	0.1-0.2	3-6	0.2-0.4	0.1-0.3
Total N_2O	*3.4*	*100*	*6*	*5*
Total CFC			*24*	*12*
Total enhanced greenhouse effect			*100*	*100*

ABATEMENT

The prevention of the formation (abatement) of greenhouse gases from coal-fired power generation ideally requires in depth knowledge of all energy use and greenhouse gas emissions over the complete fuel cycle. Progress towards rigorous treatment over the complete fuel cycle is currently in its infancy so this section examines that part which concerns improving the efficiency of coal use. Extracting more useful energy from the coal reduces emissions of CO_2, the most important greenhouse gas from coal use, as well as other emissions in most cases. Much may be gained by increasing the combustion efficiency in countries such as China and India where a good deal of coal is burnt inefficiently. Even where the combustion efficiency is high there may be scope for improving the overall thermal efficiency.

It is important to be aware of the limitations of comparing efficiencies cited for different power generating systems without insight into the details of each project. One limitation is the different use of heating values for the fuel (HHV/LHV). Another important factor is the steam cycle condenser pressure. A low condenser pressure (or high vacuum) enables use of a steam turbine low pressure stage that can extract significantly more power than if the condenser pressure were higher. These factors together can easily add up to a 5% points difference in efficiencies between similar plants (Jansson, 1993).

The power generating efficiencies of various coal utilisation technologies are summarised in Table 3.

Table 3 Reductions in CO_2 emissions from coal-fired plants (Smith and others, 1994)

Technology			Net plant efficiency, % LHV	CO_2 emission factor, gC/kWh			CO_2 reduction, %
				coal	limestone	total plant	
Conventional systems	Pulverised coal	Reference plant	36	252	6	258	0
		Subcritical steam	39	233	5	238	8
		Supercritical steam	42-45	202-216	4-5	206-221	14-20
		Ultra-supercritical steam	47	193	4	197	24
	AFBC	Subcritical steam	39	233	10	243	6
Combined cycles	IGCC	Demonstrated systems	38-43	211-239	0	211-239	7-18
		Advanced systems	45-47	193-202	0	193-202	22-25
	PFBC	Subcritical steam	44	206	4	210	19
		Supercritical steam	46	197	4	201	22
	Hybrid*	Subcritical steam	47-49	185-193	4	189-197	24-27
		Supercritical steam	52	174	3	177	31
	MHD	Subcritical steam	42-47†	193-216	0	193-216	16-25
	Fuel cells	Subcritical steam	47-60†	151-193	0	151-193	25-42
Combined heat and power	Pulverised coal	Subcritical steam	85†	107	2	109	58
		Supercritical steam	91-92	99-100	2	101-102	61
	PFBC	Subcritical steam	86	106	2	108	58
Fuel blending	Pulverised coal	Subcritical steam, coal/natural gas (85:15)	37	231	5	236	9
		Subcritical steam, coal/oil (47-53)	36	224	5	229	11
	Topping GT/PC	Subcritical, natural gas/coal (33:67)	41	121	4	225	13
		Supercritical, natural gas/coal (33:67)	49	161	3	164	36

* gasifier+PFBC

† converted from HHV using a conversion factor of 1.04

Emission factors are assumed in LHV for hard coal as 25.2 gC/MJ from Marland and others (1994), for oil as 20.0 gC/MJ and for natural gas as 15.3 gC/MJ from Marland (1983). From calculations by Smith and others (1994), by Maude (1993) and Audus (1993), it seems possible to reduce CO_2 emissions by up to about 20% by replacing existing plants with new conventional technology; by about 30% by using technologies based on combined cycles; and by about 60% by cogeneration of heat and power. However, when replacing an existing power plant and heating unit, a typical fuel saving would be about 30% with a corresponding reduction in CO_2 emissions (Pedersen and Staerkind, 1993). Another means of reducing CO_2 emissions from power plants is by blending coal with fuels containing a lower carbon to hydrogen ratio per unit of energy released. CO_2 reductions of about 10% have been calculated for typical blending ratios of natural gas or oil with coal in conventional steam cycles or 36% in combined cycles.

The specific investment cost of generating power is the total cost divided by the nominal power. Thus it is related to plant size. Maude (1993) calculated the specific and power cost for a number of plants with a nominal output of 300 MWe and 90% sulphur removal and 25.2g C/MJ (HHV) reference coal.

Plant	CO_2 emission factor, total plant, gC/kWh	Specific cost, $/kWe	Power cost c/kWh, 5 % DCF
Pulverised coal, supercritical steam	231	1631	4.6
AFBC, subcritical steam	242	1393	4.2
IGCC, fluidised bed, air blown, hot gas cleaning	204	1353	4.0
PFBC, supercritical steam	209	1267	3.8
Gasifier+PFBC, subcritical steam, hot gas cleaning	201	1380	3.9

The IGCC plant listed was selected as being the most economically attractive version of IGCC. The results show that the PFBC, IGCC and hybrid (gasifier and PFBC) had the lowest specific and power costs in the study. All the options in the study have considerably lower specific and power costs and reduced CO_2 emission factors compared to the PC plant.

Even though the installation of new, more efficient, coal use technologies would result in considerable CO_2 reductions, it appears unlikely that an appreciable decrease in global emissions of CO_2 from coal combustion will be realised in the short term. Progress will depend on how fast the new technologies can be introduced and replace existing plants. For economic reasons, most existing power plants will continue to operate until the end of their useful life before being replaced, in many cases another 20-30 y unless legislation dictates otherwise.

It should also be noted that the most efficient power generation technology may not necessarily be the most favourable when considering the complete fuel cycle. Stringent CO_2 emission limits may be enforced requiring CO_2 removal. In this case the power generating technology will affect CO_2 capture and maximum efficiency generation may not be the most appropriate choice.

CONTROL TECHNOLOGIES

Control of CO_2 requires its separation or capture from the flue gas, followed by storage or reuse. The ease of capture of CO_2 is influenced by the concentration and pressure of CO_2 in the flue gas, and the presence of other gases. The capture and storage of CO_2 incur energy penalties and extra costs at each stage in CO_2 capture, transport and disposal.

CO_2 capture processes have been compared by Riemer (1993), Schütz and others (1992) and Summerfield and others (1993a) in terms of efficiency and cost penalties for three coal utilisation technologies. The results of these studies, giving the lowest cost of capturing at least 90 % of the CO_2 in the flue gas compared with the PC + FGD base case, were summarised by Smith and others (1994):

Technology	Capture process	Cost (times base case)
PC+FGD	-	1
PC+FGD	MEA absorption	1.5
IGCC	cryogenics	1.5
IGCC+shift	physical absorption	1.3
CO_2 recycle	membrane	1.7

CO_2 capture and disposal from a 500 MW PC power plant could reduce the net power output by about 35%, with a net heat rate of 15.8 MJ/kWh. The net output of a 400 MW IGCC plant would be reduced by only about 12%, with a net heat rate of 12.6 MJ/kWh (Smelser and Booras, 1992).

Transport of CO_2 from the power plant to the disposal site adds to the cost. Skovolt (1993) estimates that the transport unit cost for a fully utilised large diameter pipeline over 1500 km is approximately $\$6/tCO_2$, while transport through a 40 cm pipeline, corresponding to CO_2 from a single 1000 MWe gas fired power station, over the same distance is approximately $\$42/tCO_2$. Skovolt (1993), Summerfield and others (1993b) and Ormorod and others (1993) estimated the cost of a pipeline for ocean disposal of CO_2 to be approximately $1 million per kilometre, depending on the pipeline diameter, length and the landform through which it runs. Thus it is likely that ocean disposal will only be cost-effective for new power plants constructed near the coast.

Estimates of global CO_2 storage potential ($GtCO_2$) are summarised by Smith and others (1994):

Oceans	73,000,000
Aquifers	320-425
Natural gas fields	304-520
Oil fields	154
Forestry	180-370
Short rotation cropping (emissions avoided)	3
Halophytes	3
Enhanced oil recovery	62

The largest storage potential is in the oceans. Hence most research has focused on ocean disposal. Ocean disposal costs were estimated for a 640 km pipeline (480 km overland and 160 km offshore) for disposal in the ocean at 450 m depth by Smelser and Booras (1992). The costs were judged also to be reasonable estimates for disposal in large, depleted natural gas fields. The cost of CO_2 disposal ranges from 35 - 60 % of the incremental costs. Total incremental capital requirements are the difference between the cost of the CO_2 removal plant and the cost of the base case plant, plus the replacement power costs. The IGCC incremental plant costs are much lower than the costs for PC plants because CO_2 removal from high pressure syngas requires less energy and uses lower cost processes than CO_2 recovery from low pressure flue gas.

Koide and others (1992) estimated the cost of storing 4,500 tCO_2 in an underground repository to be $\$72/t\ CO_2$. This compares with van Engelenburg and Blok (1993) who found the cost of CO_2 disposal in aquifers ranged from about $\$0.5 - 2/tCO_2$, and the cost of recovery ranged from $\$13-33/tCO_2$ avoided. Krom and others (1993) comment that the establishment and operation of a facility which can sequester CO_2 in a deep lying saline aquifer is expensive - about $\$14.7/t$ when sequestering 1.397 $MtCO_2$ per year including transport, energy and operational costs for a typical scenario but excluding removal from the flue gas.

Storage of CO_2 in biomass obviously does not incur capture or transport costs. In the US the marginal cost of carbon sequestration ranges from $7 - 54/tC, in nominal dollars, that is, in the dollars of the year in which the carbon is sequestered. The present cost of a programme to sequester 49 GtC over 160 years approaches $250 billion ($5.1/tC) (Richards and others, 1993). The costs are on a similar scale to estimates by Nakicenovic and others (1993) for a global plantation programme (comprising 265 Mha for forest and 85 Mha for agroforestry) which would cost $520 billion over the period 1995 - 2095, sequestering some 120 GtC ($4.4/tC). However, the cost estimates do not include major expenses such as obtaining the land. The IEA GHG (1993) included estimates for land purchase, plantation and maintenance expenses and found average carbon sequestration costs to be $16/tC in tropical countries and $76/tC in the industrialised countries, adding $0.004/kWh and $0.017/kWh respectively to the power generating costs.

CONCLUSIONS

Coal production and use is responsible for about 32% of total CO_2 emissions, around 8% of the CH_4 emissions and 5% of N_2O emissions from human activities. The enhanced greenhouse effect is that part of the total greenhouse effect which is due to human activities. In 1990, coal's contribution from emissions of CO_2, CH_4 and N_2O to the enhanced greenhouse effect may be estimated at about 19%, or 24% when considering their effect over a 100 y (*see* Table 2).

Expressing the greenhouse effect of emissions in common terms is vital for evaluations of emissions. The least complicated, common parameter is the greenhouse effect (radiative forcing) of a gas. Global warming potentials currently used have the disadvantage of not including the indirect effects of gases such as CH_4. They are not applicable for gases with widely varying horizontal or vertical distributions. There are major shortcomings in choosing CO_2 as a reference gas hence several authors are moving towards use of absolute measures of the potential effect of each gas. Recent attempts to account for uncertainties in calculating global warming potentials have increased the global warming potentials of CH_4 and N_2O relative to that of CO_2. The lack of a means of rigorously quantifying the effects of the other greenhouse gases is a major handicap to evaluations over the complete fuel cycle so that the current focus remains on CO_2.

The efficiency of coal utilisation may be improved considerably with proportionate reductions in CO_2 emissions as summarised in Table 3. The cost of an increase in efficiency is site and plant specific. Compared with the world average efficiency of coal-fired plants, efficiency improvements resulting in CO_2 reductions ranging from about 20-60% appear achievable by means of conventional steam cycles < combined cycles < combined heat and power. These reductions can only be realised to the extent that existing power plants are replaced by new, more efficient technologies. The full reduction potential may not be achievable in the near future. Another means of reducing CO_2 emissions from power plants is by blending coal with fuels containing a lower carbon to hydrogen ratio.

Higher CO_2 reductions, over 60%, will necessitate other kinds of actions such as concentrating the CO_2 in the flue gas by flue gas recycling or shift reactions with subsequent separation; or recovery of CO_2 from the flue gas of the existing system. All these alternatives incur decreased efficiencies and increased costs of about 1.5 times the cost without CO_2 capture.

Following capture, long term disposal is an essential part of CO_2 control. The oceans are potentially the largest carbon sink. However, the construction costs of ocean disposal appear to add 50 % to the cost of the power plant for both PC+FGD and integrated gasification combined cycle (IGCC). Thus the total cost for CO_2 capture and disposal may approximately double the cost of the base case plant.

Other cost estimates for storage are \$8 - 280/tCO_2 for biomass and \$0.5 - 72/tCO_2 for aquifers. However, there is still a lack of data, particularly on the costs of the various disposal options as well as their long term efficacy.

REFERENCES

Audus H (1993) *Greenhouse gas releases from fossil fuel power stations* IEAGHG/SR1, Cheltenham, UK, IEA Greenhouse Gas R&D Programme, 178 pp

Berdowski J J M, Olivier J G J, Veldt C (1993) Methane emissions from fuel combustion and industrial processes. In: *Proceedings of the international IPCC workshop methane and nitrous oxide: methods in national emission inventories and options for control.* A R van Amstel (ed.), Amersfoort, The Netherlands, 3-5 February 1993. Bilthoven, The Netherlands, National Institute of Public Health and Environmental Protection, pp 131-141

Broecker W S, Peng T-H (1992) Interhemispheric transport of carbon dioxide by ocean circulation. *Nature;* 356 (6370); 587-589
Broecker W S, Peng T-H (1993) Evaluation of the ^{13}C constraint on the uptake of fossil fuel CO_2 by the ocean. *Global Biogeochemical Cycles;* 7 (3); 619-626
Brown S, Lugo A E, Wisniewski J (1992) Missing carbon dioxide. *Science;* 257 (5066); 11
Caldeira K, Kasting J F (1993) Insensitivity of global warming potentials to carbon dioxide emission scenarios. *Nature;* 366 (6452); 251-253
CIAB (1992) *Global methane emissions from the coal industry*. Paris, France, Coal Industry Advisory Board, Global Climate Committee/International Energy Agency, 42 pp
Dai A, Fung I Y (1993) Can climate variability contribute to the "missing" CO_2 sink? *Global Biogeochemical Cycles;* 7 (3); 599-609
Daniel M (1991) *Power stations coal use: prospects to 2000*. Report IEACR/41, London, UK, IEA Coal Research, 61 pp
De Soete G, Sharp B (1991) *Nitrous oxide emissions: modifications as a consequence of current trends in industrial fossil fuel combustion and in land use*. EUR 13473 EN, Luxembourg, Commission of the European Communities, 259 pp
Harrison K, Broecker W, Bonani G (1993) A strategy for estimating the impact of CO_2 fertilization on soil carbon storage. *Global Biogeochemical Cycles;* 7 (1); 69-80
Harvey L D (1993) A guide to global warming potentials (GWPs). *Energy Policy;* 21 (1); 24-34
Hesshaimer V, Heimann M, Levin I (1994) Radiocarbon evidence for a smaller oceanic carbon dioxide sink than previously believed. *Nature;* 370 (6486); 201-203
Houghton R A (1993) Is carbon accumulating in the northern temperate zone? *Global Biogeochemical Cycles;* 7 (3); 611-617
IEA GHG (1993) *Carbon dioxide utilisation: evaluation of long term forestry and short rotation cropping as two schemes for compensating or avoiding the CO_2 emissions from a 500 MW(e) coal-fired power station*. OE16A; Cheltenham, UK, IEA Greenhouse Gas R&D Programme, vp
IPCC (1990) *Climate change: the IPCC scientific assessment*. J T Houghton, G J Jenkins, J J Ephraums (eds.), Cambridge, UK, Cambridge University Press, 414 pp
IPCC (1992) *Climate change 1992: the supplementary report to the IPCC scientific assessment*. J T Houghton, B A Callander, S K Varney (eds.), Cambridge, UK, Cambridge University Press, pp 212
Jansson S A (1993) Comparing coal power generation technologies In: *World Coal Institute conference on coal for development*, London, UK, 24-26 Mar 1993. London, UK, World Coal Institute, pp 38-46
Joos F (1994) Imbalance in the budget. *Nature;* 370 (6486); 181-182
Khalil M A K, Rasmussen R A (1992) Nitrous oxide from coal-fired power plants: experiments in the plumes. *Journal of Geophysical Research;* 97 (D13); 14,645-14,649
Koide H, Tazaki Y, Noguchi Y, Nakayama S, Iijima M, Ito K, Shindo Y (1992) Subterranean containment and long-term storage of carbon dioxide in unused aquifers and in depleted natural gas reservoirs. *Energy Conversion and Management;* 33 (5-8); 619-626
Krom T D, Jacobsen F L, Ipsen K H (1993) Aquifer based carbon dioxide disposal in Denmark. *Energy Conversion and Management;* 34 (9-11); 933-940
Lelieveld J, Crutzen P J, Brühl C (1993) Climate effects of atmospheric methane. *Chemosphere;* 26 (1-4); 739-768
Marland G (1983) Carbon dioxide emission rates for conventional and synthetic fuels. *Energy;* 8 (12); 981-992
Marland G, Andres R J, Boden T (1994) Magnitude and trends of CO_2 emissions. Presented at: Air & Waste Management Association International Specialty Conference *Global climate change: science, policy, and mitigation strategies*, Phoenix, AZ, USA, 5-8 April 1994, pp 16
Maude C (1993) *Advanced power generation - a comparative study of design options for coal* IEACR/55, London, UK, IEA Coal Research, 90 pp
Nakicenovic N, Grübler A, Inaba A, Messner S, Nilsson S, Nishimura Y, Rogner H, Schafer A, Schrattenholzer L, Strubegger M, Swisher J, Victor D, Wilson D (1993) Enhancing carbon sinks. *Energy;* 18 (5); 499-522
Ormerod W G, Webster I C, Audus H, Riemer P W R (1993) An overview of large scale CO_2 disposal options. *Energy Conversion and Management;* 34 (9-11); 833-840
Pedersen S L, Stærkind K (1993) Large scale deployment of cogeneration in the Danish Energy System: regulatory, institutional, economic and technical aspects. In: *New electricity 21: power industry technology and*

management strategies for the twenty-first century. Tokyo, Japan, 12-14 May 1992. Paris, France, OECD/IEA, pp 267-272
Quay P D, Tilbrook B, Wong C S (1992) Oceanic uptake of fossil fuel CO_2: carbon-13 evidence. *Science;* 256 (5053); 74-79
Richards K R, Moulton R J, Birdsey R A (1993) Costs of creating carbon sinks in the US. *Energy Conversion and Management;* 34 (9-11); 905-912
Riemer P (1993) *The capture of carbon dioxide from fossil fuel fired power stations.* IEAGHG/SR2, Cheltenham, UK, IEA Greenhouse Gas R&D Programme, 418 pp
Rotmans J, Den Elzen M G J (1992) A model-based approach to the calculation of global warming potentials (GWP). *International Journal of Climatology;* 12; 865-874
Rotmans J, Den Elzen M G J (1993) Modelling feedback mechanisms in the carbon cycle: balancing the carbon budget. *Tellus;* 45B (4); 301-320
Sarmiento J L, Sundquist E T (1992) Revised budget for the oceanic uptake of anthropogenic carbon dioxide. *Nature;* 356 (6370); 589-593
Schütz M, Daun M, Weinspach P-M, Krumbeck M, Hein K R G (1992) Study on the CO_2-recovery from an ICGCC-plant. *Energy Conversion and Management;* 33 (5-8); 357-366
Schwartz S E (1993) Does fossil fuel combustion lead to global warming? *Energy;* 18 (12); 1229-1248
Shine K P, Sinha A (1991) Sensitivity of the Earth's climate to height-dependent changes in the water vapour mixing ratio. *Nature;* 354 (6352); 382-384
Siegenthaler U, Sarmiento J L (1993) Atmospheric carbon dioxide and the ocean. *Nature;* 365 (6442); 119-125
Skovolt O (1993) CO_2 transportation system. *Energy Conversion and Management;* 34 (9-11); 1095-1104
Smelser S C, Booras G S (1992) An engineering and economic evaluation of CO_2 removal from fossil fuel-fired power plants. In: *EPRI ninth conference on gasification power plants.* Palo Alto, CA, USA, 17-18 Oct 1990. Palo Alto, CA, USA, EPRI Distribution Center, EPRI TR-100466, pp 30/1-30/25
Smith I M, Sloss L L (1992) *Methane emissions from coal.* IEAPER/04, London, UK, IEA Coal Research, 27 pp
Smith I M, Thambimuthu K V (1991) *Greenhouse gases, abatement and control: the role of coal.* IEACR/39, London, UK, IEA Coal Research, 88 pp
Smith I M, Nilsson C, Adams D M B (1994) *Greenhouse gases - perspectives on coal.* IEAPER/12, London, UK, IEA Coal Research, 41 pp
Sundquist E T (1993) The global carbon budget. *Science;* 259 (5097); 934-941
Summerfield I R, Goldthorpe S H, Bower C J (1993a) Combating global warming - reducing CO_2 emissions from coal-fired plant. *Proceedings of the Institute of Mechanical Engineers Part A: Journal of Power and Energy:* 207; 81-88
Summerfield I R, Goldthorpe S H, Williams N, Sheikh A (1993b) Costs of CO_2 disposal options. *Energy Conversion and Management;* 34 (9-11); 1105-1112
Takahashi T, Tans P P, Fung I (1992) Balancing the budget. *Oceanus;* 1 (spring); 18-28
Takeshita M, Sloss L L, Smith I M (1993) *N_2O emissions from coal use.* IEAPER/06, London, UK, IEA Coal Research, 28 pp
Tans P P, Fung I Y, Takahashi T (1990) Observational constraints on the global atmospheric CO_2 budget. *Science;* 247 (4949); 1431-1438
van Engelenburg B C W, Blok K (1993) Disposal of carbon dioxide in permeable underground layers: a feasible option? *Climatic Change;* 23; 55-68
Wallis M K, Lucas N J D (1994) Economic global warming potentials. *International Journal of Energy Research:* 18 (1); 57-62
Wigley T M L (1993) Balancing the carbon budget. Implications for projections of future carbon dioxide concentration changes. *Tellus;* 45B (5); 409-425
Wuebbles D J, Edmonds J (1991) *Primer on greenhouse gases.* Chelsea, MI, USA, Lewis Publishers, 230 pp
Wuebbles D J, Patten K O, Grant K E, Jain A K (1992) *Sensitivity of direct global warming potentials to key uncertainties.* UCRL-ID-111461, Livermore, CA, USA, Lawrence Livermore National Laboratory, 48 pp
Zetterberg L (1993) *A method for assessing the expected climatic effects from emission scenarios using the quantity radiative forcing.* IVL-B 1111, Stockholm, Sweden, Swedish Environmental Research Institute, 19 pp